The roles of microRNAs in proteostasis in *C. elegans*

by

İsa Özdemir

A Thesis Submitted to the

Graduate School of Sciences and Engineering

in Partial Fulfillment of the Requirements for

the Degree of

Master of Science

in

Molecular Biology and Genetics

Koc University

August 2017

Koc University

Graduate School of Sciences and Engineering

This is to certify that I have examined this copy of a master's thesis by

İsa Özdemir

and have found that it is complete and satisfactory in all respects,

and that any and all revisions required by the final

examining committee have been made.

Committee Members:

_____

Assistant Prof. Dr. Funda Şar (Advisor)

_____

Associate Prof. Dr. Nurhan Özlü

_____

Asistant Prof. Dr. Elif Uz

_____

ABSTRACT

microRNAs (miRNAs) are ~22 nt long small non-coding RNAs involved in post-transcriptional gene regulation (PTGR) [1, 2]. The first discovered miRNAs, *lin-4* and *let-7*, act on a nematode specific "heterochronic" pathway [3, 4]. Since then, miRNAs are associated with a plethora of biological processes including apoptosis, cell differentiation and immune system [5-7].

While studies using the knockouts of miRNA biogenesis genes showed that miRNAs are essential for both embryonic and larval development, it was not possible to address post-developmental roles of miRNAs till a temperature sensitive DGCR8/*pash-1* mutant, here after called *pash-1ts*, was isolated in *C. elegans* [8]. Using this allele, post-developmental expression of miRNAs was shown to be essential for normal life span and physiology in *C. elegans* [8]. However, the underlying mechanisms behind the rapid aging phenotype of *pash-1ts* animals remained elusive.

One of the important hallmarks of aging is the decline in proteostatic capacity. Proteostasis is the process in which the functional proteome has been maintained by proteostasis network (PN), including molecular chaperones, proteasome and autophagy. Defects in PN result in cytotoxic protein aggregations, rapid aging and deterioration of the locomotion in *C. elegans*.

Here, I showed that *pash-1ts* animals phenocopied the proteostasis defects which could be rescued by the enhancement of proteostasis by Thioflavin T (ThT). Then, I examined how PN was affected in the absence of miRNAs. Our results indicated that the mRNA levels of small heat shock proteins were altered in *pash-1ts* animals. Of 24 chaperones, *sip-1*, *Q9N350*, *hsp-25*, and *hsp-60* were downregulated while *F08H9.4a*, *F44E5.4*, *F08H9.3* and *ZK1128.7* were upregulated in *pash-1ts* animals compared to wild type and *pash-1* rescue animals. Moreover, I have tested the protein degradation systems. First I examined the transcript levels of proteasome genes by quantitative RT-

PCR. Interestingly, the mRNA levels of the longevity determining proteasome genes, *pbs-5* and *rpn-6.1*, increased in the absence of miRNAs. However, these have not been phenotypically reflected on *pash-1ts* animals. Lastly, I have examined the activity of autophagy in the absence of miRNAs. I have knocked-down *unc-51* and *bec-1* by RNAi and observed that it did not affect the life span of *pash-1ts* animals, suggesting that autophagy was already impaired in the absence of miRNAs. To validate, we visualized autophagic vesicles using translational LGG-1 reporter fused with GFP. Even though LGG-1 protein level was higher in *pash-1ts* animals compared to wild type and *pash-1* rescue animals, we observed that a decrease in the number of autophagic vesicles formed in *pash-1ts* mutants.

Overall, these results suggested that miRNAs are essential for the regulation of protein folding and degradation. In future, miRNAs can be potentially used for diagnostic and therapeutic purposes against the diseases associated with proteostasis defects.

Key Words: miRNAs, *C. elegans*, *pash-1*, aging, proteostasis, proteostasis network (PN)

ÖZETÇE

mikroRNA'lar (miRNA'lar), transkripsiyon sonrası gen kontrolünde (PTGR) yer alan 22 nt uzunluğunda protein kodlamayan küçük RNA'lardır [1, 2]. İlk keşfedilen miRNA'lar, *lin-4* ve *let-7*, nematod'a özgü "heterochronic" yolak üzerinde etki yapmaktadır [3,4]. Daha sonra, miRNA'ların apoptoz, hücre farklılaşması ve bağışıklık sistemi gibi biyolojik olgularla da ilişkili olduğu gösterilmiştir [5-7].

miRNA biyogenez genlerinin nakavtları kullanılarak yapılan çalışmalar, miRNA'ların hem embriyo hem de larva gelişimi için gerekli olduğunu gösterdi; ancak, *C. elegans*'da izole edilen sıcaklığa duyarlı DGCR8 / *pash-1* mutantına kadar, kısaca *pash-1ts,* gelişme sonrası miRNA'ların rollerine değinmek mümkün değildi [8]. *pash-1ts* mutantını kullanarak, gelişim sonrası ortaya çıkan miRNA'ların ekspresyonunun *C. elegans*'daki normal ömür ve fizyoloji için gerekli olduğu bulundu [8]. Bununla birlikte, *pash-1ts* hayvanlarının hızlı yaşlanan fenotipinin altında yatan mekanizmalar belirsiz kaldı.

Yaşlanmanın önemli özelliklerinden biri proteostatik kapasitenin azalmasıdır. Proteostaz proteomun moleküler şaperonlar, proteazom ve otofaji dahil olmak üzere proteostaz ağı (PN) tarafından işlevselliğinin korunmasıdır. PN'deki bozukluklar sitotoksik protein agregasyonlarına, hızlı yaşlanmaya ve *C. elegans*'da hareket kaybına neden olur.

Burada, *pash-1ts* hayvanlarının proteostaz ile ilişkilendirilmiş fenotipleri yansıttığını ve bunların proteostatik kapasitenin Thioflavin T (ThT) tarafından arttırılmasıyla kurtarılabildiğini gösterdim. Daha sonra, miRNA'ların yokluğunda PN'nin nasıl etkilendiğini inceledim. Bulgularımız, küçük şaperon proteinlerinin mRNA düzeylerinin *pash-1ts* hayvanlarında değiştiğini gösterdi. 24 şaperon içinden, *pash-1ts* hayvanlarında doğal suş ve *pash-1* kurtarma hayvanlarına kıyasla *sip-1*, *Q9N350*, *hsp-25* ve *hsp-60*'ın miktarının azaldığını, *F08H9.4a*, *F44E5.4*, *F08H9.3* ve *ZK1128.7* miktarının

arttığını gözlemledim. Ayrıca, protein yıkım sistemlerini test ettim. Öncelikle, proteazom genlerinin transkript seviyelerini inceledim. İlginç bir şekilde, ömrü uzatan *pbs-5* ve *rpn-6.1* proteazom genlerinin mRNA seviyeleri, miRNA'ların yokluğunda artmıştır. Bununla birlikte, bunlar *pash-1ts* hayvanlarına fenotipik olarak yansımış değildir. Son olarak, miRNA'ların yokluğunda otofajinin aktivitesini inceledim. *unc-51* ve *bec-1* seviyelerinin RNA interferaz teknolojisi ile düşüşünün *pash-1ts* hayvanlarının ömrünü etkilemediğini gözlemledim. Bu yüzden, miRNA'ların yokluğunda otofajinin çalışmadığını hipotize ettim. Bu hipotezi doğrulamak için, otofajik veziküller GFP ile işaretlenmiş LGG-1 proteinini kullanarak görselleştirdik. LGG-1 protein seviyesi *pash-1ts* hayvanlarında vahşi tip ve *pash-1* kurtarma hayvanlarına kıyasla daha yüksek olmasına rağmen, *pash-1ts* mutantlarında otofajik veziküllerin sayısının azaldığını gözlemledik.

Genel olarak, bu sonuçlar, miRNA'ların protein katlama ve yıkımının düzenlenmesi için şart olduğunu önermiştir. Gelecekte, miRNA'lar, proteostaz kusurlarıyla ilişkili hastalıklara karşı teşhis ve tedavi amacıyla kullanım potansiyeli taşımaktadır.

Anahtar Kelimeler: miRNAlar, *C. elegans*, *pash-1*, yaşlanma, proteostaz, proteostaz ağı (PN)

ACKNOWLEDGEMENTS

I want to thank my supervisor, Dr. Funda Şar for all her support and giving me opportunity to work on such an interesting project. I am grateful to Dr. Şar for her unceasing enthusiasm, and endless interest to discuss new ideas.

Thanks to everyone in Şar laboratory for making the laboratory an excellent place to study. First, I would like to thank to Dr. Nihal Gülseren Çakmakçı for teaching me how to work with the worms, and lifespan experiments. I am also grateful to current Şar laboratory members, Fatma, Hale, and Mukadder, for creating friendly environment to study.

I want to thank our collaborator Janine Kirstein for her contribution to the study.

I would like to thank Dr. Patricija van Oosten-Hawle and her laboratory members for teaching me how to do quantitative RT-PCR and for encouraging scientific discussions.

I would like to thank to my thesis committee members, Dr. Nurhan Özlü and Dr. Elif Uz, for their contribution to my thesis.

I would like to thank Dr. Halil İ. Kavaklı and his laboratory members for allowing me to use their qPCR machine.

Also, I would like to thank to my close friends, Osman, Bayram and Yiğit, for their life-long support. Whenever I needed them, they were always with me.

Most of all, I am grateful to my parents Adil and Fatma and my brother Cem for their love, encouragement and support under all conditions. Undoubtedly, I cannot explain how I am happy to have such a family.

Lastly, I would like to thank my dear love Hazal Ergüneş for her unceasing love.

TABLE OF CONTENTS

LIST OF FIGURES

LIST OF TABLES

ABBREVATIONS

AGO: Argonoute Protein

atg: *Autophagy related gene*

C. elegans: Caenorhabditis elegans

CMA: Chaperone mediated autophagy

DHIC: DDL-1 containing HSF-1 inhibitory complex

E. coli: Escherichia coli

FUdR: 5-Fluoro-2′-deoxyuridine

GSK3: Glycogen Synthase Kinase 3

HD: Huntington's Diseases

HS: Heat shock

HSF-1: Heat Shock Factor 1

HSR: Heat Shock Response

IIS: Insulin and insulin-like growth factor signling

K: Lysine

lf: Loss of function

miRNA: MicroRNA

mRNA: Messenger RNA

mTORC1: Target of Rapamycin Complex 1

NGM: Nematode Growth Medium

n.s.: Not Significant

nt: Nucleotide

oe: overexpression

PC: Proteolytic core

Pre-miRNA: Precursor miRNA

Pri-miRNA: Primary miRNA

PTGR: Posttranscriptional Gene Regulation

Q: Glutamine

RISC: RNA inducing silencing complex

RNAi: RNA interference

ROS: Reactive Oxygen Species

RP: Regulatory Particle

sHSP: Small heat shock protein

ThT: Thioflavin T

ts: Temperature Sensitive

UPS: Ubiquitin-proteasome system

CHAPTERS

CHAPTER 1: INTRODUCTION

1.1. *C. elegans* as a model organism

Caenorhabditis elegans is a free living nematode that found in rotting organic matter in nature [9]. It is a transparent, non-parasitic animal, reaching to 1.2 mm in length [9] **(Figure 1)**. Half a century year ago, Sydney Brenner suggested using this tiny nematode to study the developmental biology and neurobiology. Since then, it is commonly used not only in biology, but also in other fields such as physics and chemistry due to its ease and low cost of cultivation.

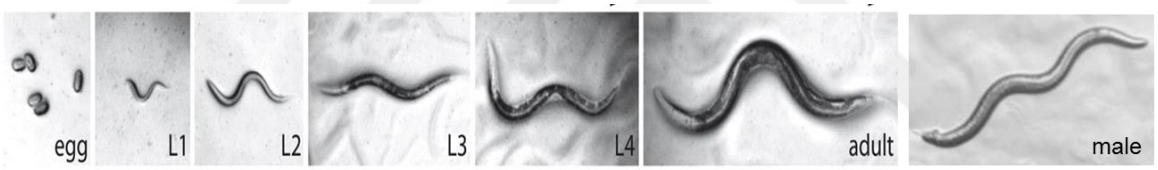

Figure 1. *C. elegans* from embryo to male. (Adapted from wormbook)

Depending on the temperature, the life cycle of *C. elegans* takes place between 2.5 and 5.5 days under favored conditions **(Figure 1)**. Optimum maintenance temperature varies between 15°C to 25°C. Above 25°C, it is not possible to propagate these animals since they become sterile. Embryogenesis starts as *in utero* and continues as *ex utero* (**Figures 1-2).** After hatching, embryos follow four successive larval stages (L1-L4) **(Figure 2).** Each stage ends with a sleep-like state called lethargus, followed by the molting of the old cuticle [10]. After L4 stage, animals become adult hermaphrodites **(Figure 2).** Each adult hermaphrodite lays 200-300 embryos; however, in the presence of the males in the population this number can go up to 1000 progenies for 3 days at 20°C [11].

Even though the development of *C. elegans* is timely regulated event, the life cycle of an animal changes depending on the environmental conditions, such as food availability and crowding. Wild type adults can live up to 20-30 days between 20℃ and 25℃ **(Figure 2)**. Under laboratory conditions, *C. elegans* is usually grown on agar plates containing a lawn of bacterium *Escherichia coli (E. coli).*

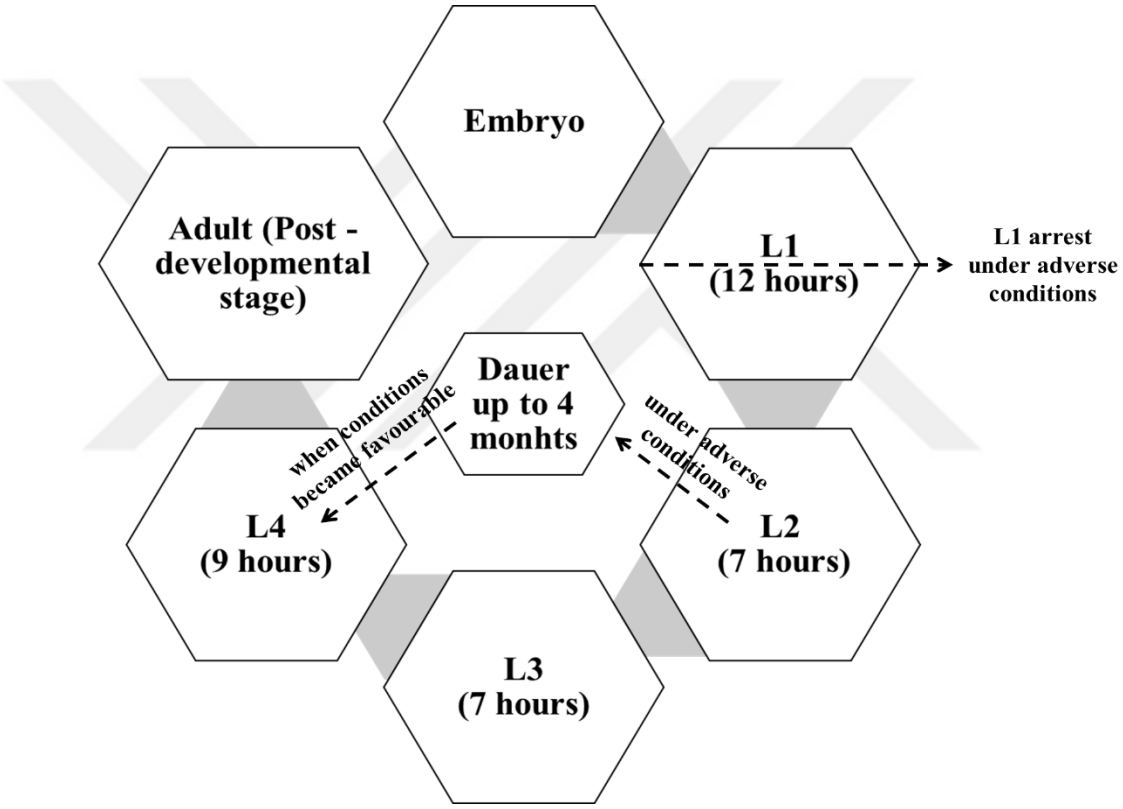

Figure 2. Complete life cycle of a *C. elegans.*

Under the adverse conditions such as starvation, crowding and temperature *C. elegans* can stop development at either L1 or L2/L3 stages to enter into an alternative stage, called dauer **(Figure 2).** Dauer worms are free from feeding, resistant to chemical insults and can survive for months [12]. When the conditions become favorable, L1 diapause and L3 dauer animals can resume their development **(Figure 2)** [12]. At dauer or L1 diapause animals, worm stocks can be

frozen at -80°C and thawed upon the necessity enabling to store various strains without accumulation of the spontaneous mutations.

C. elegans can be visualized and manipulated either using a dissecting microscope or a compound microscope. Using a dissecting microscope, it is possible to observe the live animals as they move, eat or mate; however, a compound microscope is required to visualize cellular events at higher resolution. Moreover, owing to its transparency, *C. elegans* is a very useful model organism to observe cellular events. While common techniques such as antibody staining and ß-galactosidase assay can be utilized in fixed animals, fluorescent proteins also pose many advantages to observe gene activity or protein localization in living organisms for the entirety of their life [13].

C. elegans has an invariant cell lineage and development, which makes it a powerful tool for developmental and cellular processes [14-16]. The functional conservation of biological pathways and many human related diseases enable researchers to use *C. elegans* as a model system to study a variety of biological processes and diseases [17, 18].

1.1.1. *C. elegans* genetics

C. elegans consists of two sexes, hermaphrodites and males **(Figure 1)**. Under the steady state conditions, the majority of population is self-fertilizing hermaphrodites, while only 0.2% of it is male. The genetic configuration for a hermaphrodite is XX, whereas it is X0 for a male [19]. Only small proportions of progenies are males due to rare meiotic non-disjunction in the hermaphrodites' germ line. Besides their genetic differences, they have physiologically distinguishable tail structure **(Figure 1)**.

C. elegans, due to self-fertilizing feature, is a very useful model organism to study genetics because it (i) simplifies stock maintenance, (ii) is "driven to homozygosity" meaning population tend to lose heterozygosity [9], and (iii) follows the Mendelian rules of segregation facilitating the maintenance of mutants. Hermaphrodites can also be crossed to males for the exchange of genetic material.

C. elegans genome is the first metazoan genome that is completely sequenced and annotated [20, 21]. Even though *C. elegans* and *H. sapiens* are evolutionarily distinct, comparative genetics and proteomics studies indicated that 60% of genome similarity and 38% proteome similarity exist between nematode and human [22, 23]. Additionally, numerous reverse and forward genetic techniques make *C. elegans* instrumental for the elucidation of molecular pathways implicated in human diseases [9, 24-26]. For example, the sensitivity of *C. elegans* to environmental perturbations allows designing mutational screens to isolate conditional mutants of interest [12, 27, 28].

1.2. miRNAs

MicroRNAs (miRNAs) are ~22 nt long regulatory non-coding RNAs involved in various cellular events such as embryonic development, metabolism, cell fate and apoptosis [5, 6, 29]. Together with RNA inducing silencing complex (RISC), they function in the posttranscriptional gene regulation (PTGR). Imperfect base pairing between seed sequences (2-7th nt) of miRNA and 3' UTR of target mRNA allows the target recognition leading to inhibition of protein translation or mRNA degradation.

miRNAs are the second largest gene family after transcription factors [5]. 1-2% of nematode and mammal genome is thought to comprise of miRNA genes [5]. Since miRNAs are predicted to target hundreds of genes, the majority of protein coding genes is estimated to be controlled by miRNAs. In other words, virtually every biological process is subject to PTGR by miRNAs [7].

C. elegans is the simplest multicellular organism that has miRNA genes and a conserved miRNA biogenesis pathway [30]. So far 250 miRNAs have been annotated and deletions of many of them are available through CGC (WBcel235). Most of the miRNAs are functionally conserved from nematodes to mammals. All these features make *C. elegans* a powerful model to study the functions of miRNAs and miRNA biogenesis pathway.

1.2.1. miRNA biogenesis in *C. elegans*

miRNAs can be generated by various pathways; however majority of them are produced by the canonical pathway **(Figure 3)** [31-33]. Similar to mRNAs, miRNAs are usually transcribed by RNA polymerase II in the nucleus from the intergenic regions **(Figure 3).** The initial transcript is called primary miRNA (pri-miRNA) and, like mRNAs, they possess a 3'

polyadenylated tail and 5' 7-methylguanosine cap **(Figure 3)** [34, 35]. Pri-miRNA is converted to precursor miRNA (pre-miRNA) by the microprocessor complex consisting of an RNAse III enzyme, called Drosha/DRSH-1 and its mediator DGCR8/PASH-1 in nucleus **(Figure 3)** [34, 36]. The base of the pre-miRNA stem loop has typically 5' phosphate and ~2 nt 3' overhang [37] which is exported to cytoplasm by XPO-1/Exportin 5 Ran-GTP **(Figure 3)** [38, 39]. In cytoplasm, Dicer/DCR-1, another RNAse III enzyme, trims the hairpin loop to generate 21-23 nucleotide length double stranded RNAs **(Figure 3)** [40-42]. The resultant duplex (miRNA guide and passenger strand) is loaded onto Ago/ALG-1/2, forming the pre-RISC complex. The passenger strand is peeled off, and later gets degraded. However, guide strand together with ALG-1/2 in *C. elegans* forms the RISC complex, which localizes to 3' UTR of target mRNA to mediate translational repression or mRNA degradation **(Figure 3).**

Although most miRNA genes are intergenic, some of them can be intragenic [5, 31, 43]. Intragenic miRNAs are derived from the introns of pre-mRNAs through splicing, these miRNAs are named as mirtrons [44]. They are usually found in the same orientation with the host gene [45, 46]. This mechanism is thought to provide the coordinated expression of a miRNA and the host gene [5].

A collection of knock-out strains, containing deletion of a single miRNA or all of miRNA gene family members were generated through mutational screens [47, 48]. Analysis of these strains revealed that the majority of miRNAs are dispensable for development or viability [48]. This suggests that miRNAs might be only essential under the certain genetic backgrounds due to functional redundancies [49, 50]. Therefore, disabling miRNA biogenesis eliminates the functional redundancies between the miRNA genes and have potential to be utilized to address the functions of miRNAs genes [51]. However, this is not a simple task due to the fact that

cessation of global miRNA activity is incompatible with life [5]. Therefore, global suppression of miRNA production can be achieved by conditional mutants of important miRNA biogenesis genes. Recently, in a forward genetic screen a conditional *mj-100* allele of p*ash-1,* which enables reversible and quick deactivation of miRNA biogenesis, was isolated in *C. elegans* [8]. The mutation results in substitution of a single base A to G which cause exchange of tyrosine to cysteine at 515th partially conserved amino acid residue within the dsRNA-binding domains of PASH-1 [8].

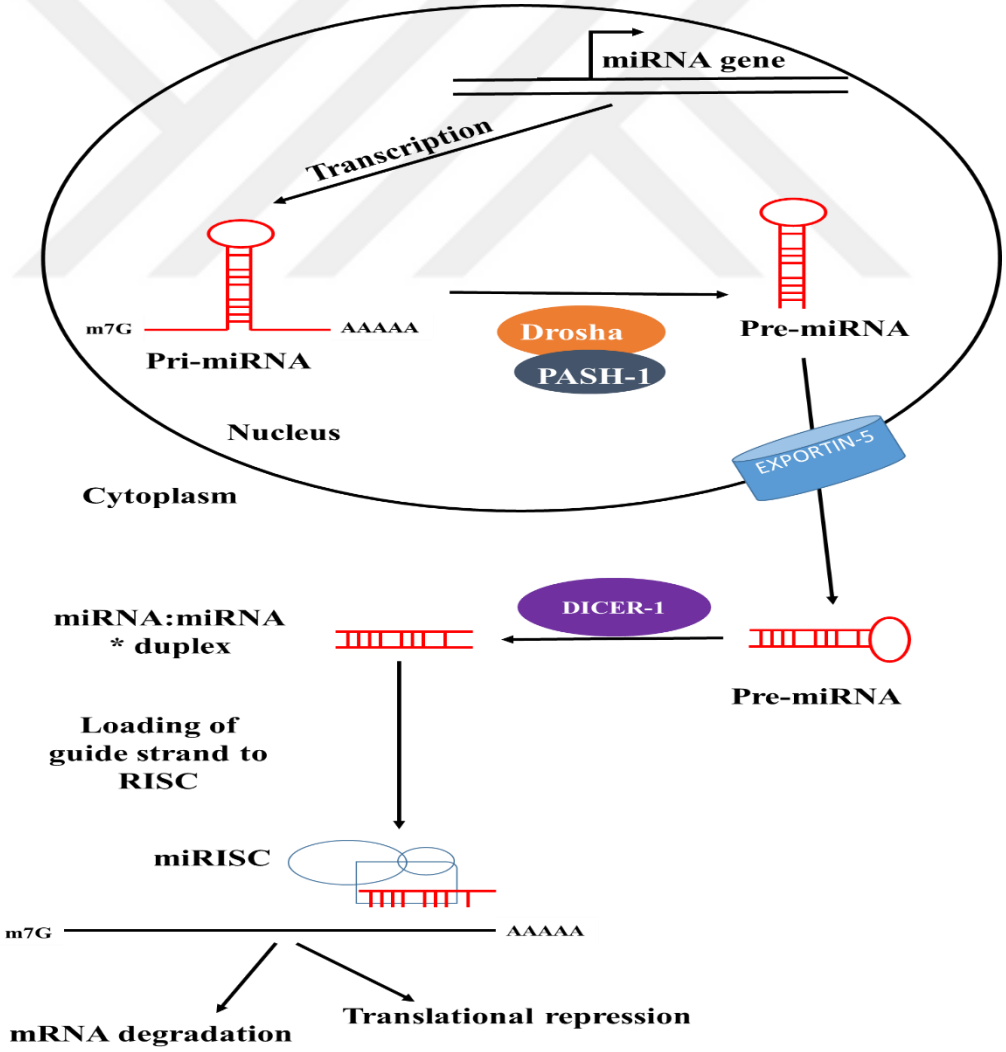

Figure 3. Canocical miRNA biogenesis pathway in *C.elegans.*

1.2.2. Functions of microRNAs (miRNAs)

miRNAs are involved in various fundamental processes both at cellular and organismal level. Some of these processes include developmental timing, cell proliferation [52], differentiation and apoptosis [53].

The heterochronic, *lin-4*, is the first discovered miRNA in *C. elegans* in 1993 [1]. In this groundbreaking study, they observed that *lin-4(lf)* mutants are retarded at L1 stage; however, no protein is expressed from the *lin-4* gene locus [1]. This astonishing finding suggested that some genes are functional at RNA level, without being translated into protein. Later on it has been understood that the retarded phenotype of *lin-4(lf)* can be suppressed by a mutation in *lin-14 3' UTR*. *lin-4* substantially reduces the amount of LIN-14 protein without affecting the mRNA level of *lin-14* [1, 54] .

After the discovery of first miRNA in *C. elegans* an extensive effort put on to discover novel miRNAs, which led to the identification of *let-7* among others. *let-7*, another heterochronic gene, which promotes the transition from L4 to young adult stage by targeting LIN-41 [4, 55]. Indeed, *let-7* is the most conserved miRNAs from nematodes to humans and involved in various biological processes such as cell differentiation and progression of cancer among species suggesting miRNAs are widespread class of small RNAs [2, 56].

In addition to larval development, miRNAs are also important for the embryonic development in *C. elegans*. Knock out of two miRNA families, *mir-35* (*mir-35-42*) and *mir-51* (*mir-51-57*), have been associated with embryonic lethality [47, 57]. The members of both miRNA families appear to act redundantly as embryonic lethality can be greatly rescued by expression of any single miRNA in the families [47, 57].

miRNAs can also play a role in organismal asymmetry. The ASE neurons are a pair of taste receptor neurons found in the left (ASEL) and right (ASER) of *C. elegans.* This asymmetry is required for chemotaxis in complex environments [58]. *lys-6* and *mir-273* have been implicated in ASEL-ASER determination in *C. elegans* [59, 60]. Whereas *lys-6* is specifically expressed in ASEL and targets COG-1 which acts in the cascade of transcription factor that regulates ASER/ASEL asymmetry [59], *mir-237* is only expressed in ASER and targets DIE-1 transcription factor in ASER neurons [60].

Similar to *lys-6* and *mir-237*, *mir-1* is a tissue specific miRNA, expressed only in muscle cells in *C. elegans*, Drosophila and mice. *mir-1* functions in the neuromuscular junctions through targeting UNC-29 and UNC-63, subunits of acetyl choline receptor in *C. elegans* [61].

Lastly, several reports indicated that miRNAs, expressed in mammals, are also known to prevent various diseases. For example, aberrant expression of miR-320 causes cerebral and cardiac ischemia; miR-1 have been demonstrated to prevent cardiac injury [66, 67]. Furthermore, three miRNAs, miR-26b, miR-106a and miR301b were shown to be significantly increased in Parkinson's disease patients resulting in aberrant α-synuclein aggregation in Lewy bodies [68].

Since their first discovery the mounting evidence, leaves no doubt that miRNAs are one of the cornerstones of regulation of gene expression [1, 3, 62].

1.2.3. miRNAs and aging

In recent years, several miRNAs have been shown to affect life span and aging related disorders such as heart disease, neurodegeneration, and cancer [63-65]. Genome-wide

studies indicated that almost 25% of miRNA genes are differentially expressed in aged *C. elegans* suggesting that miRNAs are dynamically regulated during aging [66, 67]; however, their functional significance is poorly understood [63, 68]. Up to date, all known miRNAs, which are affecting aging are listed in **Table 1**.

Besides regulating developmental timing in *C. elegans, lin-4* was shown to be the first miRNA regulating aging in *C. elegans* [69]. While decreased expression of *lin-4* shortens the life span of animals, over expression of *lin-4* extends the life span in LIN-14 and DAF-16 dependent manner [69]. Furthermore, DAF-16 has been shown to repress *lin-4* expression, implying an intricate regulation between DAF-16 and *lin-4* [70].

Knock out of, nematode specific, *mir-71* also causes shortened life span, while ubiquitously over expression of *mir -71* promotes longevity [68]. On the contrary, *mir-239* knock-out exhibits an increase in life span and over expression of *mir-239* shortens the life span [68]. Recently, it has been reported that *mir-71* and *mir-239* antagonistically act on DNA damage check point and IIS pathways to regulate aging [68]. This reveals that miRNAs can act as pro-aging and anti-aging genes.

More detailed studies on *mir-71* have also shown that expression of wild type *mir-71* only in the neurons is sufficient to extend the life span of *mir-71* mutants. However, this requires the expression of DAF-16 in the intestine. This result indicate that *mir-71* act cell-non-autonomously to regulate the life span [64].

Moreover, *mir-71,* together with *mir-228,* is critical for the life span regulation in *C. elegans* as downstream targets of PHA-4 and SKN-1 transcription factors [71]. Interestingly, *mir-71* and *mir-228* negatively regulate PHA-4 and *mir-71,* but not *mir-228,* represses SKN-1

[71]. This shows that miRNAs and transcription factors may form feedback loops to regulate aging in *C. elegans*.

mir-124 is a highly conserved miRNA from worm to human and it is abundantly expressed in neuronal cells. Genetic studies implicated that *mir-124* expression is regulated by WRN-1, a DNA helicase, and *mir-124* mutants are short lived and generate more ROS in *C. elegans* [72]. Interestingly, aging phenotype of *mir-124* can be rescued by vitamin C supplementation in *C. elegans* [72].

Knock-outs of *mir-238* and *mir-246* are also short-lived [68]. While *mir-246* overexpression can extend the life span of wild type nematode, life span extension has not been observed in *mir-238* transgenic worms suggesting *mir-238* may not be a *bona fide* aging gene [68].

miRNA name	Genotype	Phenotype	References
mir-45	*n4280*	Longevity	[64]
mir-239.1 and .2	*nDf62*	Longevity	[68]
mir-58.1	*n4640*	Shortened life span	[47, 64]
mir-61 and mir-250	*nDf59*	Shortened life span	[64]
mir-71	*n4115*	Shortened lifespan	[64, 68, 71]
mir-124	*n4255*	Shortened lifespan	[72]
mir-64-66) and mir-229	*nDf63*	Shortened lifespan	[64]
mir-80	*nDf53*	Shortened lifespan	[64]
mir-238	n4112	Shortened lifespan	[68]
mir-228	n4382	Shortened lifespan	[71]
lin-4	*e912*	Shortened lifespan	[69]

Table 1. miRNAs implicated in aging. Adapted from [47, 64, 68, 69, 71, 72].

1.3. Aging

With the advances in technology and science, life expectancy for human being has greatly expanded **(Table 2)**. Together with life span extension, prevalence of many diseases including neurodegenerative diseases, muscle dystrophy and cancer have also increased [73]. Regrettably, the main reasons underlying these non-treatable disorders have not been well characterized yet. Therefore, it is essential to identify molecular mechanisms of aging to have comprehensive understanding of aging associated diseases [74].

Aging is characterized by a progressive deterioration of cellular processes in all tissues [75]. Genomic instability [76], progressive shortening of telomeres [77], loss of epigenetic regulation [78], stem cell exhaustion [79], mitochondrial dysfunction [80] and decline in proteostasis capacity [81, 82] are important hallmarks of aging **(Figure 4)**.

Decades	Life expectancy (Years)
1950	42
1960	48
1970	55
1980	59
1990	61
2000	65
2010	71

Table 2. Life expectancy has been increasing all around the world. Numbers were taken from World Health Organization statistics, 2016.

The first aging associated genes were discovered through forward genetic screen in *C. elegans* [83-85]. In a groundbreaking study led in Cynthia Kenyon's laboratory in 1993, it has been reported that loss of function mutation in *daf-2*, a receptor tyrosine kinase, doubles the life span of nematodes in *daf-16*/FOXO3A dependent manner [86]. This pioneering study was astonishing because it indicated that aging can be genetically modulated [87] and established the field of the biology of aging.

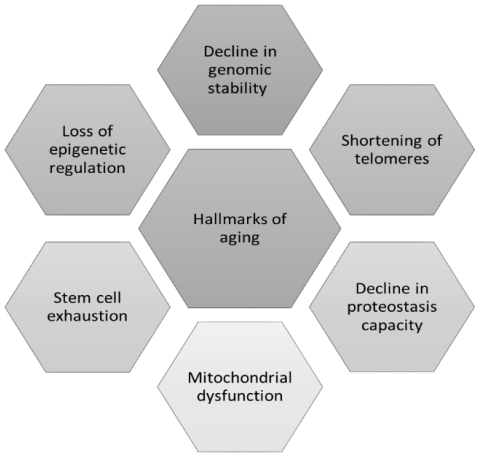

Figure 4. Hallmarks of aging.

1.3.1. Proteostasis Network

Proteins, central to all biological processes, must be kept in their native, functional state. To achieve this, protein homeostasis (proteostasis), the state in which the proteome of a living organism is in functional balance, is strictly maintained by an intricate network, known as proteostasis network (PN) **(Figure 5)** [88, 89]. PN must be upheld during development, healthy aging and in the face of environmental stresses.

Functional decline in the proteostatic capacity contributes to pathogenesis of aging associated disorders such as Alzheimer's and Huntington's diseases and muscular dystrophy while upregulation of proteostatic capacity is sufficient to prevent protein conformational diseases and extend the life span of organisms **(Figure 5)** [89-94]. Furthermore, proteostatic capacity tend to decline as organisms age and this decline is thought to rapidly occur in the early days of adulthood [89, 95].

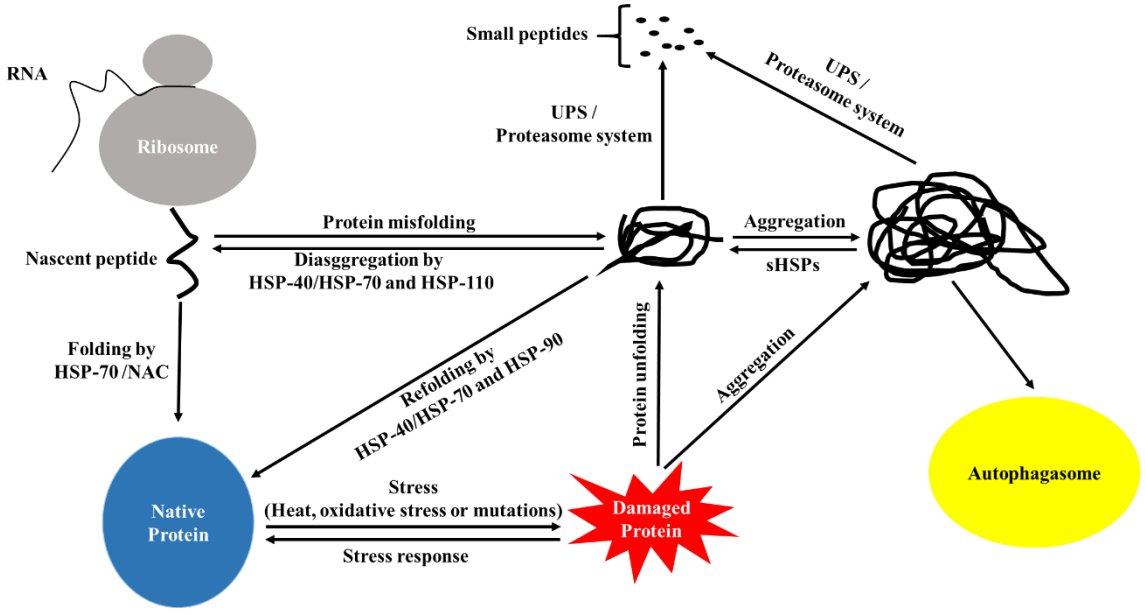

Figure 5. Proteostasis network (PN).

1.3.1.1. Stress responses

Organisms are continuously exposed to changing internal and external conditions such as DNA damage, increased reactive oxygen species (ROS), errors in protein synthesis and exposure to elevated temperatures during their lifetime. In order to combat these stresses, multiple protective responses including PN, have been employed by a set of transcription factors including HSF-1, DAF-16, and SKN-1. These proteins are collectively called stress response regulating transcription factors, in *C. elegans*. Owing to the connection between PN and aging [96, 97], the stress response signaling have been studied for a long time as an approach to understand potential treatment of age-related diseases [98, 99].

Stress response regulating transcription factors are central not only to the transcriptional regulation of PN, but also the developmental processes in *C. elegans* suggesting that these genes have pleiotropic effects during development and in the adulthood [91, 93, 100-102]. Of note, although these transcription factors have roles in distinct mechanisms, they can also regulate common downstream targets. In the rest of this section, I will briefly summarize what is currently known about these transcription factors.

Heat shock transcription factor 1 (HSF-1) is essential for the regulation of heat shock response (HSR) in metazoans [91, 103]. Heat shock challenges the organismal proteostasis by causing global protein denaturation. During recovery following heat shock, if HSF-1 fails, PN undergoes to an organismal collapse. Moreover, HSF-1 is critical for both development and life span determination [91, 104]. C-terminus truncated *hsf-1* mutant in nematode is defective in egg laying and transition from L2 to L3 stage in *C. elegans* [105]. While HSF-1 loss of function mutations cause rapid aging, HSF-1 overexpression can increase the life span of nematodes [91, 93, 103].

In vertebrates, there exist four HSF genes (HSF1-4) [106] whereas *C. elegans* harbors only one HSF gene. Heterologous expression of human HSF1 in *hsf*-1 loss of function mutations can rescue the defects in *C. elegans,* suggesting that human HSF1 and *C. elegans* HSF-1 are functionally conserved [107].

HSF-1 is normally kept as inactive through its interaction with HSP-90 or HSP-70 in the cytoplasm **(Figure 6)**. Upon exposure to stress, HSP-90 and HSP-70 preferentially bind to unfolded protein, leaving HSF-1 free to form homotrimers in the cytoplasm **(Figure 6)**. Free HSF-1 monomers can also undergo post translational modification [108] aiding in trimerization of HSF-1 to localize into the nucleus, where it binds to Heat Shok Element (HSE) consensus sequence and facilitates the transcription of heat shock proteins (HSPs), also known as molecular chaperones, and other proteins regulating proteostasis **(Figure 6)** [109].

While the transcription of HSP-70 and HSP-90 is regulated by HSF-1, in turn elevated HSP-70 and HSP-90 level suppress the HSF-1 activity forming a negative feedback loop [110]. In parallel to HSP-70 and HSP-90 regulation, DDL-1 containing HSF-1 inhibitory complex (DHIC) also negatively regulates HSF-1. DHIC is composed of DDL-1, DDL-2 and HSB-1. The interaction between DHIC and HSF-1 is disrupted upon DDL-1 phosphorylation **(Figure 6)** [111]. The function of HSB-1 and DDL-2 in DHIC remains elusive [111]. HSF-1 activity is also regulated by post-translational modifications. For example, acetylation of HSF-1 leads to dissociation of HSF-1 from HSE **(Figure 6)** [112, 113].

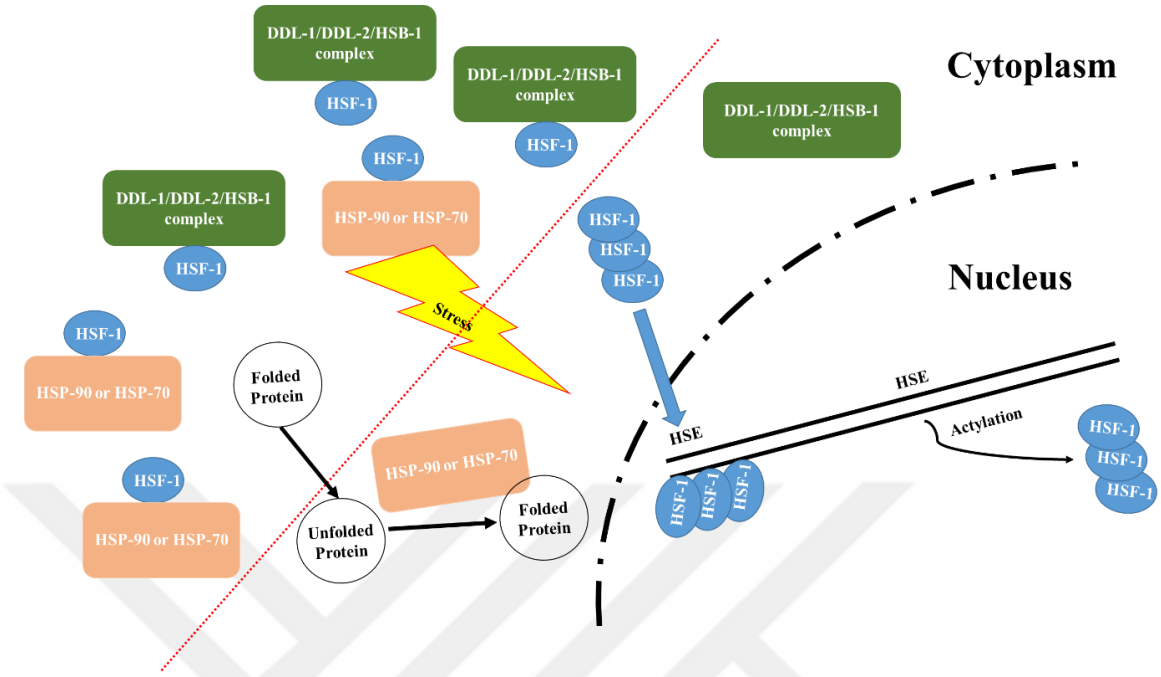

Figure 6. Stress inducible HSF-1 activity is regulated through inhibitory HSP-70/90 and/or DHIC interaction in *C. elegans*.

Insulin signaling pathway (IIS) is the first signaling pathway implicated in aging [86]. In the presence of insulin-like ligands, DAF-2, an insulin and insulin-like growth factor-1 (IGF-1), phosphorylates AGE-1/PI3K that initiates the cascade of kinase activity which results in the phosphorylation (suppression) of DAF-16 and the activation of TOR pathway **(Figure 7)** [114]. DAF-16 and TOR have been proposed to antagonize stress response and aging through DAF-2 receptor [91]. Suppression of insulin/IGF-1 signaling causes dephosphorylation (activation) of DAF-16/FOXO3A transcription factor that allows it to localize into nucleus and activates a set of genes involved in immunity, metabolism, oxidative stress, and PN **(Figure 7)** [86, 91, 115]**.** DAF-18/PTEN is a, phosphatase which activates DAF-16 and suppresses TOR pathway by inhibiting insulin signaling [116].

IIS signaling, central to stress responses, is very sensitive to environmental perturbations. IIS is suppressed upon food scarcity and overcrowding in the population and cause L2

animals to enter into dauer [117-119]. Moreover, long-lived *daf-2* mutant is heat shock resistant whereas loss of function mutations in *daf-16* mutant causes decline in HSR, suggesting that together with HSF-1, DAF-16 is also necessary for the regulation of HSR **(Figure 7)** [91].

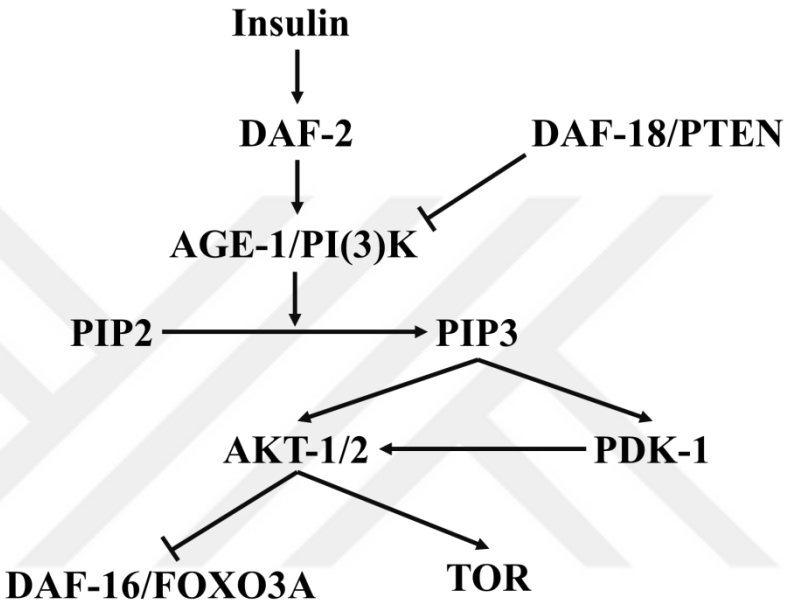

Figure 7. Insulin/IGF-1 signaling pathway antagonistically regulates DAF-16 activity and TOR pathway.

SKN-1/Nrf2 is a ß-zip transcription factor that responds to environmental and endogenous stresses, including pathogens, ROS and xenobiotics [101, 120]. In parallel to IIS [101], SKN-1 is also regulated by MAPK/ERK pathway [121], ER stress [122], mTORC2 [123] and glycogen synthase kinase 3 (GSK3) [124]. However, whether these pathways act independently or together in the regulation of SKN-1 remains to be discovered. Mutations in *skn-1* have been shown to influence life span in *C. elegans* through proteasome dysregulation and TOR activity. [101, 120, 125, 126].

Besides functions in adult animals, SKN-1 also plays essential roles in regulating development and cellular homeostasis [101, 120, 127]. For example, it is essential for the development and differentiation of digestive system in *C. elegans* embryos [128].

1.3.1.2. Molecular Chaperones

Molecular chaperones are group of safe guarding proteins against acute and chronic proteostatic challenges [129]. They are mainly controlled by HSF-1, but also other stress response regulating transcription factors [91, 130, 131]. Historically, molecular chaperones were named as heat shock proteins (HSPs) due to quick up regulation in the presence of heat shock [132].

Upon exposure to stress, the level of HSPs is elevated in order to increase the fitness of the organism. Chaperome consisting of HSPs, co-chaperones and adaptors constitute 219 and more than 300 different members in *C. elegans* and human, respectively [133]. The HSPs are organized according to their molecular size as HSP-100, HSP-90, HSP-70/40, HSP-60/10, and small HSPs (sHSPs) ranging between 10 kDa to 42 kDa [134-136]. These classes of HSPs can operate at different level of PN such as folding, refolding, and disaggregation **(Figure 5)** [109].

Chaperones bind their clients by hydrophobic sequences that are not exposed in native protein conformation [137]. The specificity between chaperones and their substrates are provided by co-chaperones such as HSP-40 and nucleotide exchange factors (NEFs) [138]. Co-chaperones are important for the ATP cycle mediated folding. *C. elegans* possesses only one HSP-90 protein, DAF-21, but it has 13 HSP-70 homologues and 16 sHSPs [25, 35, 58].

On the other hand, HSP-90 is the most abundant protein in humans and human genome comprises of only ten sHSPs [18,41, 42].

HSP-70 must be present and active at the ribosome to maintain faithful folding and ensure fidelity of nascent polypeptides [139]. HSP-70 recognizes a seven amino acid motif that occurs every 50-100 residue in an average protein [140]. Upon failure to fold, HSP-70 transfers the clients to HSP-90 [141]. Repetitive HSP-90 binding and dissociation proceed until client protein is properly folded [140].

HSP-100 family members solubilize the aggregated proteins, which can be refolded by HSP-70/40 machines or sequestered by sHSPs [54]. So far, HSP-100 family members have not been identified in *C .elegans* and it is thought that HSP-70/40 family members may involve in disaggregation of the proteins [57].

The function of sHSPs is to prevent the association of misfolded/unfolded proteins with larger protein aggregates [60-62]. In other words, their main function is to sequester the damaged proteins until other chaperone families refold them [142, 143]. sHSPs do not participate in ATPase activity; therefore, they do not act as foldases, but rather as holdases [63]. sHSPs exist in all domains of life and characteristically they contain two a-crystallin domains in their flanking C terminus and N terminus region. Notably sHSPs in metazoan evolved from a single ancestral gene by repeated duplication [129]. Moreover, chaperones also can assist ubiquitin proteasome system (UPS) and autophagy in the degradation of the misfolded proteins in PN **(Figure 5)** [144, 145].

1.3.1.3. Autophagy

Protein degradation systems, autophagy and proteasome, are of vital importance for the removal of misfolded and aggregated proteins [146]. Autophagy is a lysosome mediated digestive process involved in the degradation of cellular materials including protein aggregates. Autophagy can be mainly classed into three which are microphagy, chaperone mediated autophagy (CMA) [144, 147] and macroautophagy **(Figure 8)**. In microautophagy, lysosome engulfs small areas of cytosol for degradation. In CMA, target proteins are directed to the lysosome by chaperones, so it is considered to be the most specific form of autophagy. However, both types of autophagy are beyond the scope of this study, therefore they will not be discussed further.

Macroautophagy, here after referred as autophagy were first identified in yeast [148] and later on, it has been shown that autophagy genes were conserved in a variety of species, from yeast to human, including *C. elegans* [149-151].

Autophagy plays an important role in the regulation of aging and age-related diseases [152]. Reduced autophagic activity in mice has been associated with protein aggregation related diseases [153-155]. However, the role of autophagy in aging and age-related diseases may have the varying outcomes depending on the context. Interestingly, increased autophagic activity alone is not sufficient to promote life span extension, however, studies have shown a decrease in autophagy and lysosome function with age [156, 157].Moreover, autophagy is required for calorie restriction and *daf-2* mediated longevity [149].

Autophagy is composed of four steps, which are induction, nucleation, elongation and recycling **(Figure8)**. Upon the environmental stresses such as nutrient starvation, TOR

pathway is suppressed leading to the induction of autophagy [158]. Phosphorylated UNC-51 forms a complex with ATG-13 and initiates the formation of a crescent shaped double membrane called phagophore **(Figure 8)**. During nucleation, controlled by BEC-1 and LET-512, phagophore is further extended and autophagosome is generated **(Figure 8)**. After nucleation, autophagosome undergoes a maturation process with the participation of LGG-1 and LGG-2 **(Figure 8)**. During elongation, autophagy substrates are loaded into autophagosome **(Figure 8)**. The activity of LGG-1 and LGG-2 is controlled by ATG-5 and ATG-7 in *C. elegans* **(Figure 8)** [159]. During recycling autophagic vesicles fuse with lysosome and biomaterials are degraded and recycled. Once the autophagic activity takes place ATG-2, ATG-9 and ATG-18 functions in the recycling system **(Figure 8)** [160, 161].

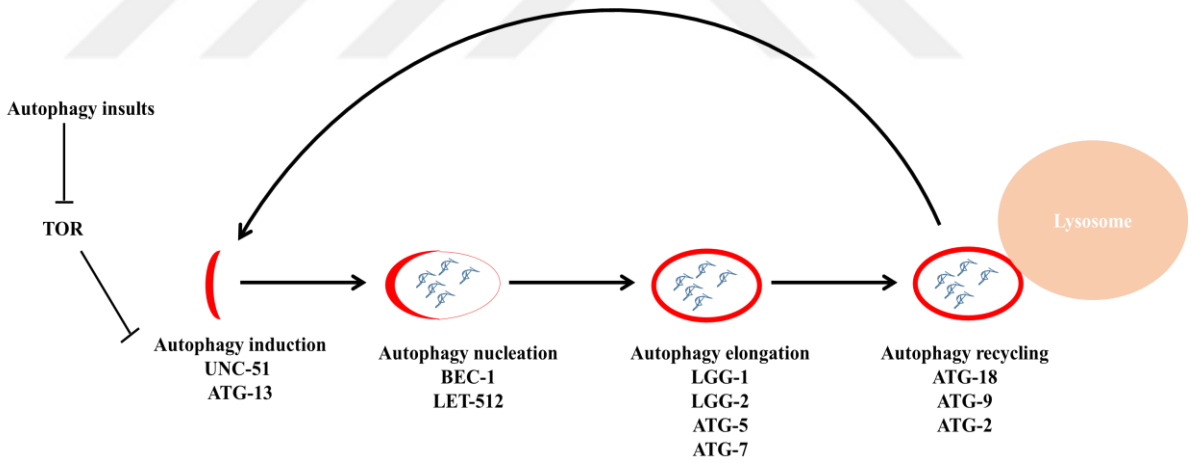

Figure 8. The schematic diagram of the steps of autophagy in *C. elegans*.

1.3.1.4. Proteasome

The ubiquitin proteasome system (UPS) is a primary proteolytic degradation system in all eukaryotes **(Figure 5)** [162]. It has the capability of degrading almost any protein, and yet it acts with exquisite specificity. The ubiquitin system selects proteins and marks them for destruction, whereas the 26S proteasome is the executioner of proteolysis.

Proteasome machinery recognizes its targets through their ubiquitylated lysine (K48) residue [163, 164] . Proteasome is an ATP-dependent 26S,/30S multi-subunit machine consisting of one/two 19S lids and one 20S proteolytic core **(Figure 9)** [165]. 19S lid recognizes ubiquitylated substrates, removes ubiquitin chains, and unfolds the client to allow entry into the proteolytic core, where it is rapidly degraded into peptides [162, 166]. Lid consists of regulatory non-ATPase (*rpn*) and ATPase (*rpt*) gene families. RPN-1, RPN-10 and RPN-13 play the key role in recognizing the ubiquitin chains [167, 168].

The proteolytic core consists of 2ß subunits (*pbs-1* to *7*) rings sandwiched by 2α subunits rings (*pas-1* to *7*) **(Figure 9)**. ß subunits host the proteolytic active sites. Among them ß1, ß2 and ß5 are responsible for the proteasome hydrolyzing activity of acidic (caspase-like activity), basic (trypsin-like activity) and hydrophobic (chymotrypsin-like activity) amino acids respectively [169].

Proteasome machinery is assembled with the following events: (i) biosynthesis of α and ß subunits, (ii) the arrangement of α subunits with the assistance of proteasome assembling chaperones (PACs), (iii) conjugation of a and ß sub-units with UMP1/POMP accessory proteins, (iv) dimerization of half α-ß subunit complex [170].

Many studies on worms, flies and mice have shown that defects in proteasome shorten the life span [171, 172]. In recent studies, overexpression *pbs-5* and *rpn-6.1* has been reported to be sufficient to extend life span of wild type *C. elegans* [173, 174]. This suggests that *pbs-5* and *rpn-6.1* are rate-limiting factors to assemble the 26S proteasome machinery. Consistently, *rpn6.1* has been demonstrated to enhance the attachment of 19S lids assemblies to the 20S proteolytic core [175].

Interestingly, it has been indicated that proteasome activity increases in aged animals which suggests that increased proteasome activity, by itself, might be a futile effort to degrade substrates.

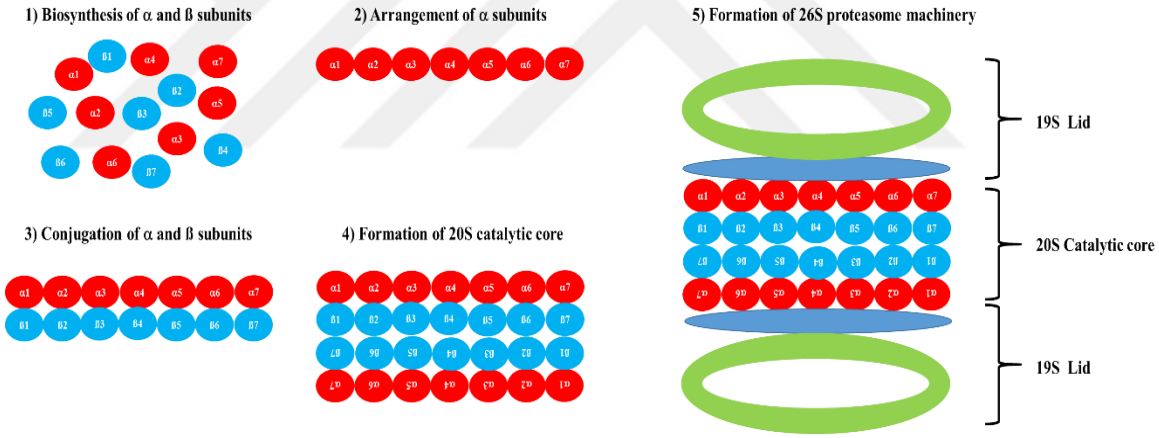

Figure 9. The formation of 26S proteasome complex.

1.3.1.5. Chemical regulators of Proteostasis

A growing number of disorders including neurodegenerative diseases and cancer have been associated with protein conformational diseases; however, not any affective treatment method against these diseases has been developed yet. Therefore, pharmacological strategies offer the great possibility of treating protein aggregations. Chemicals involved in the

enhancement of proteostasis are divided into three main categories (i) chemical chaperones (ii) pharmacological chaperones and (iii) proteostasis regulators [176, 177]

The chemical chaperone refers to the compounds that stabilize the native conformation of proteins. The therapeutic use of chemical chaperones in the treatment of misfolding diseases is limited due to the requirement of high concentration and lack of specificity [178, 179].

Pharmacological chaperones specifically and reversibly target misfolded proteins and induce the conformational stabilization of them. Unlike chemical chaperones, pharmacological chaperones are effective even at low concentrations. Their targets must have a mutation, which renders the protein unstable but not inactive [180].

A new group of chemicals have been identifies as the regulators of proteostasis that alleviates the consequence of protein misfolding by boosting the intracellular proteostasis capacity [181].

In order to chemically modulate the proteostasis in *pash-1ts* animals, I have employed Thioflavin T (ThT), a benzathiazole dye **(Figure 10)**. Recently, ThT has been shown to extend the life span of wild type nematodes at 20°C and reduce the proteotoxicity of metastable proteins by binding to protein aggregations and increasing the proteostasis capacity [182]. These results suggest that ThT can act as both pharmacological chaperone and proteostasis regulator.

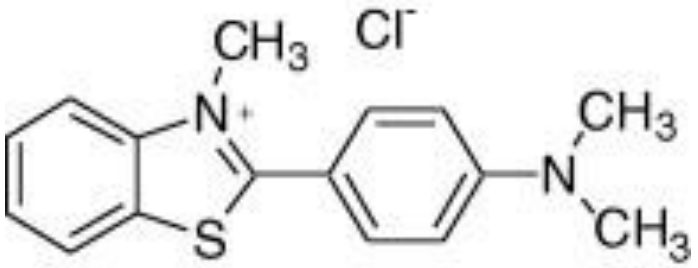

Figure 10. The structure of Thioflavin T (ThT). Image was taken from Khurana et. al. [183].

CHAPTER 2: MATERIALS AND METHODS

2.1. Materials

Unless otherwise stated, all chemicals were purchased from Sigma Aldrich, Fisher Scientific or Merck. All oligonucleotide DNA primers were manufactured by Macrogen. RNA miniprep kit was purchased from Zymo Research and cDNA synthesis kit was ordered from Bioline. A full list of manufacturers and suppliers is given below.

AppliChem	Ottoweg, GERMANY
Bioline	London, UK
Conda	Madrid, SPAIN
Fisher Scientific	Hampton, New Hapshire, USA
Gibco	Carlsbad, CA, USA
Macrogen	Geumcheon-Gu, S. Korea
Merck	Kenilworth, New Jersey, US
Sigma Aldrich	St. Louis, MO, USA.
PAN Biotech	Eidenbach, GERMANY
Zymo Research	Orange, CA, USA.

2.2. Methods

2.2.1. Preparations of the reagent and buffers

B-Broth: 10 g of bacto tryptone and 5 g of NaCl were dissolved in 1 double distilled H_2O. The solution was aliquoted into 100 or 250 ml bottles and autoclaved (121°C for 10 mins in liquid mode). After autoclaving, B-broth was stored at room temperature.

LB medium: 10 g of bacto tryptone, 5 g of yeast extract and 5 g of NaCl were dissolved in 1 L double distilled H_2O. The solution was aliquoted into 100 ml bottles and autoclaved (121°C for 10 mins in liquid mode). LB medium was stored at room temperature.

LB agar: 10 g of bacto tryptone, 5 g of yeast extract, 5 g of NaCl and 15 g of agar were added on 1 L double distilled H_2O. The mixture was then autoclaved (121°C for 10 mins in liquid mode) and cooled to 55°C in a water bath before use.

Super broth: 144 g of bacto tryptone, 288 g of yeast extract, and 48 ml of 100% glycerol were mixed in double distilled H_2O. Then the volume was completed to 10 L with double distilled H_2O. The mixture was aliquoted into 900 ml portions and autoclaved (121°C for 10 mins in liquid mode). Super broth was stored at room temperature.

Potassium orthophosphate: 23.1 g of KH_2PO_4 and 125.4 g of K_2HPO_4 were dissolved in double distilled H_2O. Then the total volume was completed to 1 L with double distilled H_2O. The mixture was autoclaved (121°C for 10 mins in liquid mode) after dispensed into 100 ml bottles.

Nematode growth media (NGM): 3 g of NaCl, 17 g of agar and 2.5 g of bacto peptone were added on 970 ml of double distilled H_2O. The mixture was autoclaved (121°C for 10 mins in liquid mode) and cooled to 55°C in water bath. Filter-sterilized NGM supplements (1 ml of 5mg/ml

cholesterol (in ethanol), 1 ml of 1M MgSO4 and 1 ml of 1M $CaCl_2$) were added. Other supplements such as FUdR, IPTG and antibiotics were added at this step, if necessary.

KH_2PO_4 buffer: 272 g of KH_2PO_4 was dissolved in double distilled H_2O. Then the total volume was completed up to 1L with double distilled H_2O in 2L graduated cylinder. pH was adjusted to 6.0 by gradually adding KOH (potassium hydroxide) pellets. Then the total volume was adjusted to 2L and autoclaved (121°C for 10 mins in liquid mode).

5mg/ml Cholesterol solution: 1 g of cholesterol was dissolved in 100% ethanol. The volume was completed to 200 ml with 100% ethanol and it was filter sterilized in a laminar flow hood. Cholesterol solution was stored at 4°C.

1 M $CaCl_2$ solution: 73.51 g of $CaCl_2.2H_2O$ was dissolved in double distilled H_2O. Then the volume was completed to 500 ml with double distilled H_2O. The mixture was filter sterilized, and aliquoted into 100 ml portions in a laminar flow hood.

1 M $MgSO_4$ solution: 123 g of $MgSO_4.7H_2O$ was dissolved in double distilled H_2O. Then the volume was completed to 500 ml with double distilled H_2O. The mixture was filter sterilized, and aliquoted into 100 ml portions in a laminar flow hood.

M9 medium: 12 g of $Na_2HPO_4.12H_2O$, 6 g of KH_2PO_4 and 6 g of NaCl were dissolved in double distilled H_2O. Then the volume was completed to 2 L with double distilled H_2O and autoclaved (121°C for 10 mins in liquid mode). M9 medium was stored at room temperature. 2 ml of 1 M $MgSO_4$ solution was added near flame before use.

10 M NaOH solution: 40 g of NaOH pellets were dissolved in double distilled H_2O. The volume was completed to 100 ml with double distilled H_2O. NaOH solution was stored at room temperature.

Bleach solution: 3.5 ml of 10 M NaOH, 3.5 ml of 15% sodium hypo chloride (stored at 4°C) and 43 ml of double distilled H_2O were mixed in a 50 ml falcon tube. Bleach solution was kept at room temperature.

2X Freezing buffer: 100 ml of 1M NaCl, 50 ml of 1M KH_2PO_4 and 300 ml of glycerol were mixed and the volume was completed to 1L with double distilled H_2O. The mixture was filter sterilized, and aliquoted into 100 ml portions in a laminar flow hood. 300 µl of 0.1 M $MgSO_4$ was added onto 100 ml in a laminar flow hood before use.

10 mM 5-Fluoro-2'-deoxyuridine (FUdR) solution: 0.1231 g of FUdR was dissolved in double distilled H_2O. The volume was completed to 50 ml with double distilled H_2O. The solution was filter sterilized in a laminar flow hood and stored at 4°C.

4 mM Thioflavin T (ThT) stock: 0.0638 g of ThT was dissolved in double distilled H_2O. Then the volume was completed to 50 ml with double distilled H_2O, and immediately used.

1 M Isopropyl ß-D-1 thiogalactopyranoside (IPTG) solution: 13.8 g of IPTG was dissolved in double distilled H_2O. The volume was completed to 100 ml with double distilled H_2O. The solution was filter sterilized, and aliquoted into 1 ml portions in a laminar flow hood and stored at -20°C.

4 % Paraformaldehyde (PFA) solution preparation: 0.04 g of PFA was dissolved in 1 ml of double distilled H_2O in 55°C water bath (Waited until solution becomes clear). Then the mixture was aliquoted into 20 µl portions and stored at -20°C.

0.125 % ThT for staining: 0.0125 g of ThT was dissolved in 5 ml of 50% ethanol. The solution volume was completed to 10 ml with 50% ethanol. It was stable for one week in 4°C and dark room.

Antibiotics:

Carbenicillin (50 mg/ml): 0.5 g of disodium carbenicillin was dissolved in 9.5 ml of double distilled H2O. The solution was filter sterilized, and aliquoted into 1 ml portions in a laminar flow hood and stored at -20°C.

Ampicillin (100 mg/ml): 1 g of ampicillin was dissolved in 10 ml of double distilled H2O. The solution was filter sterilized, and aliquoted into 1 ml portions in a laminar flow hood and stored at -20°C.

Streptomycin (100 mg/ml): 1 g of streptomycin was dissolved in 10 ml of double distilled H_2O. The solution was filter sterilized, and aliquoted into 1 ml portions in a laminar flow hood and stored at -20°C.

2.2.2. Bacterial glycerol stock preparation

Bacterial glycerol stocks were prepared as follows: 500 µl of the overnight bacterial culture was mixed with 500 µl of 50% glycerol in an Eppendorf tube. The solution was gently mixed with pipetting up and down. Then the mixture was aliquoted into 100 µl portions and stocked at -80°C.

2.2.3. Bacterial Food Source

Glycerol stock of *E.coli* HB101 was streaked LB agar plate containing streptomycin and incubated overnight at 37°C. Next day, single colony was inoculated in B-broth medium with 100 µg/ml streptomycin containing under aseptic conditions. The inoculated culture was grown overnight at 37°C. The liquid culture was seeded onto NGM plates in dropwise manner. The NGM plates were incubated for 2-3 days for the growth of bacterial lawn, then stored at 4°C. The liquid B-broth medium was immediately stored at 4°C.

2.2.3.1. Thick Food Preparation

900 ml of super broth, 100 ml of potassium orthophosphate and 50 ml of freshly opened HB101 bacteria culture in broth were mixed in a 4 L flask near the flame. The mixture was incubated over night at 37°C. Next morning, the culture was centrifuged at 5000g for 15 minutes at 4°C. The resulting supernatant was discarded and the pellet was dissolved in 30 ml of autoclaved freshly opened double distilled H_2O. 300 µl of 100 mg/ml of streptomycin was added on the mixture and it was vigorously vortexed until all pellets were dissolved in double distilled H_2O. 10 ml aliquotes were frozen at -80°C.

2.2.4. Nematode Culture and strains

C. elegans strains were grown and maintained at the temperatures shown on nematode growth medium (NGM) agar [9]. *E. coli* strain HB101 was used as the food source (*Caenorhabditis* Genetics Center, University of Minnesota, Twin Cities, MN, USA). Strains were maintained either by chunking a piece of agar to a new plate in upside down or transferring animals to a new plate using a platinum wire and Nikon SMZ729 microscope. Strains carrying fluorescent markers were verified by using Nikon SMZ18 microscope with GFP and mCherry filters.

The details of the strains used or generated in this study can be found in **Appendix 1**.

2.2.5. Genetic manipulation by setting up crosses with *pash-1ts* mutant

In *C. elegans*, double homozygotes can be easily generated by mating males and hermaphrodites. To generate males of desired strains, wild type male animals were employed. Since *pash-1ts* mutant males, even at 15°C, were sterile, I first crossed wild type male worms with mid-L4 hermaphrodites of the strain to be crossed with *pash-1ts*. The success of the cross was determined by the frequency of males among the progenies, which hypothetically

should be around 50%. Of note all progenies should be heterozygotes. Then the heterozygous males of the strain were crossed with *pash-1ts* at 15°C. Again, the success of the cross was checked by the number of the male progenies. Among the progenies, 6-8 hermaphrodites were picked into separate plates for self-fertilization to generate homozygotes of both *pash-1ts* and the desired mutant or transgenic line. *Pash-1ts* homozygotes were verified by 100% embryonic lethality at 25°C. At least 32 hermaphrodites from F_2 generation were examined at 25°C, to see whether they are 100% embryonically lethal. After *pash-1ts* homozygotes were handled, they were tested for the second mutation or transgenic line. Transgenic lines were identified with genetic markers such as GPF and *rol-6(su1006).*

2.2.6. Generation of extrachromosomal *pash-1 overexpression*

SX1359 strain carrying the extrachromosomal wild type *pash-1* transgene was crossed with wild type males at 25°C to remove *pash-1ts* mutation. 4 Hermaphrodite progenies carrying extrachromosomal *pash-1* transgene from the cross were singled out to new plates and allowed self-crossing. Then 8 hermaphrodites from F2 generation were singled out and allowed giving rise to F3 generation. The plates containing 100% endogenous wild type *pash-1* were isolated and extrachromosomal *pash-1* transgene were verified by the presence of *myo-2p::mCherry* coinjection marker.

2.2.7. Generation of integrated *pash-1 overexpression*

200 L4 hermaphrodites carrying the extrachromosomal wild type *pash-1* copies in *pash-1(mj100)* mutant background in a 100 mm plate were irradiated with 60 Gy for 40 minutes using RX-650 Faxitron X-ray source. The plate was chunked to 5 new plates and incubated at 25°C until starved. A piece of agar was then chunked from the starved plates and allowed to grow for one generation. The plates were screened for 100% transmission rate of transgene.

From candidate plates, next generation was also screened for 100% transmission rate of transgene. Hermaphrodites from these plates were out-crossed 5 times to wild type males to remove background mutations.

2.2.8. Synchronization

Gravid adults grown on 100 mm plates were collected into 15 ml canonical tubes. Samples were centrifuged for 2 minutes at 2000 rpm at room temperature. Supernatant was discarded and pellet was washed by adding 15 ml of M9 buffer. Washing was repeated for two more times with M9 buffer. 6 ml of bleach solution was added onto pellets and tubes were vigorously vortexed at room temperature until adult animals completely dissolved. Then 9 ml of sterile M9 buffer was added onto samples. Tubes were centrifuged for 2 minutes at 2000 rpm at room temperature. After the supernatant was discarded, 15 ml of sterile M9 was added onto tubes and centrifuged for 2 minutes at 2000 rpm at room temperature three more times. After discarding the supernatant, the pellet was suspended with 2 ml sterile M9 buffer and embryos were allowed to hatch rotating at 15°C for 28 hours. Synchronized starved L1 diapause animals were then counted and placed onto directly onto bacterial lawn on the NMG plates to ensure the effective synchronization.

2.2.9. Freezing the strains

Starved worms in 100 mm NGM plates were collected with 2.5 ml of M9 buffer and mixed with 2.5 ml of 2X freezing buffer. 1 ml of solution was individually placed into 5 cryo tubes and frozen at -80°C. Within the next 2 days, the quality of freezing was examined by checking the recovery of population by thawing one of the aliquots.

2.2.10. Thermotolerance assay

2.2.10.1. Thermotolerance assay for *pash-1ts* animals

40 synchronized late L4 animals, grown at 15°C, were picked to 5 different plates. One plates for each day was selected and heat shocked at 35°C for 6 hours. Animals were at 15°C and kept at 25°C on the following days **(Figure 11)**. Day 0 animals were recovered at 15°C for 1 hour whereas samples from other days were recovered at 25°C for 1 hour after heat shock **(Figure 11)**.

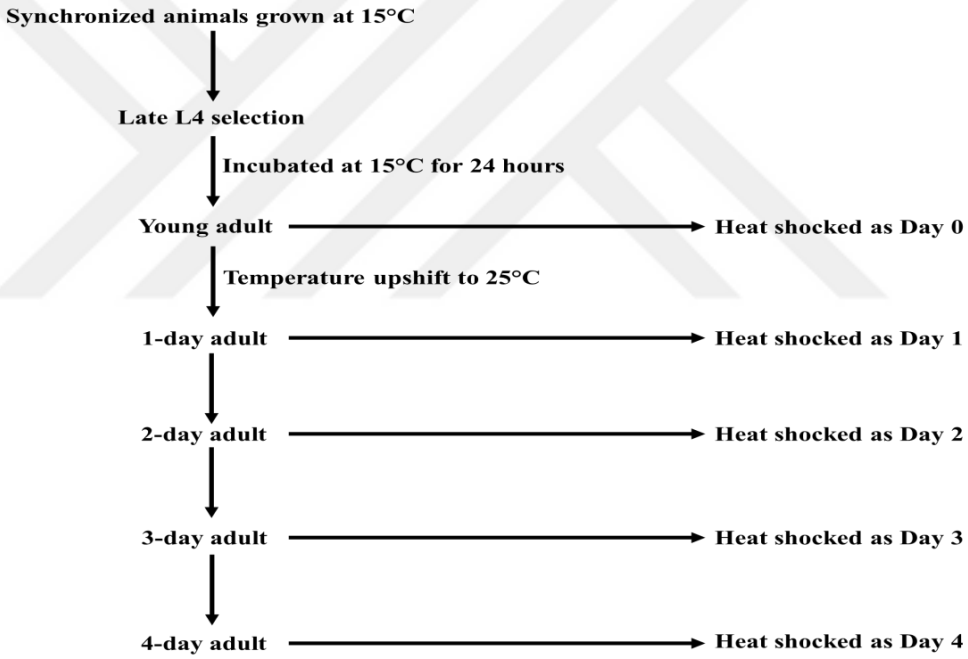

Figure 11. The schematic diagram of the thermotolerance assay of *pash-1ts* animals.

2.2.10.2. Thermotolerance assay for *eft-3::pash-1* transgenic animals

40 synchronized late L4 animals were picked onto 2 different plates. Animals on one of the plates were heat shocked at 37°C for 6 hours. Following the heat shock, animals were allowed to recover at 20°C for 1 hour. Remaining animals on the second plate served as

controls and kept at 20°C. Control and heat shock treated animals were scored for viability and movement by prodding with the platinum pick. Day 0 refers the young adult stage.

2.2.11. Lifespan and motility assay

Lifespan experiments were performed essentially as described in Kenyon et. al. 1993 [86]. Late L4 stage animals were transferred to a new plate and kept at their growing temperature for 24 hours. Young adults were placed onto NGM plates supplemented with 20 μM FUdR (5-fluoro-2'-deoxyuridine, Sigma Aldrich) at experimental temperature (either 20°C or 25°C.). This day refers to day 0 in the analysis and all the experimental manipulations including stopping miRNA biogenesis, RNAi knock-down and ThT supplementation started at this point. Animals were transferred to new plates every 2 days for the first 10 days of the assay. After the 10^{th} day, they were transferred onto new plates if necessary. On each day, 60 to 100 animals per experimental group were scored as dead if they failed to display touch provoked movement or as paralyzed if they twitch in response to prodding. Animals crawled off the plate, showed bagging or gonadal extrusion were censored in the analysis.

2.2.12. RNAi plate preparation

RNAi by feeding was performed using *E. coli* HT115 carrying Ahringer library or Vidal library vectors [24, 184]. Animals fed on empty RNAi vector were used as controls. RNAi was initiated in young adults and carried out at 20°C or 25°C on the RNAi plates supplemented with 20 μM FUdR, 4 mM IPTG and 25 μg/ml carbenicillin. The lifespan and motility of ~60 animals were analyzed. No more than 30 worms were present on each plate. RNAi knock down efficiency was tested by qPCR on day 3 adults as described in 2.2.16.

2.2.13. Preparation of ThT supplemented plates

4 mM filter-sterilized stock ThT solution in distilled water (Sigma Aldrich) was freshly prepared for each experiment. 200 µl ThT was spread over 8 ml NGM agar containing 20 µM FUdR in 60 mm glass plates as soon as agar was solidified. *E. coli HB101* or *HT115* dsRNA expressing bacterial cultures were spotted on the 3rd day of the following ThT supplementation. Plates were kept at room temperature for 3 more days and placed to 4°C to be used in life span experiments.

2.2.14. *C. elegans* total RNA isolation

20 animals were transferred in to a 20 µl M9 buffer containing RNAse free Eppendorf tube. Animals were spun down and frozen at -80°C. 250 µl TRIsure reagent (BIOLINE) was added on to samples and vigorously vortexed at 4°C for 20 minutes. After adding 50 µl chloroform, the tubes were vortexed for 30 seconds and incubated for 3 minutes at room temperature. The mixture was then centrifuged at 12700 rpm for 15 minutes at 4°C and the aqueous phase was transferred to a new tube. The same amount of 100% ethanol was mixed with the aqueous solution and the mixture was transferred into Zymo-Spin IIc column (provided by the RNA miniprep kit). The column was centrifuged for 10 seconds at maximum rpm. The flow through was discarded and 400 µl RNA pre-wash buffer (provided by the RNA miniprep kit) was added to column. Again the mixture was centrifuged for 10 seconds at maximum rpm. The flow through was discarded and 700 µl RNA wash buffer (provided by the RNA miniprep kit) was added and it was centrifuged at maximum rpm for 10 seconds. Lastly, the column was transferred to a new tube and 20 µl RNAse free water was added for elution and centrifuged at maximum rpm for 40 seconds. Isolated RNA concentration was

measured by Nanodrop and immediately used. The RNA concentration usually varies between 40ng-70 ng per µl.

2.2.15. Reverse Transcription

BIOLINE sensiFAST cDNA synthesis kit was used for reverse transcription. 50 ng total RNA was mixed with 4 µl 5X TransAmp buffer and 1 µl reverse transcriptase and reaction mixture volume was completed to 20 µl with RNAse free water. The reaction condition was set to 25°C for 5 minutes, 42°C for 30 minutes and 85°C for 5 minutes in BIORAD T100 thermocycler. The products were stored at 4°C for short-term use.

2.2.16. Real-Time Quantitative PCR

The real-time quantitative PCR was performed using SYBR green PCR reaction mixture (BIOLINE Sensi FAST 2X SYBR Green No-ROX Mix or BioRAD) in BioRAD CFX96 connect real-time PCR detection system. The reaction buffer contained 1 µl cDNA, 0.4 µl 10 µM forward primer, 0.4 µl 10 µM reverse primer, 8.2 µl water and 10 µl 2X SYBR green. The conditions of the qPCR reaction are as follows: 7 minutes at 95°C (1 cycle), 8 seconds at 95°C, 10 seconds at 56°C, and 20 seconds at 72°C (40 cycles), 10 seconds at 95°C (1 cycle) and 70°C-95°C increase point temperature after 2 cycle by 0.5°C.

Fold induction of genes of interest was normalized to the housekeeping genes *cdc-42* [185]. Data were analyzed with the comparative ΔΔCt method [186]. Primers used can be found in the **Appendix 2**.

2.2.17. Western Blot for aggregation quantification

2500 starvation synchronized L1 worms were seeded on 100 mm thick food containing Petri dish. Samples were grown at 15°C until they become young adult and shifted to 25°C. This

day is counted as day 0 and 4-day adults were collected for analysis. 30000 worms on day 0 and day 4 per strain were collected to obtain 100 µl packed worm pellets in an Eppendorf tube. Tubes were immediately frozen at -80°C. To prevent progeny contamination and have the same conditions with life span experiments animals were seeded on 100 mm NGM plates supplemented with 20 µM FUdR after day 0.

2.2.18. Protein aggregation staining with ThT

Worms were mounted on 2 % agarose pad covered with fixation solution (4% PFA). The samples were incubated in PFA solution at 4°C for 24 hours. Next day, samples were washed three times with M9 buffer and exposed to 0.125 % (w/v) ThT solution. After 2 minutes incubating samples in ThT solution, 50% ethanol was dropped three times onto samples for 4 minutes intervals for destaining. Then, samples were transferred to new agarose pad and imaging process was immediately started. Zeiss LSM700 microscope was used for imaging.

2.2.19. Data Analysis

All raw data were saved in Excel files. Graphpad Prism 6 was used to form the figures and perform the statistical analysis. Figures were saved in Power Point. Life span graphs were statistically tested and plotted by Kaplan-Meier analysis and p-values were determined by log rank test. Motility, thermotolerance and quantitative RT-PCR results were statistically tested using 2-way ANOVA. ThT imagings were analyzed in ImageJ and protein aggregations were counted manually. To show the distribution, the data were presented using whisker bar plot.

CHAPTER 3: RESULTS

3.1. 20 μM FUdR does not affect the life span and motility of wild type, *pash-1ts* and *pash-1* rescue animals at 25°C.

One difficulty in nematode life span assays is the large number of offsprings produced during the reproductive period. If the offspring is not carefully eliminated from the plates, they can easily mix with their parents in two days. In addition, some of progenies can hatch within the hermaphrodite and begin to feed upon the tissues of the parent animal, leading to a phenotype named as "bag-of worms". This decreases the number of test animals in the analysis. Bag-of-worms phenotype is observed at a higher rate in sick mutants. To overcome these problems, FUdR, a thymdylate synthase inhibitor, has been frequently used to inhibit the development of the progeny [187]. In early reports, it has been demonstrated that adults have no morphological abnormalities when exposed to 400 μM FUdR [187, 188]. Since then, FUdR has been used in numerous studies, as an effective treatment to obtain synchronous adult *C. elegans* population [68, 182, 189].

On the other hand, it has recently been reported that acute 400 μM FUdR exposure can affect the longevity and stress response in certain genetic backgrounds including *daf-2*, *gas-1* and *glp-1* in *C. elegans* [190-192]. To eliminate such effects, I first optimized minimal FUdR concentration that slowed down reproduction without a significant effect on life span or motility of animals **(Table 3)**. 20 fold lower concentration (20 μM) of FUdR did not affect the survival and motility of the strains that were used in this study **(Table 3)**.

FUdR concentration (μM)	Lifespan effect	Motility effect
0	-	-
20	No effect	slightly suppresses in *pash-1ts* mutant
50	toxic for *pash-1* rescue	-
100	Toxic (data not shown)	Toxic (data not shown)

Table 3. The concentrations of FUdR tested for the effect on life span and motility of wild type, *pash-1ts* and *pash-1* rescue animals.

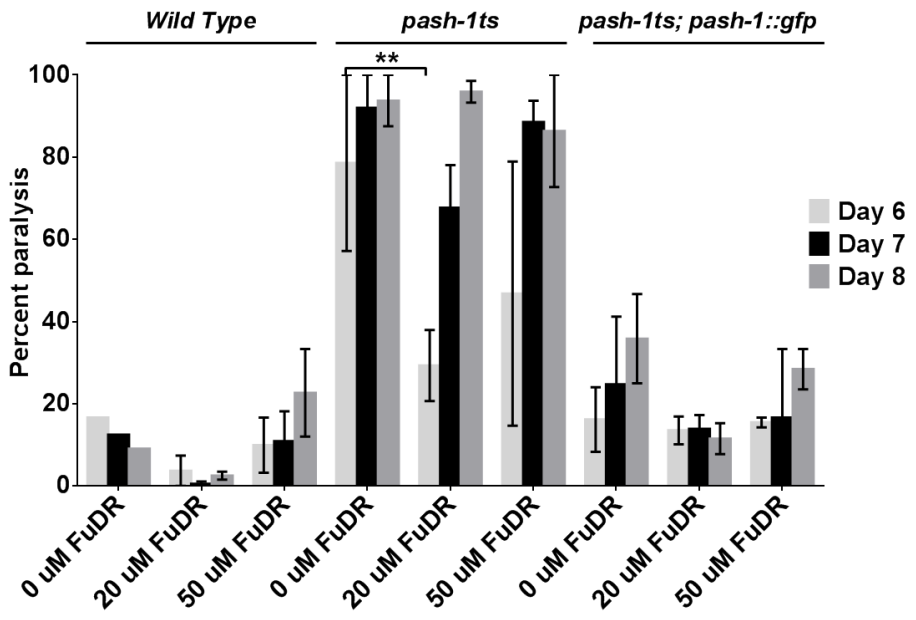

Figure 12. The effect of 20 μM and 50 μM FUdR on the motility of wild type, *pash-1ts* and *pash-1* rescue adults on the days 6 to 8.

In the presence of either 20 or 50 μM FUdR, motility of wild type and *pash-1* rescue animals were not significantly affected **(Figure 12)**. While, 20 μM FUdR ameliorated the motility defects in the absence of miRNAs only on day 6, 50 μM FUdR did not show the same effect **(Figure 12)**. Even though 50 μM FUdR decreased the maximal life of *pash-1 rescue*, the

mean and maximal life span of all three strains did not significantly change in the presence of 20 μM FUdR **(Figure 13)**.

Despite the suppression of motility defects of *pash-1ts* on day 6 by 20 μM FUdR, these animals still showed more than 20% motility defects, which did not impede further analysis of the changes in the locomotion **(Figure 12)**. Moreover, 50 μM FUdR was toxic for the maximal life of *pash-1* rescue animals **(Figure 13)**. Therefore, I decided to use 20 μM FUdR, for the remaining part of the study (unless otherwise stated) to eliminate offspring contamination and decrease the internal hatching and formation of bag of worms in the analysis of life span **(Table 3)**.

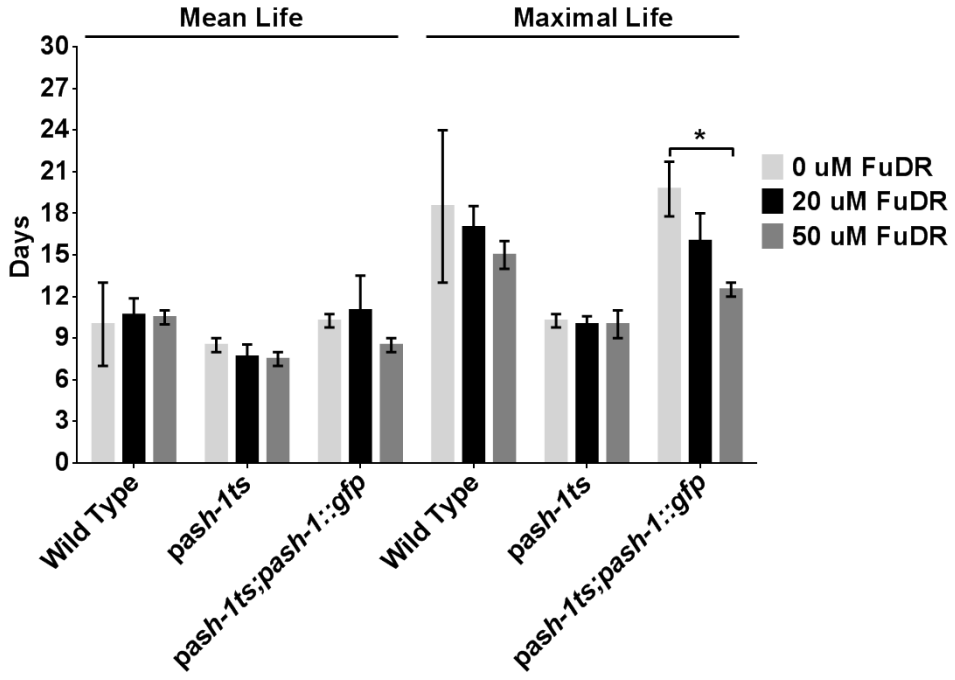

Figure 13.The effect of 20 μM and 50 μM FUdR on the mean and maximal life span of wild type, *pash-1ts* and *pash-1* rescue animals at 25°C.

3.2. miRNA biogenesis pathway genes involved in aging.

3.2.1. miRNA biogenesis ensures healthy aging in adult animals.

Canonical miRNA biogenesis pathway is essential during development; therefore, the studies using knock-outs of individual miRNA biogenesis genes are restricted to developmental stages [36]. In 2012, a temperature sensitive allele of *pash-1*, *mj100*, referred as *pash-1ts*, in *C. elegans* was isolated in a forward genetic screen [8]. Using this allele, it was possible to address the post developmental functions of miRNAs [8]. A study using these mutants showed that *pash-1* is required for normal aging and physiology of *C. elegans* adults [8].

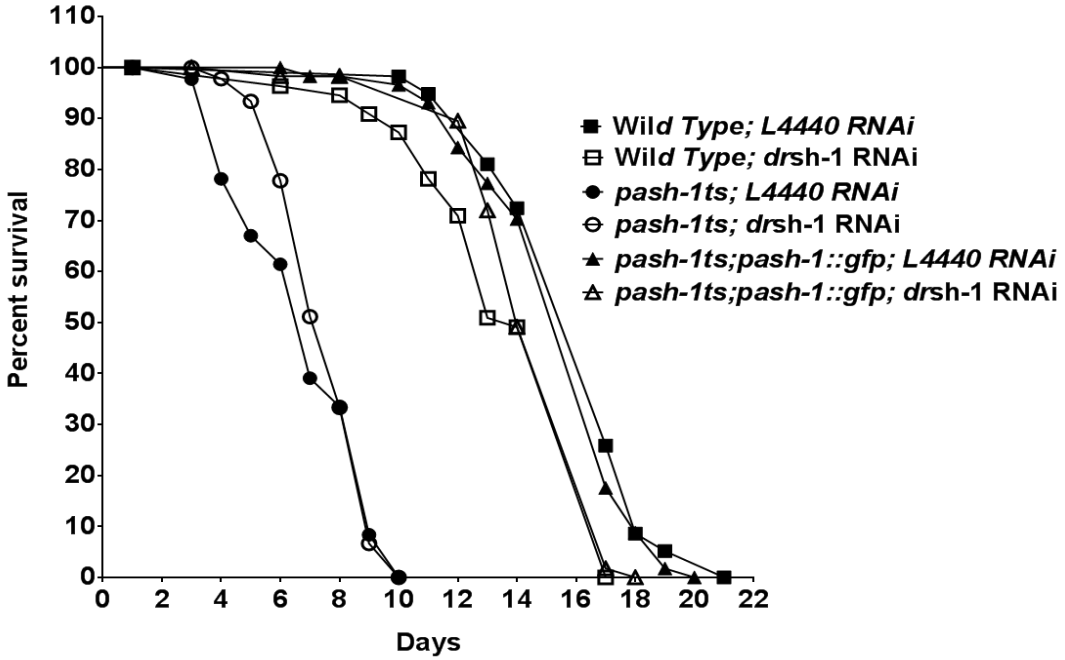

Figure 14. The effect of RNAi knock-down of *drsh-1* on the life span of wild type, *pash-1ts* and *pash-1* rescue animals at 25°C.

To independently validate the importance of miRNAs for normal aging, I employed RNA interference (RNAi) in the adults. For this purpose, I targeted three important miRNA biogenesis genes, *pash-1*, *drsh-1* and *dcr-1* in the wild type, *pash-1ts* and *pash-1* rescue animals. When *drsh-1*, partner of *pash-1*, was knocked down in the wild type or *pash-1* rescue animals at restrictive temperature, it caused to 13 and 20% decrease in the life span respectively (**Figure 14, and Table 4**). However, it did not significantly change the life span of *pash-1ts* animals suggesting function of microprocessor complex is already impaired due to the mutation in *pash-1* gene (**Figure 14, and Table 4**).

Strain	Mean Life ± SEM (Day)	75th Percentile ± SEM (Day)	Maximal Lifespan ± SEM (Day)	% Mean Lifespan change	% 75th Percentile change	% Maximal Lifespan change	p Value (Log Rank Test)
Wild Type	14,33 ± 1,19	16,33 ± 0,72	19,33 ± 0,72	-	-	-	-
Wild Type; drsh-1 RNAi	12,33 ± 0,72	15 ± 0,94	16,67 ± 0,27	-13,96	-8,14	-13,76	< 0.05
pash-1ts	7,33 ± 0,27	8,33 ± 0,54	10 ± 0	-	-	-	-
pash-1ts; drsh-1 RNAi	7 ± 0,47	7,67 ± 0,27	9,33 ± 0,27	-4,50	-7,92	-6,70	n.s.
pash-1ts;pash-1::gfp	14,67 ± 1,19	16 ± 0,47	19,33 ± 0,54	-	-	-	-
pash-1ts;pash-1::gfp; drsh-1 RNAi	11,67 ± 1,19	14 ± 1,41	15,33 ± 1,44	-20,45	-12,50	-20,69	< 0.05

Table 4. The changes in the life span of wild type, *pash-1ts* and *pash-1* rescue animals following RNAi knock-down of *drsh-1*.

Similar to *drsh-1,* RNAi knock down of *dcr-1*, another RNAse III enzyme involved in pre-miRNA processing in the cytoplasm, resulted in 15 and 25% reduction in life span in wild type and *pash-1* rescue animals, respectively **(Figure 15, and Table 5)**. Consistent with the knockdown of dr*sh-1,* lowering the levels of *dcr-1* by RNAi also did not result in the reduction of life span of *pash-1ts* mutant animals **(Figure 15, and Table 5)**.

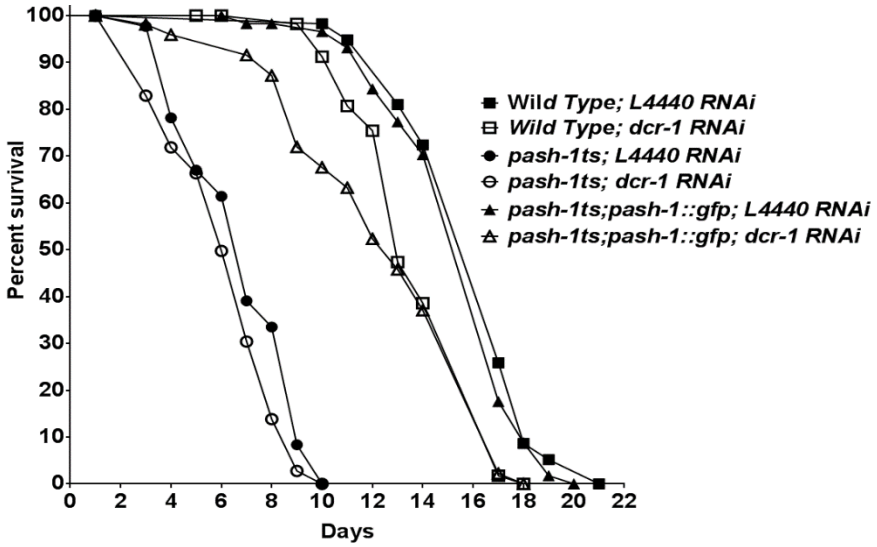

Figure 15. The effect of RNAi knock-down of *dcr-1* on the life span of wild type, *pash-1ts* and *pash-1* rescue animals at 25°C.

Strain	Mean Life ± SEM (Day)	75th Percentile ± SEM (Day)	Maximal Lifespan ± SEM (Day)	% Mean Lifespan change	% 75th Percentile change	% Maximal Lifespan change	p Value (Log Rank Test)
Wild Type	14,5 ± 1,77	17 ± 0,71	20 ± 0,71	-	-	-	-
Wild Type; dcr-1 RNAi	12,5 ± 0,35	14,50 ± 1,77	17 ± 0,71	-13,79	-14,71	-15,00	< 0.0001
pash-1ts	7 ± 0	8,5 ± 0,35	10 ± 0	-	-	-	-
pash-1ts; dcr-1 RNAi	6 ± 0	7,5 ± 0,35	9 ± 0,71	-14,29	-11,76	0,00	n.s.
pash-1ts;pash-1::gfp	14,5 ± 1,77	16,5 ± 0,35	20 ± 0	-	-	-	-
pash-1ts;pash-1::gfp; dcr-1 RNAi	12 ± 0,71	14,5 ± 1,77	15 ± 2,12	-17,24	-12,12	-25,00	< 0.0001

Table 5. The changes in the life span of wild type, *pash-1ts* and *pash-1* rescue animals following RNAi knock-down of *dcr-1*.

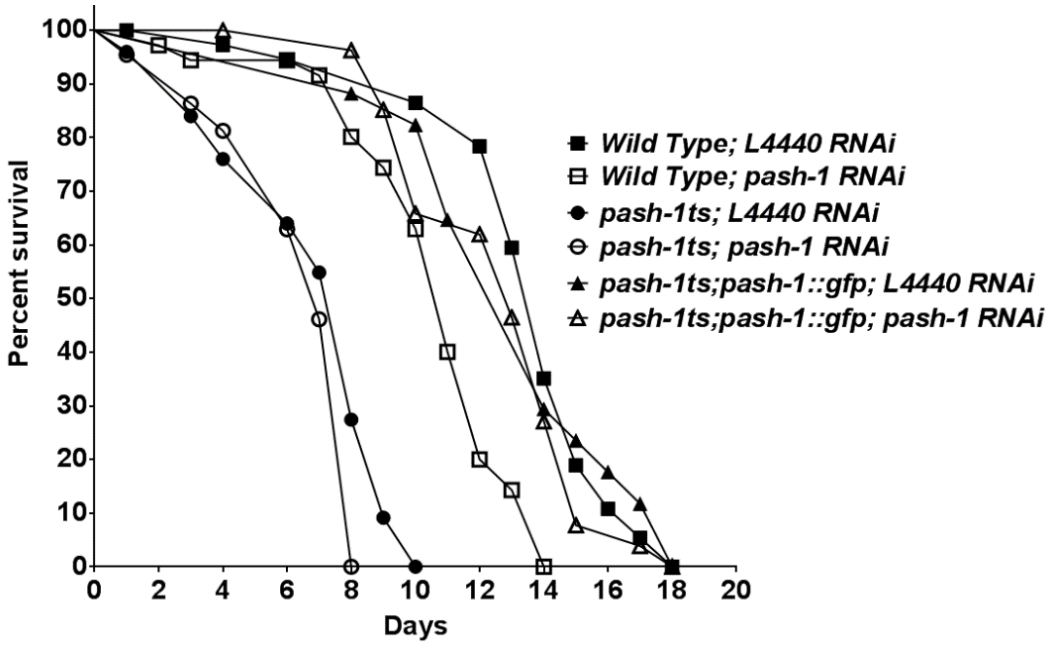

Figure 16. The effect of RNAi knock-down of *pash-1* on the life span of wild type, *pash-1ts* and *pash-1* rescue animals at 25°C.

Strain	Mean Life ± SEM (Day)	75th Percentile ± SEM (Day)	Maximal Lifespan ± SEM (Day)	% Mean Lifespan change	% 75th Percentile change	% Maximal Lifespan change	p Value (Log Rank Test)
Wild Type	14,33 ± 1,19	16,33 ± 0,72	19,33 ± 0,72	-	-	-	-
Wild Type; pash-1 RNAi	11,67 ± 0,98	13,67 ± 1,36	15 ± 1,25	-18,56	-16,29	-22,40	< 0.0001
pash-1ts	7,33 ± 0,27	8,33 ± 0,54	10 ± 0	-	-	-	-
pash-1ts; pash-1 RNAi	6,67 ± 0,27	7,67 ± 0,27	8,67 ± 0,27	-9,00	-7,92	-13,30	n.s.
pash-1ts;pash-1::gfp	14,33 ± 1,19	16 ± 0,47	19,33 ± 0,54	-	-	-	-
pash-1ts;pash-1::gfp; pash-1 RNAi	12,33 ± 0,98	14,33 ± 1,44	17 ± 0,82	-13,96	-10,44	-12,05	n.s.

Table 6. The changes in the life span of wild type, *pash-1ts* and *pash-1* rescue animals following RNAi knock-down of *pash-1*.

Lastly, I have knocked down *pash-1* by RNAi in wild type, *pash-1* rescue and *pash-1ts* mutant adults. Although RNAi knock-down of *pash-1* shortened the life span of wild type animals, it did not change the life span of *pash-1* rescue suggesting *pash-1* RNAi knock down is not sufficient to decrease the abundant *pash-1* level in *pash-1* rescue animals **(Figure 16, and Table 6)**. Moreover, the elimination of *pash-1* by RNAi knock down did not affect the lifespan of *pash-1ts* suggesting *pash-1ts* allele is a complete loss of function mutant **(Figure 16, and Table 6)** [8]. Because RNAi knock down of miRNA biogenesis genes had no additive effect on aging phenotype of *pash-1ts* mutant animals, it is very unlikely that rapid aging phenotype of *pash-1ts* mutant adults was due to a secondary function of PASH-1 **(Figures 14-15)**.

mj100 allele of *pash-1* is a missense mutation which causes to conversion of 515^{th} amino acid residue from cysteine to tyrosine **(please see 1.2.1 for more details)** [8]. Missense mutations can lead to protein misfolding [193, 194]. In this case, it is hard to interpret whether the effect of mutation is due to loss of gene function or a proteostatic challenge. If mutant PASH-1 protein poses a challenge to proteostasis, then lowering the level of mutated protein should reverse the phenotype, at least to some extent, as this would lower the amount of aggregated protein in the mutant animals [195, 196]. However, RNAi knockdown of *pash-1* in *pash-1ts* animals did not extend the life span **(Figure 16, and Table 6)** suggesting that PASH-1 protein does not aggregate in *pash-1ts* mutant animals and rapid aging of these animals results from the loss of miRNA production.

Interestingly, despite rapid aging, we did not observe any motility defect in the adult-specific knockdown of miRNA biogenesis genes as reported in *pash-1ts* mutants **(data not**

shown) [8]. This might be due to the fact that RNAi knockdown is usually not as effective as complete loss of function mutations.

3.2.2. *pash-1* overexpression is sufficient to extend the life span of *C. elegans*

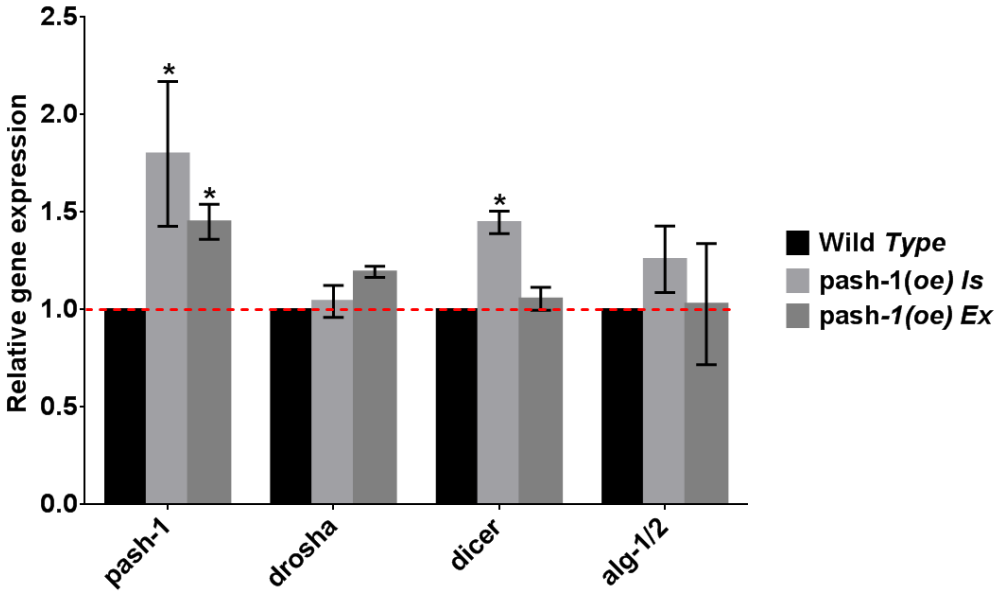

Figure 17. Quantitative RT-PCR results of miRNA biogenesis genes in 4-day adult *pash-1(oe)* transgenic animals relative to wild type animals. Red line represents the level of corresponding gene in the wild type animals. Results show the mean ± SEM of three independent experiments.

Rapid aging could simply result from a decline in the physiology of animals, rather than its active role in aging. Overexpression of a real aging gene often extends the lifespan and suppresses the motility defects. I next investigated how longevity and motility are affected upon ubiquitous overexpression of PASH-1. For this purpose, two independent *eft-3p::pash-1* transgenic lines have been isolated. The first line contains an extra chromosomal array of wild type *pash-1* gene and in the second line the array is integrated into the genome

following gamma radiation. Quantitative RT-PCR results showed that *pash-1* mRNA levels of *pash-1* were increased by 1.9 and 1.4 fold in the first and second lines as compared to wild type, respectively **(Figure 17)**, which was sufficient to extend the life span of *eft-3::pash-1* transgenic animals by 15% **(Figure 18, and Table 7)**. These results showed that *pash-1* is an aging gene and *pash-1ts* mutants can be utilized to address the roles of miRNAs in aging.

I have also quantified the level of other miRNA biogenesis genes by quantitative RT-PCR in *eft-3::pash-1* transgenic animals. The mRNA levels of *drsh-1* and *alg-1/2* did not change upon the ubiquitous overexpression of *pash-1* **(Figure 17)**. Although *dcr-1* transcript level increased significantly in the animals with integrated transgene expressing *pash-1*, this result did not reproduce in the transgenic animals expressing *pash-1* from the extrachromosomal array **(Figure 17)**. Further experiments should be carried out to the specificity of this observation. Since increasing *pash-1* transcript level without affecting other miRNA biogenesis genes is sufficient to extend the life span of animals, PASH-1 might be a rate limiting factor in miRNA biogenesis pathway.

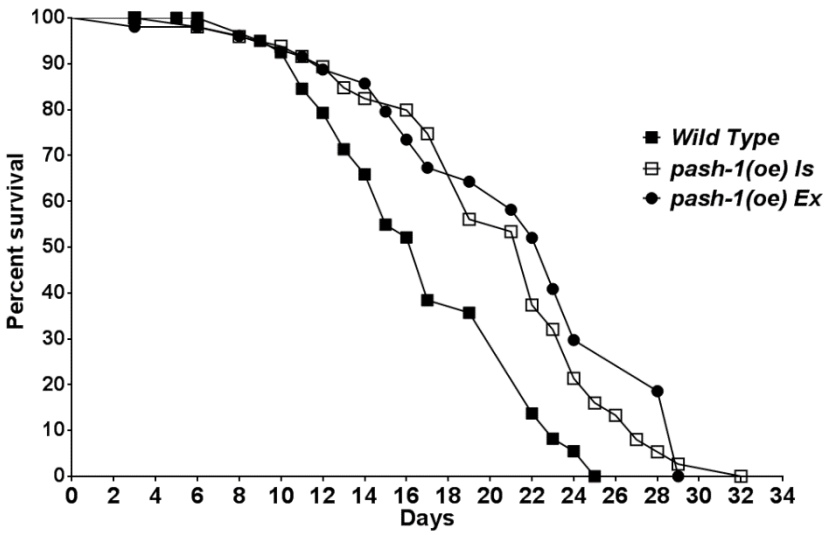

Figure 18. Life span of *pash-1(oe)* transgenic animals at 20°C.

Strain	Mean Life ± SEM (Day)	75th Percentile ± SEM (Day)	Maximal Lifespan ± SEM (Day)	% Mean Lifespan change	% 75th Percentile change	% Maximal Lifespan change	p Value (Log Rank Test)
N2 (Wild Type)	19 ± 0,72	23,67 ± 0,98	28,33 ± 1,44	-	-	-	-
pash-1(oe) Is	21,67 ± 0,98	25,67 ± 1,41	32,33 ± 1,19	14,05	8,45	14,12	p<0.01
pash-1(oe) Ex	21,67 ± 0,27	25 ± 0,27	32 ± 1,25	14,05	5,62	12,95	p<0.001

Table 7. The changes in the life span of *eft-3p::pash-1* transgenic animals at 20°C.

3.3. Heat shock response

3.3.1. Heat shock response declines in adult animals unable to synthesize miRNAs

Disruption of protein homeostasis often leads to shortened life span and abnormal locomotion. Therefore, I asked whether rapid aging and motility defects in *pash-1ts* mutants reflect a defect in proteostasis. To test this, I first examined whether animals that are deficient in miRNA biogenesis would exhibit an increased sensitivity when global protein folding environment has been challenged. For this purpose, we exposed *pash-1ts* animals to heat shock either as young adults, who are still capable of synthesizing miRNAs, or on

different days of adulthood after the miRNA production have been ceased by a temperature up-shift **(please see 2.2.10.1)**. We then examined the impact of heat shock on the survival and the motility of *pash-1ts* animals and compared them to wild type N2, *pash-1* rescue.

Interestingly, when *pash-1ts* mutants were subjected to heat shock for 6 hours, the survival of the animals declined significantly on day 2 and continued to decrease to a survival rate of about 60% until day 4 (**Figure 19**). Likewise, 60 % of the survivors were paralyzed on day 2 (**Figure 20**). However, the survival and the motility of both wild-type and *pash-1* rescue animals were not affected until day 4 (**Figures 19-20**). Neither survival nor the motility of the *pash-1ts* animals able to synthesize miRNAs during the development and in adulthood, demonstrated a significant change (**Figures 21-22)**. These results indicated that the cessation of miRNA biogenesis renders the *pash-1ts* animals susceptible to heat shock.

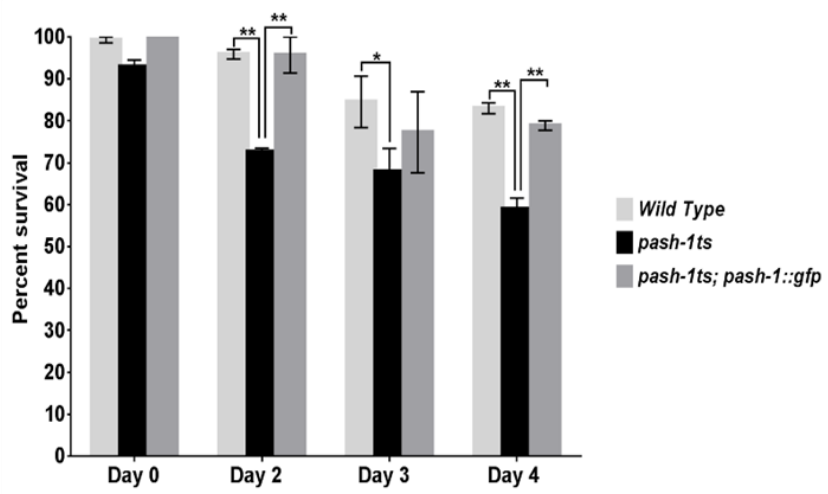

Figure 19. The survival of wild type, *pash-1ts* and *pash-1* rescue adult animals upon the heat shock at 35°C. Animals were at 15^{o}C on day 0 and kept at 25^{o}C on the following days. Data represents mean ± SEM of six independent experiments (*p<0.05 and **p<0.01).

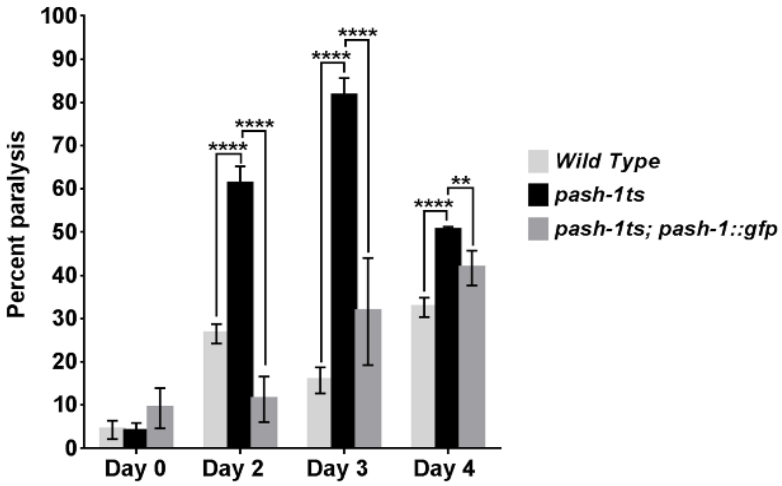

Figure 20. The motility of wild type, *pash-1ts* and *pash-1* rescue adult animals upon the heat shock at 35°C. Animals were at 15°C on day 0 and kept at 25°C on the following days. Data represents mean ± SEM of 6 independent experiments (**p< 0.01, and ****p<0.0001).

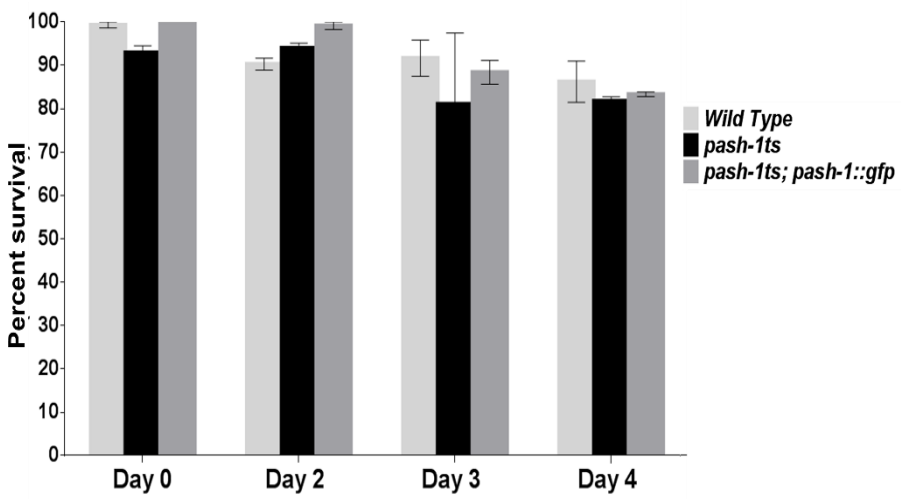

Figure 21. The survival of wild type, *pash-1ts* and *pash-1* rescue animals maintained at 15°C following heat shock at 35°C. Data represents mean ± SEM of 6 independent experiments.

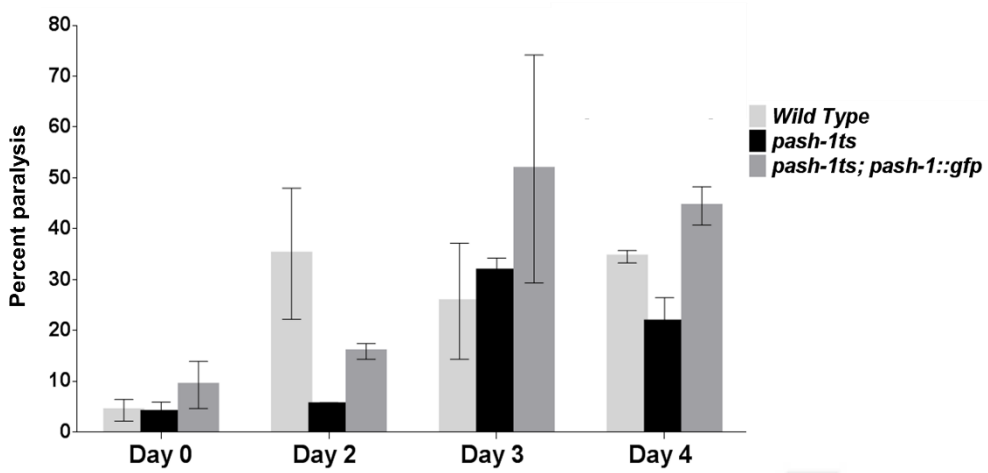

Figure 22. The motility of wild type, *pash-1ts* and *pash-1* rescue animals maintained at 15°C following heat shock at 35°C. Data represents mean ± SEM of 6 independent experiments.

3.3.2. The animals overexpressing p*ash-1* animals are resistant to heat shock.

Having observed that short-lived *pash-1ts* mutants were sensitive to heat shock, I asked whether overexpression of *pash-1* confers animals resistant to heat shock. Since the wild type animals are resistant to heat shock condition applied in section 3.3.1 **(Figures 19-20)**, higher level of heat shock (37°C) was employed for 5 hours to young adult (D0) and 1-day adult animals **(please see 2.2.10.2)**.

Young adult (D0) and 1-day adult animals were examined after exposure to heat shock. While more than 70% of *pash-1(oe)* adults were alive, half of the wild type population died upon heat shock **(Figure 23)**. Moreover, 70% of wild type animals showed motility defects, whereas only 35% of *pash-1* overexpressing animals became paralyzed after exposure to heat shock **(Figure 24)**. These results suggested that increasing the expression of *pash-1* not only extended the lifespan, but also protected the animals against heat shock in *C. elegans*.

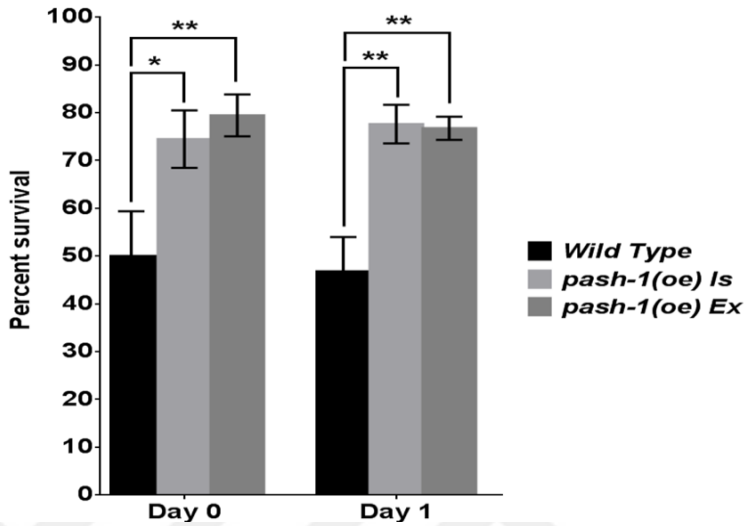

Figure 23. The survival of wild type and two independently isolated *eft-3p::pash-1* transgenic animals following heat shock at 37°C. Data represents mean ± SEM of 5 independent experiments (*p< 0.05, and **P<0.01).

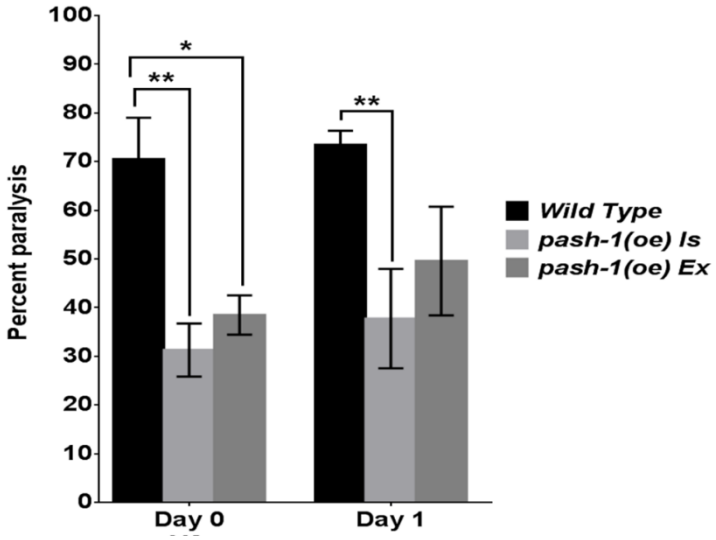

Figure 24. The motility of wild type and two independently isolated *eft-3p::pash-1* transgenic animals following heat shock at 37°C. Data represents mean ± SEM of 5 independent experiments (*p< 0.05, and **P<0.01).

3.4. Disruption of miRNA biogenesis enhances the proteotoxicity in *C. elegans*

It has been well established that expression of aggregation prone or metastable proteins in *C. elegans* challenges the protein-folding environment, which can be utilized to probe the defects in proteostasis. Initially, we utilized heterologous disease model strain, AM141 (*rmIs133 [unc-54p::Q40::YFP]*), expressing 40 amino acid long glutamine (Q) stretch fused to YFP (Q40m) that is known to aggregate in the body wall muscle [92]. Thus, we crossed Q40m transgenic animals and examined the alterations in the lifespan and onset of motility defects of double homozygotes. The expression of Q40m in *pash-1ts* animals shortened the mean lifespan by 31% when compared to *pash-1ts* (**Figure 25, and Table 8**). Remarkably, motility defects were observed at much earlier time-points in double homozygotes than either *pash-1ts* mutants or Q40m transgenic animals (**Figure 26**). Expressing the wild type copy of *pash-1* in the double homozygotes rescued the shortened lifespan and motility defects to a similar level observed in the Q40m transgenic animals (**Figures 25-26; and Table 8**). In addition, the effect of Q expression was length dependent, because the expression of the non-aggregating Q24m in the *pash-1ts* background did not significantly affect the mean life span and the onset of paralysis **(data not shown)**. Therefore, these findings strongly suggested that absence of miRNA production aggravates the cytotoxicity of Q40 expression in body-wall muscle cells.

Even though Q40m expansion mediated protoetoxicity is an effective model to study proteostasis defects in *C. elegans*, it is a non-native toxic specie in nematodes [92]. This led me to test the proteotoxicity of *pash-1ts* by chronic expression of an endogenous metastable *unc-52ts* mutation [197]. At permissive temperature, UNC-52 protein was soluble and *unc-52ts* animals did not display any distinct abnormal phenotype **(data not shown)**. However, at the nonpermissive temperature (25°C), UNC-52 aggregated and disrupted the connection

between hypodermis and body-wall muscle cells, causing uncoordinated phenotype (unc), followed by the complete paralysis of the animals [197].

unc-52ts animals had normal life span at 25°C, and co-expression of *unc-52ts* and *pash-1ts* did not further decrease the lifespan compared to *pash-1ts* mutant animals **(Figure 27, and Table 9)**. Importantly, when the motility was examined, nearly 100% of double homozygote animals were observed to be paralyzed by day 4, whereas either single mutants demonstrated no significant loss of motility (**Figure 28**). Upon restoring miRNA biogenesis in *unc-52ts*, *pash-1ts* mutants, the number of paralyzed animals was reduced by 50% (**Figure 28**).

Taken together, these results suggested that absence of miRNAs enhanced the aggregation propensity of Q40m and UNC-52 mutant proteins. Furthermore, these data showed that the protein folding environment was already impaired in the body wall muscle in *pash-1(ts)* mutants which might underlie the shortened lifespan and motility defects in these animals.

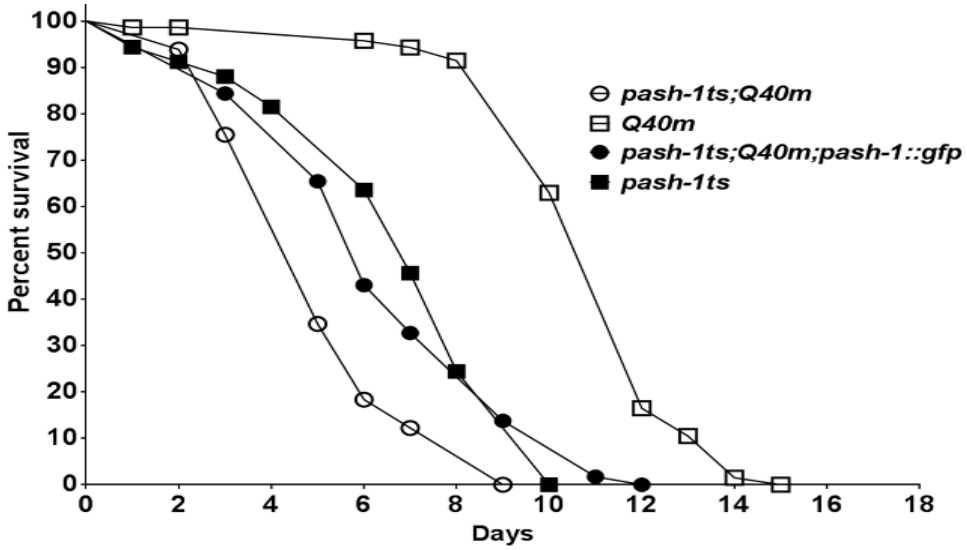

Figure 25. The life span of *pash-1ts,* Q40m, *pash-1ts*;Q40m and *pash-1ts*;Q40m*;pash-1::gfp* animals at 25°C.

Strain	Mean Lifespan ± SEM (Day)	75th Percentile ± SEM (Day)	Maximal Lifespan ± SEM (Day)	% Mean Lifespan change	% 75th Percentile change	% Maximal Lifespan change	p Value (Log Rank Test)
pash-1ts	8 ± 0,71	9 ± 0	10,5 ± 0,35	-	-	-	-
pash-1ts; Q40m	5,5 ± 0,35	7,5 ± 0,35	8,5 ± 0,35	-31,25	-16,67	-19,05	<0,0001
pash-1ts; Q40m; pash-1::gfp	9,5 ± 2,47	11 ± 1,41	13,5 ± 1,06	18,75	22,22	28,57	<0,0001

Table 8. The changes in the life span of *pash-1ts;Q40m* and *pash-1ts;Q40m;pash-1::gfp* animals compared to *pash-1ts* animals at 25°C.

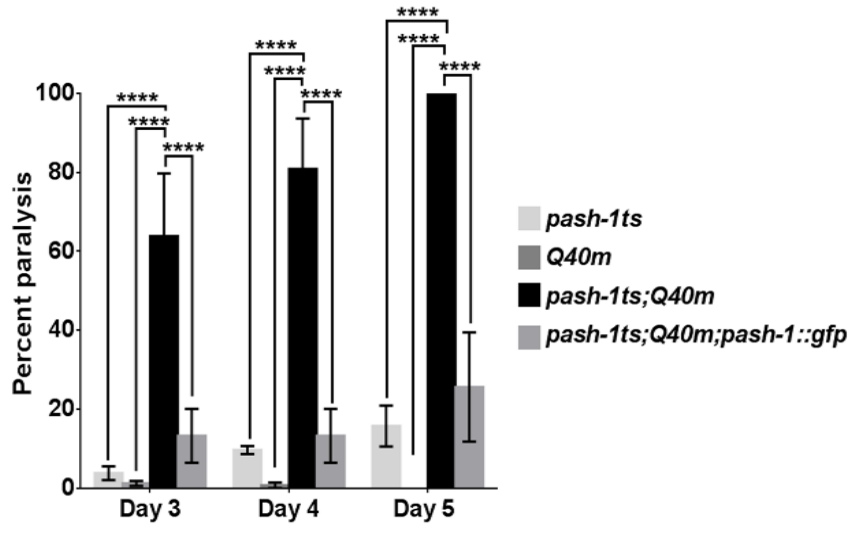

Figure 26. The motility of *pash-1ts*, Q40m, *pash-1ts*;Q40m and *pash-1ts*;Q40m;*pash-1::gfp* animals on days 3 to 5 at 25°C. Results show the mean ± SEM of three independent experiments (****p<0.0001).

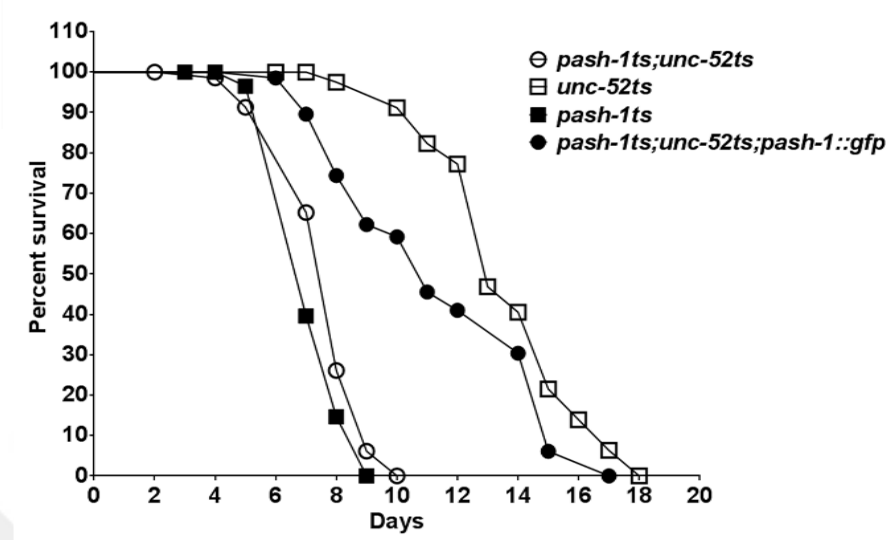

Figure 27. The life span of *pash-1ts*, *unc-52ts*, *pash-1ts;unc-52ts* and *pash-1ts;unc-52ts;pash-1::gfp* animals at 25°C.

Strain	Mean Life ± SEM (Day)	75th Percentile ± SEM (Day)	Maximal Lifespan ± SEM (Day)	% Mean Lifespan change	% 75th Percentile change	% Maximal Lifespan change	p Value (Log Rank Test)
pash-1ts	7,25 ± 0,22	8,25 ± 0,22	9,75 ± 0,41	-	-	-	-
pash-1ts;unc-52ts	7,25 ± 0,41	7,25 ± 0,41	9,5 ± 0,25	0,00	-12,12	-2,56	n.s.
pash-1ts;unc-52ts;pash-1::gfp	10,33 ±0,54	14,67 ±0,27	18 ±0,47	42,48	77,82	84,62	<0,001

Table 9. The changes in the life span of *pash-1ts;unc-52ts* and *pash-1ts;unc-52ts;pash-1::gfp* animals compared to *pash-1ts* animals at 25°C.

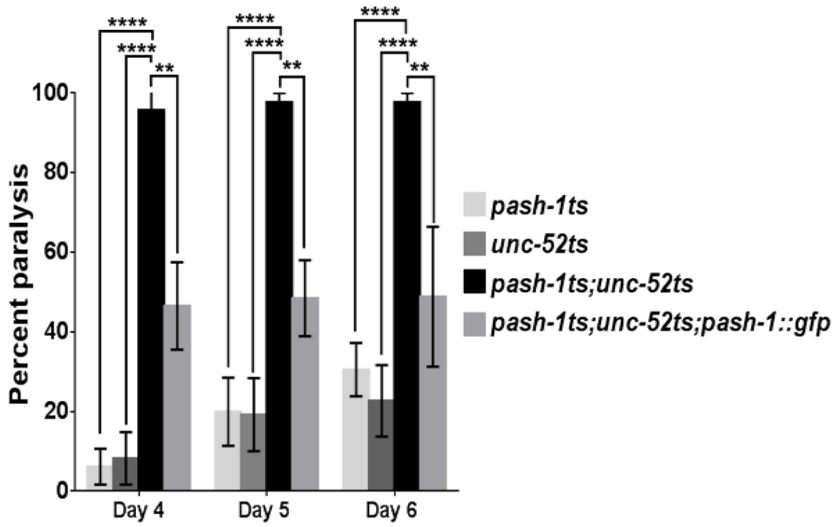

Figure 28. The motility of *pash-1ts, unc-52ts, pash-1ts;unc-52ts* and *pash-1ts;unc-52ts;pash-1::gfp* animals on days 4 to 6 at 25°C. Results show the mean ± SEM of three independent experiments (**p<0.01, and ****p<0.0001).

3.5. Animals lacking miRNA biogenesis have higher levels of protein aggregations.

Thus far, our results indicated a collapse of PN in the *pash-1ts* animals, which prompted us to ask whether *pash-1ts* animals would have higher levels of protein aggregations under normal conditions. Next, we measured the level of protein aggregation every 24 hours for four consecutive days following the temperature up-shift by two independent methods.

First I stained and quantified protein aggregates by using a benzothiazole dye, Thioflavin T (ThT) [198, 199]. Because it emits increased fluorescence upon binding to protein aggregates, ThT has been very instrumental to stain and quantify protein aggregates in cell cultures and in nematodes [200].

Strikingly, ThT staining results indicated that the number of protein aggregation increased 24 hours after stopping miRNA biogenesis **(Figure 29)**. ThT foci were more visible in the

anterior part of the animals, therefore, I only quantified ThT foci formed in the anterior section of the animals **(Figure 30)**. To verify ThT staining results, I have collected 100 µl packed worm pellets for the D0 at 15°C and for the first 4 day of adulthood at 25°C. The samples were sent to Janine Kirstein's group for analysis of protein aggregates **(please see 2.2.17).** Protein aggregates were isolated and quantified by filter trap method. Starting on day 3, *pash-1ts* animals as compared to *pash-1* rescue had more pronounced protein aggregation confirming the findings obtained with ThT staining **(Figure 31)**.

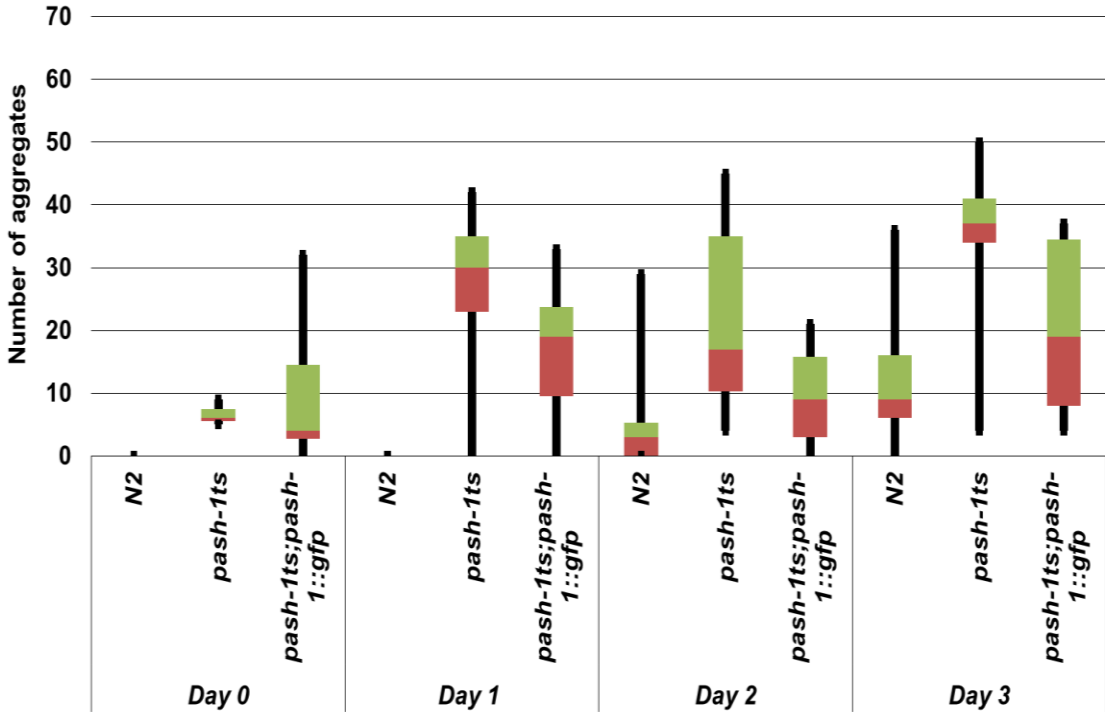

Figure 29. Quantification of protein aggregates in wild type, *pash-1ts* and *pash-1* rescue animals by Thioflavin T (ThT) staining. Animals were at 15°C on D0, and kept at 25°C on the following days.

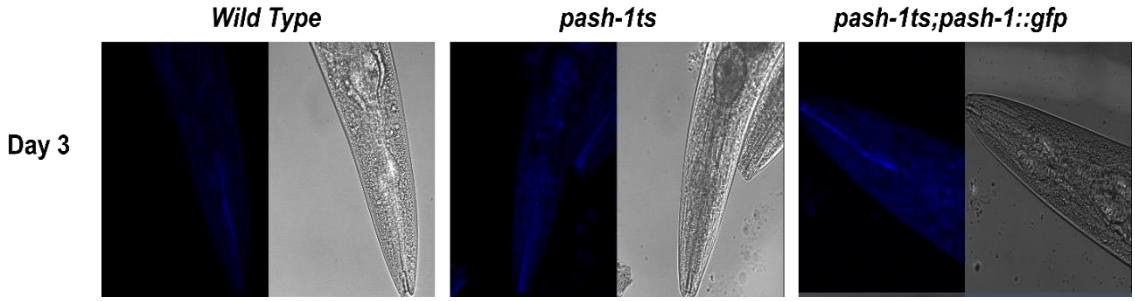

Figure 30. Representative Thioflavin T (ThT) staining images of wild type, *pash-1ts* and *pash-1* rescue animals on day 3.

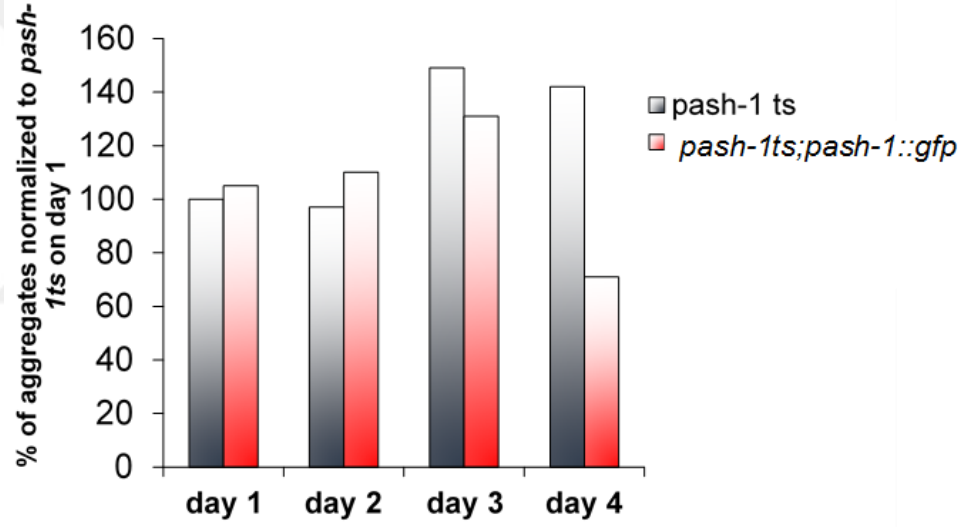

Figure 31. Biochemical isolation of protein aggregates by filter trap technique. Data was generated by Janine Kirstein.

3.6. Increasing proteostasis capacity of miRNA biogenesis deficient animals by ThT, can extend life span and suppress the motility in *C. elegans.*

3.6.1. ThT treatment ameliorates aging related defects in *pash-1ts* animals

Recently, ThT has been shown to protect the worms against the toxic effects of protein aggregation by enhancing the proteostasis in *C. elegans*. Not only the maximal life of wild type worms maintained on ThT containing plates was increased by 60%, but also the age-associated

decline in motility was suppressed in the presence of ThT [182]. It is conceivable that the rapid aging of *pash-1ts* animals and their sensitivity to proteotoxic stress may reflect a defect in proteostasis, hence, we examined how the life span and motility of *pash-1ts* animals were affected upon enhancement of proteostasis by ThT treatment. To address this hypothesis, we placed the *pash-1ts* animals into ThT containing plates on day 1 of the adulthood and shifted the temperature to 25°C to stop the miRNA biogenesis. Notably, ThT treatment increased the maximal life span of *pash-1ts* mutants by 40% at 25°C (**Figure 32, and Table 10**). Moreover, ThT remarkably diminished the motility defects of *pash-1ts* adults up to 40% from day 6 to day 8 (**Figure 33)**. The level of reduction of the paralyzed animals by ThT was indeed comparable to the reduction exerted by the expression of wild type *pash-1* transgene in *pash-1ts* animals (**Figure 33**).

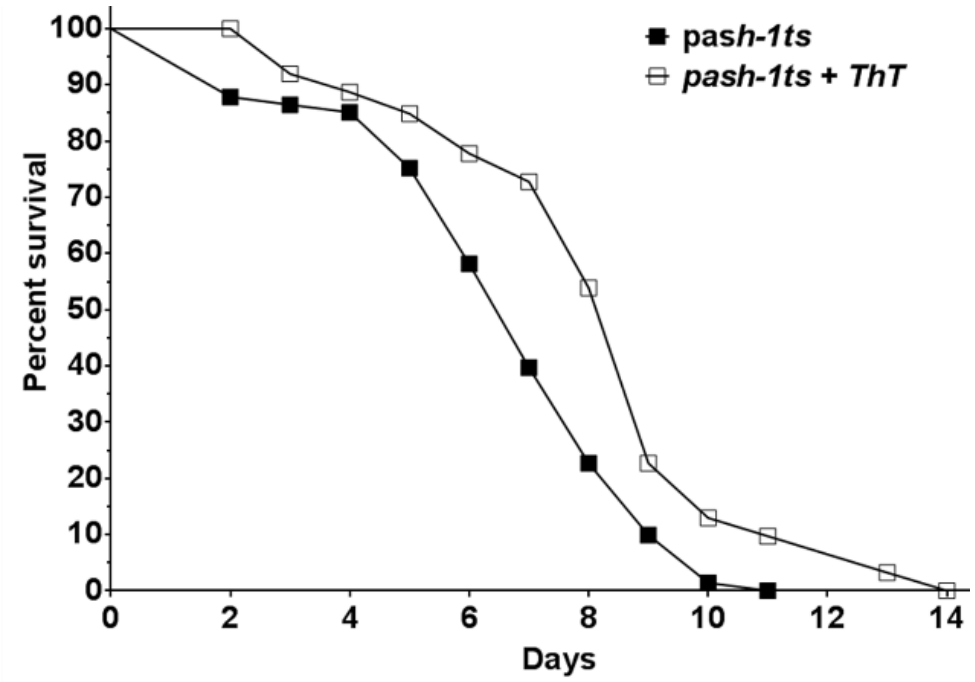

Figure 32. The life span of *pash-1ts* animals supplemented with 100 μM Thioflavin T (ThT) at 25°C.

Strain	Mean Lifespan ± SEM (Day)	75th Percentile ± SEM (Day)	Maximal Lifespan ± SEM (Day)	% Mean Lifespan change	% 75th Percentile change	% Maximal Lifespan change	p Value (Log Rank Test)
Wild Type	15,67 ±1,91	16,33 ±1,78	21,67 ±0,27	-	-	-	-
Wild Type + ThT	13 ± 0,82	16,67 ± 1,09	20,33 ± 0,27	-17,04	2,08	-6,18	<0,05
pash-1ts	7 ± 0	8 ± 0	9 ± 0	-	-	-	-
pash-1ts + ThT	9 ± 0	10 ± 0	12,67 ± 0,27	28,57	25,00	40,78	<0,001
pash-1ts;pash-1::gfp	14 ± 0	15,67 ± 0,27	20,33 ± 0,54	-	-	-	-
pash-1ts;pash-1::gfp + ThT	11 ± 0,94	12 ± 0,47	17,67 ± 0,98	-21,43	-23,42	-13,08	<0,0001

Table 10. The changes in the life span of wild type, *pash-1ts*, and *pash-1* rescue animals supplemented with 100 μM ThT at 25°C.

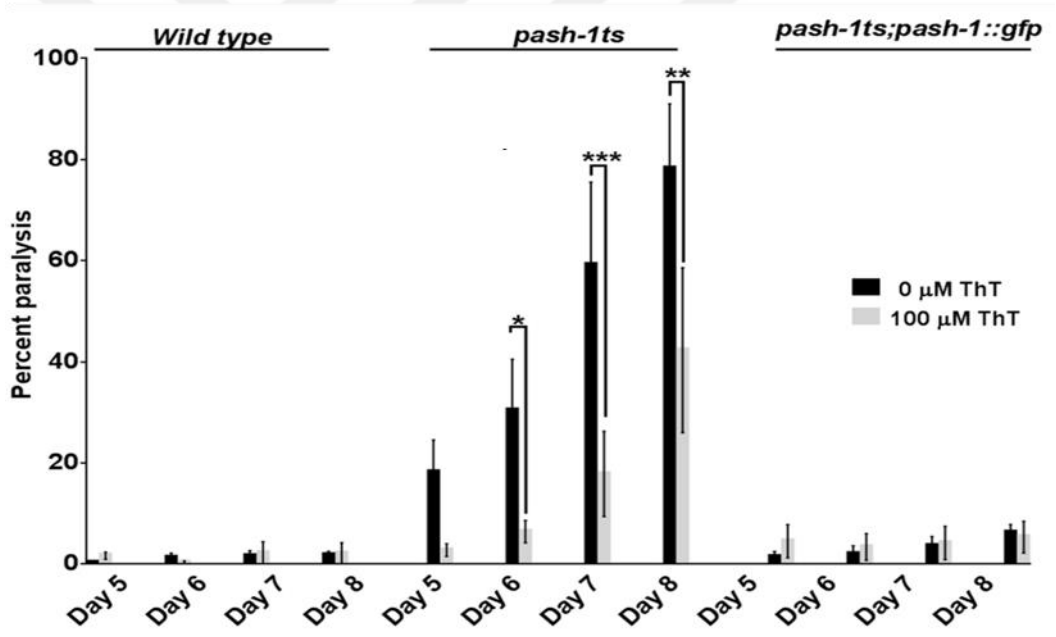

Figure 33. The motility of wild type, *pash-1ts* and *pash-1ts;pash-1::gfp* animals supplemented with 100 μM Thioflavin T (ThT) on days 5 to 8 at 25°C. Results show the mean ± SEM of three independent experiments (*p<0.05, **p<0.01, and ***p<0.001).

3.6.2. The positive effect of ThT on wild type animals depends on the temperature

Interestingly, ThT treatment had a mild toxicity to wild type and *pash-1* rescue animals at 25°C which raised a question as to temperature that might confer to its toxicity (**Figures 34-35, and Table 10**). To address this, I analyzed the effect of ThT at 20°C. I observed an increase in the median lifespan of wild type animals as reported previously, however, to a lesser degree [182]. At 20°C, *pash-1ts* animals have near normal levels of miRNAs; therefore, in order to reduce the miRNA levels, I have knocked down *pash-1* by RNAi in the wild type animals and determined 15% reduction in the maximal lifespan (**Figure 36; Table 10**). In the presence of ThT, downregulating *pash-1* levels by RNAi did not significantly change the lifespan of wild type animals, suggesting that at both 20°C and 25°C, absence of miRNAs leads to a proteostasis defect, and the resulting phenotypes could be suppressed by the ThT treatment (**Figures 32, and 36, and Tables 9-10**). Of note, *pash-1* level was reduced to 50% of control RNAi in the ThT containing or control plates (**Figure 37**).

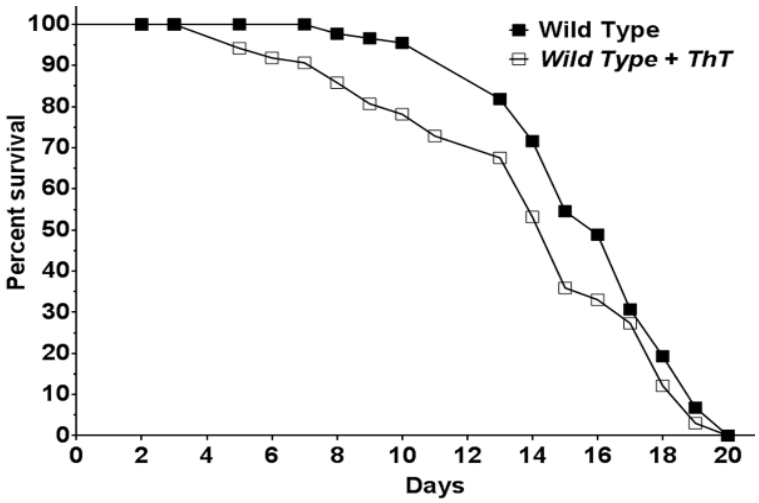

Figure 34. The life span of wild type animals supplemented with 100 μM Thioflavin T (ThT) at 25℃.

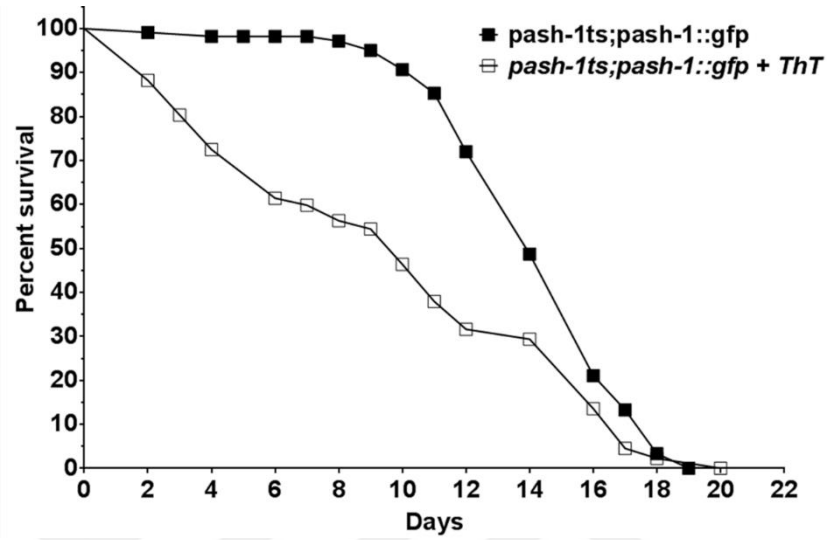

Figure 35. Life span of p*ash-1* rescue animals supplemented with 100 μM Thioflavin T (ThT) at 25°C.

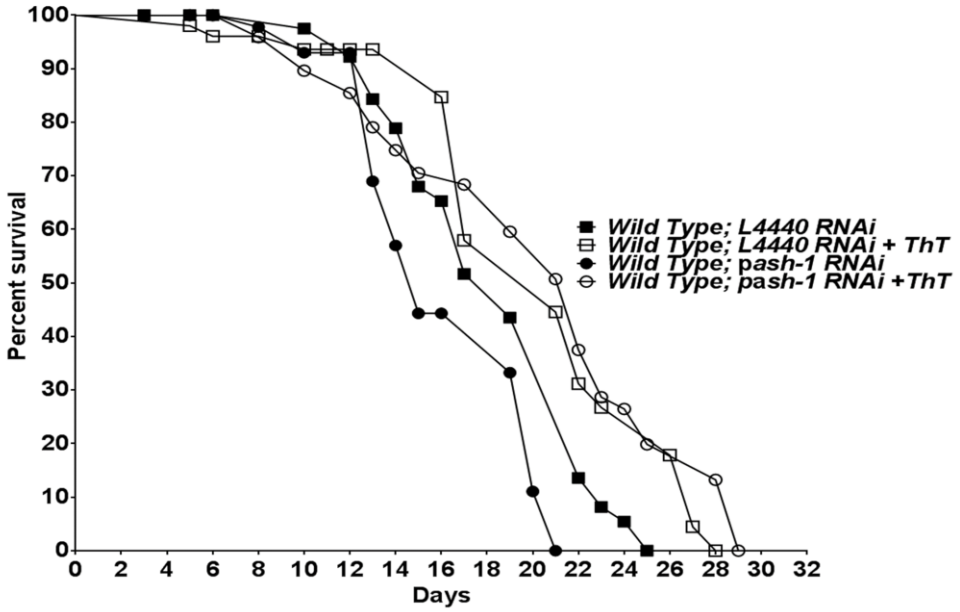

Figure 36. The effect of RNAi knock-down of *pash-1* on the life span of wild type animals supplemented with 100 μM Thioflavin T (ThT) at 20°C.

Strain	Mean Life ± SEM (Day)	75th Percentile ± SEM (Day)	Maximal Lifespan ± SEM (Day)	% Mean Lifespan change	% 75th Percentile change	% Maximal Lifespan change	p Value (Log Rank Test)
Wild Type; L4440 RNAi	19,33 ± 0,72	23,33 ± 0,98	28,33 ± 1,44	-	-	-	-
Wild Type; L4440 RNAi + ThT	22 ± 0,82	26,33 ± 0,27	32 ± 1,25	13,81	12,86	12,95	<0,0001
Wild Type;pash-1 RNAi	18 ± 1,41	21,33 ± 0,54	24 ± 1,25	-	-	-	-
Wild Type; pash-1 RNAi + ThT	20,33 ± 1,36	24,33 ± 0,54	30,67 ± 0,98	12,94	14,06	27,79	<0,0001

Table 11. The changes in the life span of wild type animals following RNAi knock-down of *pash-1* supplemented with 100 μM Thioflavin T (ThT) at 20°C.

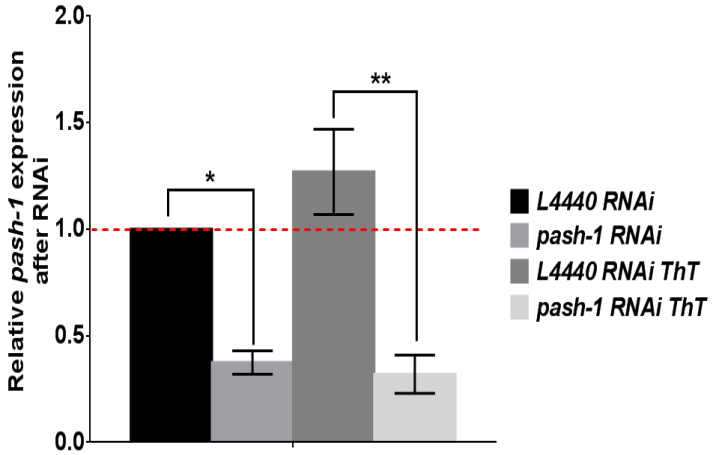

Figure 37. RNAi knock-down efficiency of *pash-1* in wild type animals supplemented with 100 μM Thioflavin T (ThT) determined by quantitative RT-PCR on day 3 at 20°C. Results show the mean ± SEM of three independent experiments (*p<0.05, and **p<0.01).

3.6.3. ThT requires HSF-1 and SKN-1, but not DAF-16 at restrictive temperature for its positive effect on *pash-1ts* adults.

If the influence of ThT on lifespan and motility of *pash-1ts* animals was due to its effect on proteostasis then, ThT treatment would depend on *hsf-1* and *skn-1* and be independent of *daf-16* [182]. To investigate this, we RNAi-knocked down *hsf-1, skn-1* and *daf-16* in *pash-1ts, pash-1* rescue and wild type animals. As expected, ThT did not increase the survival or suppress the motility defects of *pash-1ts* animals upon *hsf-1* or *skn-1* RNAi (Figures 38-41, and Tables 12-13). However, ThT was able to increase the maximal lifespan and suppress the motility defects by 29% and 20%, respectively following RNAi knockdown of *daf-16* (Figures 42-43; Table 14). The efficiency of the RNAi knockdown of *hsf-1, skn-1* and *daf-16* was determined by qPCR after animals were fed with bacteria expressing dsRNA for 3 days (Figure 44). The mRNA levels of *hsf-1, skn-1* and *daf-16* were decreased more than 50% in wild type and in *pash-1ts* animals (Figure 44). Despite the seemingly negligible decrease of *hsf-1, skn-1* and *daf-16* in *pash-1* rescue, the level of reduction in the survival of *pash-1* rescue was comparable to wild type animals (Figures 44-51; Tables 15-20). These data showed that the beneficial effect of ThT on *pash-1ts* animals is indispensable of *skn-1* and *hsf-1* and it is independent of *daf-16*. These findings suggested that ThT exerted its effect through enhancement of proteostasis, rather than on other, yet uncharacterized processes. Interestingly, the toxic effect of ThT on wild type and *pash-1* rescue animals was augmented by *hsf-1* and *skn-1* RNAi, providing further evidence on differential behavior of ThT at 25°C (Figures 45-51; Tables 15-20).

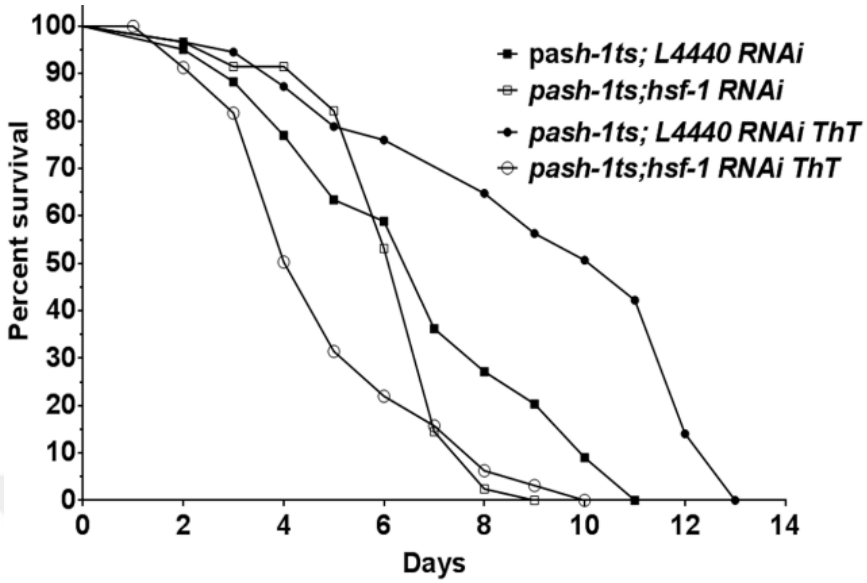

Figure 38. The effect of RNAi knock-down of *hsf-1* on the life span of *pash-1ts* animals supplemented with 100 μM Thioflavin T (ThT) at 25°C.

Strain	Mean Life ± SEM (Day)	75th Percentile ± SEM (Day)	Maximal Lifespan ± SEM (Day)	% Mean Lifespan change	% 75th Percentile change	% Maximal Lifespan change	p Value (Log Rank Test)
pash-1ts; L4440 RNAi	7,75 ± 0,22	9 ± 0	10,75± 0,22	-	-	-	-
pash-1ts; hsf-1 RNAi	7,25 ± 0,22	8,33 ± 0,47	10 ± 0,35	-6,45	-7,44	-6,98	n.s.
pash-1ts; L4440 RNAi + ThT	8 ± 0,79	9,67 ± 0,85	13,25 ± 0,22	3,23	7,44	23,26	<0.0001
pash-1ts; hsf-1 RNAi + ThT	5,75 ± 0,54	7 ± 0,41	9,25 ± 0,41	-25,81	-22,22	-13,95	<0.01

Table 12. The changes in the life span of *pash-1ts* animals supplemented with 100 μM Thioflavin T (ThT) following RNAi knockdown of *hsf-1* at 25°C.

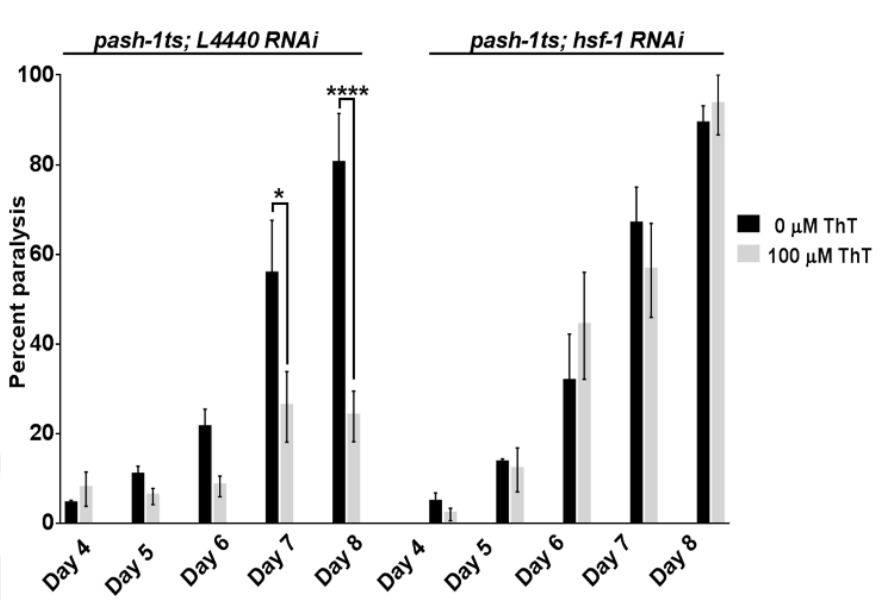

Figure 39. The effect of RNAi knock-down of *hsf-1* on the motility of *pash-1ts* animals supplemented with 100 μM Thioflavin T (ThT) on days 4 to 8 at 25°C. Results show the mean ± SEM of three independent experiments (*p<0.05, **p<0.01).

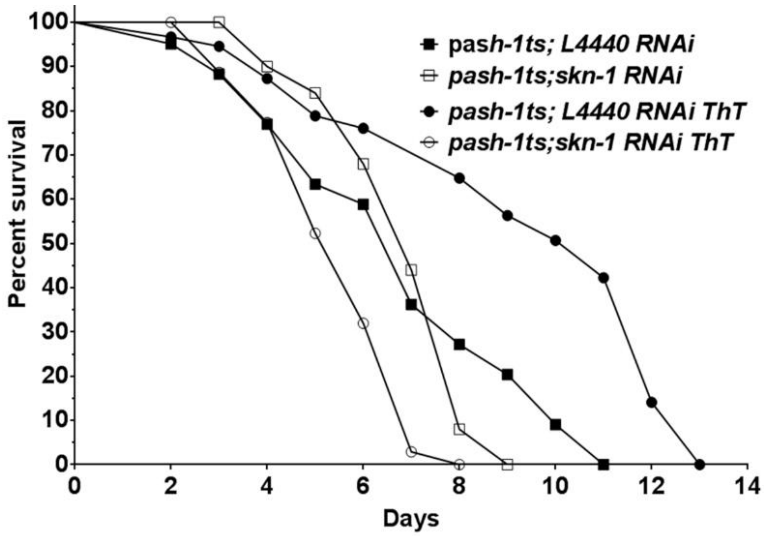

Figure 40. The effect of RNAi knock-down of *skn-1* on the life span of *pash-1ts* animals supplemented with 100 μM Thioflavin T (ThT) at 25°C.

Strain	Mean Life ± SEM (Day)	75th Percentile ± SEM (Day)	Maximal Lifespan ± SEM (Day)	% Mean Lifespan change	% 75th Percentile change	% Maximal Lifespan change	p Value (Log Rank Test)
pash-1ts; L4440 RNAi	7,67 ± 0,27	9 ± 0	10,67± 0,27	-	-	-	-
pash-1ts;skn-1 RNAi	7,67 ± 0,27	9 ± 0,47	10 ± 0,47	0,00	0,00	-6,28	n.s.
pash-1ts; L4440 RNAi + ThT	7,67 ± 0,98	9,67 ± 0,98	13 ± 0	0,00	7,44	21,84	<0.0001
pash-1ts; skn-1 RNAi + ThT	6,33 ± 0,54	7,67 ± 0,27	10 ± 0,82	-17,47	-14,78	-6,28	<0.01

Table 13. The changes in the life span of *pash-1ts* animals supplemented with 100 μM Thioflavin T (ThT) following RNAi knock-down of *skn-1* at 25°C.

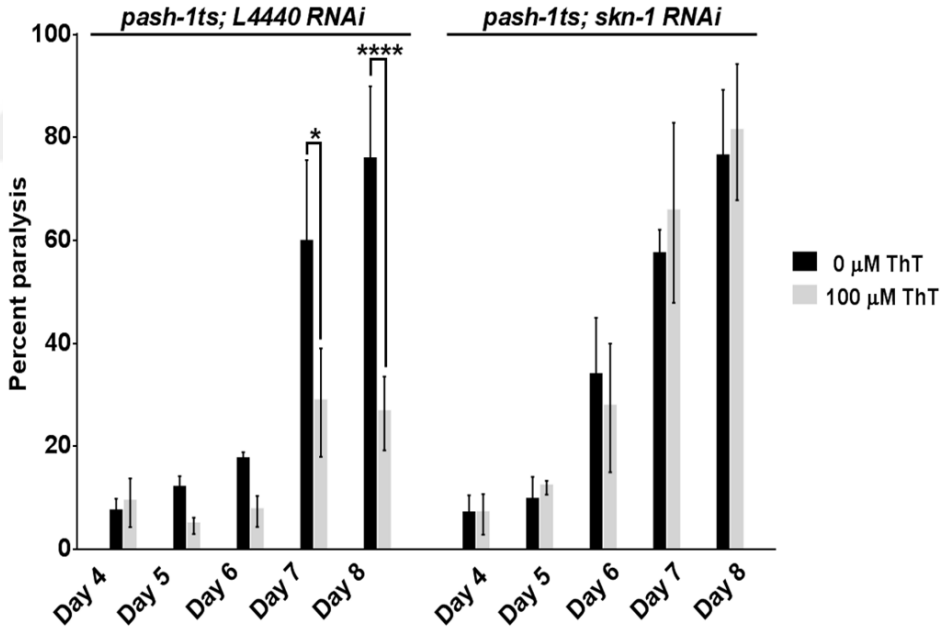

Figure 41. The effect of RNAi knock-down of *skn-1* on the motility of *pash-1ts* animals supplemented with 100 μM Thioflavin T (ThT) on days 4 to 8 at 25°C. Results show the mean ± SEM of three independent experiments (*p<0.05, ****p<0.0001).

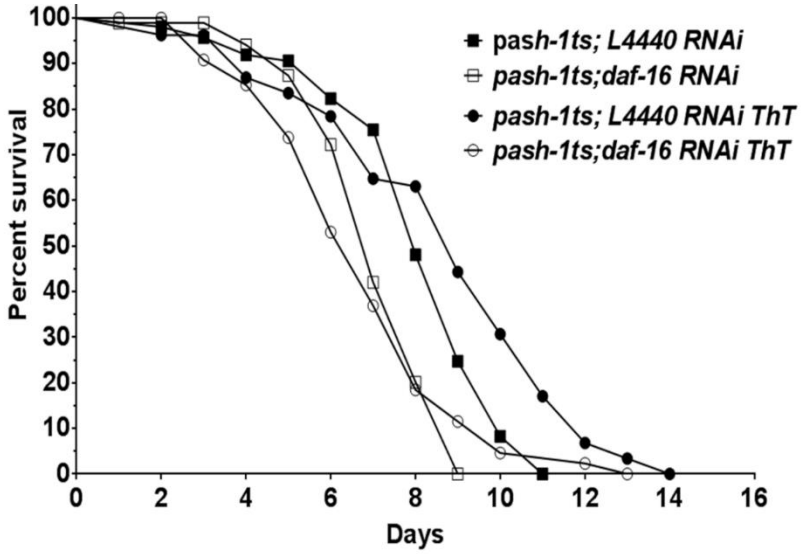

Figure 42. The effect of RNAi knock-down of *daf-16* on the life span of *pash-1ts* animals supplemented with Thioflavin T (ThT) at 25°C.

Strain	Mean Life ± SEM (Day)	75th Percentile ± SEM (Day)	Maximal Lifespan ± SEM (Day)	% Mean Lifespan change	% 75th Percentile change	% Maximal Lifespan change	p Value (Log Rank Test)
pash-1ts; L4440 RNAi	7,33 ± 0,33	8,33 ± 0,44	10,33 ± 0,18	-	-	-	-
pash-1ts;daf-16 RNAi	6,50 ± 0,22	7,17 ± 0,28	9,00 ± 0,49	-11,32	-13,93	-12,88	<0,0001
pash-1ts; L4440 RNAi + ThT	7,67 ± 0,54	10 ± 0,47	14 ± 0,47	4,64	20,05	35,53	<0,0001
pash-1ts; daf-16 RNAi + ThT	6,33 ± 0,54	9,33 ± 1,52	13,33 ± 0,72	-13,64	12,00	29,04	<0,01

Table 14. The changes in the life span of *pash-1ts* animals supplemented with 100 μM Thioflavin T (ThT) following *daf-16* RNAi knock-down at 25°C.

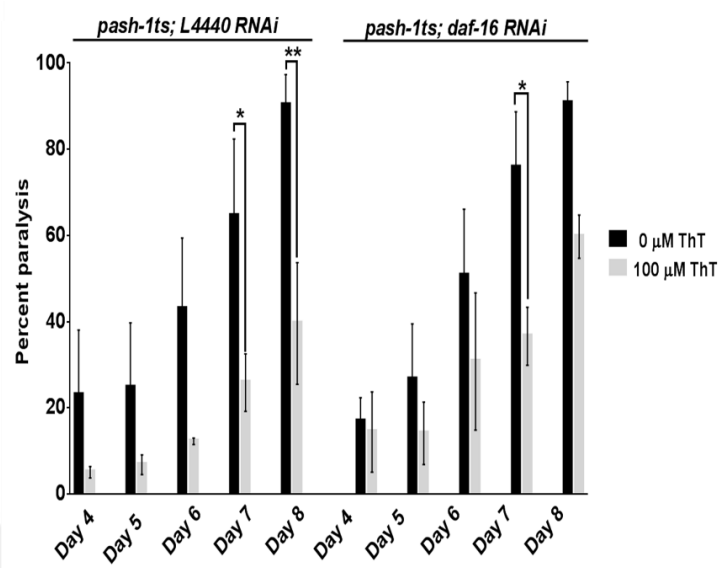

Figure 43. The effect of RNAi knock-down of *daf-16* on the motility of *pash-1ts* animals supplemented with 100 μM Thioflavin T (ThT) on days 4 to 8 at 25°C. Results show the mean ± SEM of three independent experiments (*p<0.05, **p<0.01).

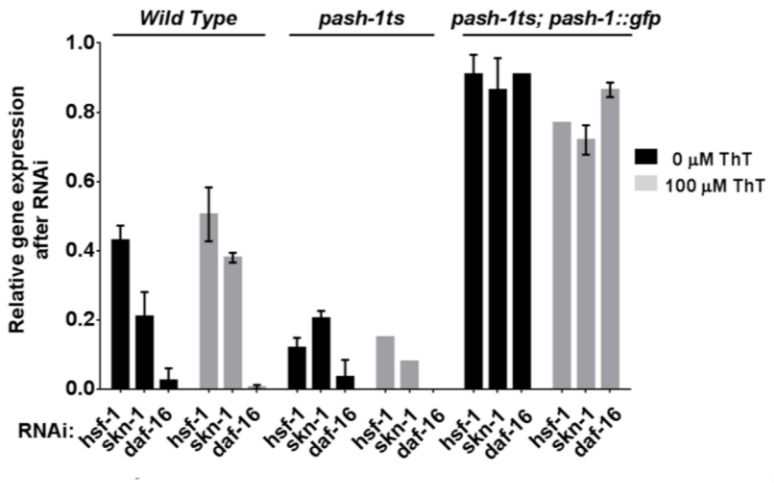

Figure 44. RNAi knock-down efficiency of *hsf-1*, *skn-1* and *daf-16* in wild type, *pash-1ts* and *pash-1* rescue animals supplemented with 100 μM Thioflavin T (ThT) determined by quantitative RT-PCR on day 3 at 25°C. Results show the mean ± SEM of three independent experiments.

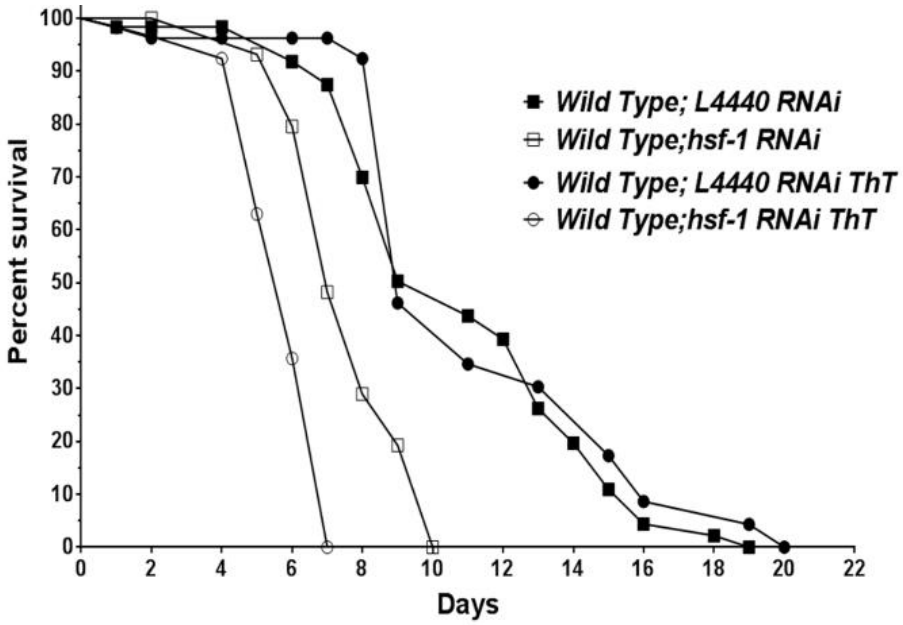

Figure 45. The effect of RNAi knock-down of *hsf-1* on the life span of wild type animals supplemented with 100 μM Thioflavin T (ThT) at 25°C.

Strain	Mean Life ± SEM (Day)	75th Percentile ± SEM (Day)	Maximal Lifespan ± SEM (Day)	% Mean Lifespan change	% 75th Percentile change	% Maximal Lifespan change	p Value (Log Rank Test)
Wild Type; L4440 RNAi	14,25 ± 1,24	16,33 ± 1,03	19,75 ± 0,22	-	-	-	-
Wild Type; L4440 RNAi + ThT	12 ± 1,12	14,67 ± 0,62	19,25± 0,74	-15,79	-10,17	-2,53	n.s.
Wild Type;hsf-1 RNAi	9,5 ± 0,83	9,67 ± 0,62	12,5 ± 0,90	-	-	-	-
Wild Type; hsf-1 RNAi + ThT	6,75 ± 0,41	7 ± 0	10 ± 1,50	-28,95	-27,61	-20,00	<0,0001

Table 15. The changes in the life span of wild type animals supplemented with 100 μM Thioflavin T (ThT) following *hsf-1* RNAi knock-down at 25°C.

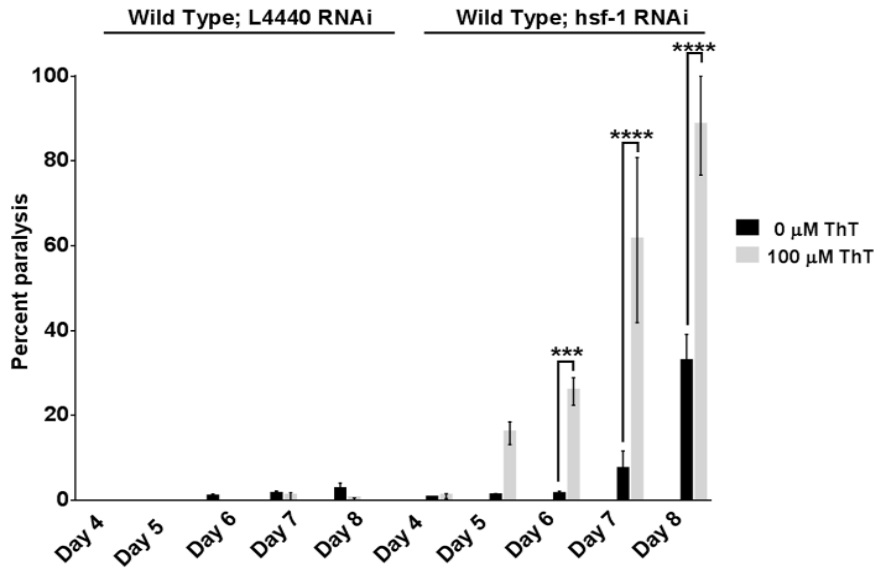

Figure 46. The effect of RNAi knock-down of *hsf-1* on the motility of wild type animals supplemented with 100 μM Thioflavin T (ThT) on days 4 to 8 at 25°C. Results show the mean ± SEM of three independent experiment (***p<0.001, ****p<0.0001).

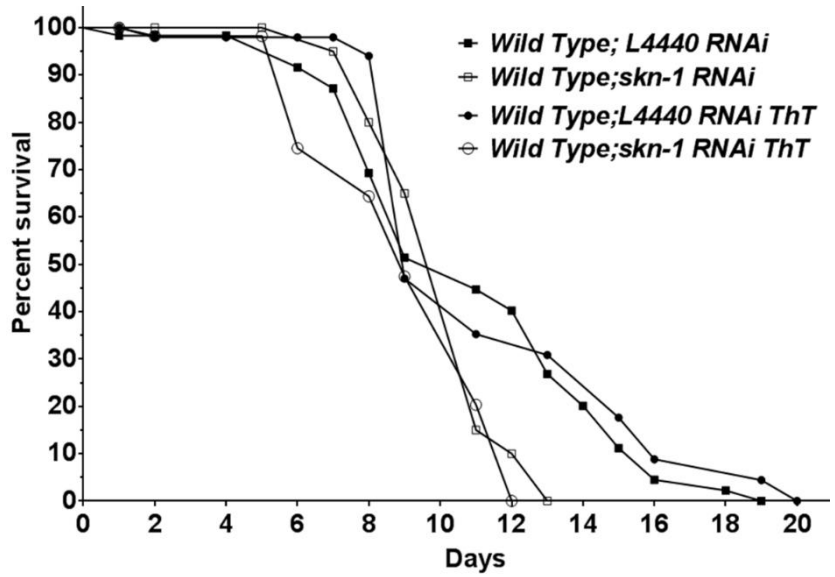

Figure 47. The effect of RNAi knock-down of *skn-1* on the life span of wild type animals supplemented with 100 μM Thioflavin T (ThT) at 25°C.

Strain	Mean Life ± SEM (Day)	75th Percentile ± SEM (Day)	Maximal Lifespan ± SEM (Day)	% Mean Lifespan change	% 75th Percentile change	% Maximal Lifespan change	p Value (Log Rank Test)
Wild Type; L4440 RNAi	14,33 ± 1,66	16 ± 1,41	19,67 ± 0,27	-	-	-	-
Wild Type;skn-1 RNAi	13 ± 0,82	13,67 ± 1,09	16,33 ± 1,36	-9,28	-14,56	-16,98	n.s.
Wild Type; L4440 RNAi + ThT	11,67 ± 1,44	14,67± 0,72	19,33± 0,98	-18,56	-8,31	-1,73	n.s.
Wild Type; skn-1 RNAi + ThT	9,33 ± 0,27	11,67 ± 0,27	14 ± 0,94	-34,89	-27,06	-28,83	<0,01

Table 16. The changes in the life span of wild type animals following *skn-1* RNAi knock-down in the presence of 100 μM Thioflavin T (ThT) at 25°C.

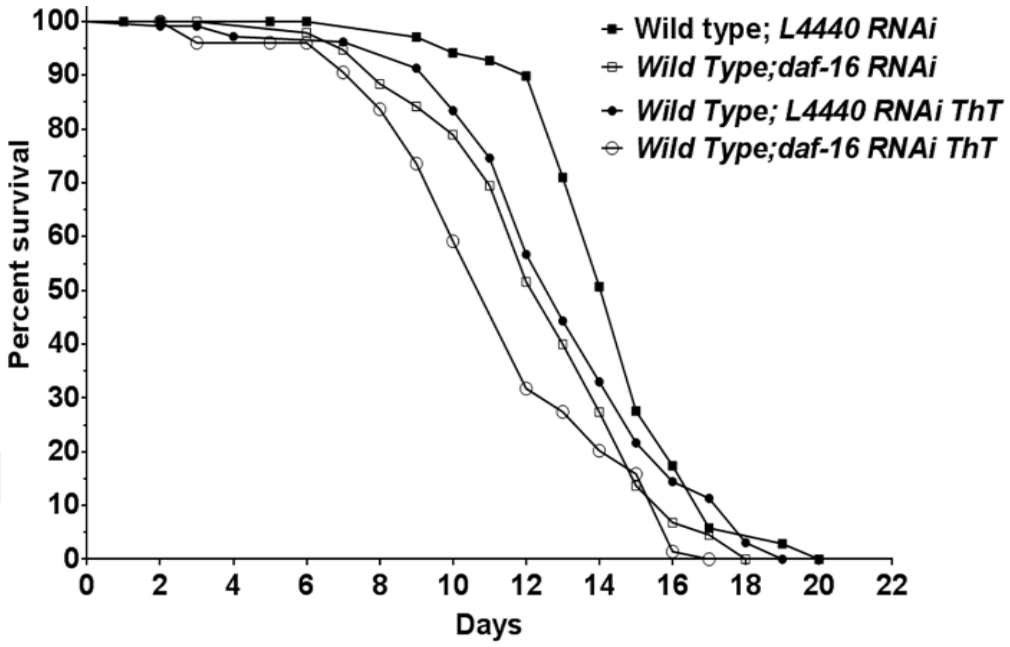

Figure 48. The effect of RNAi knock-down of *daf-16* on the life span of wild type animals supplemented with 100 μM Thioflavin T (ThT) at 25°C.

Strain	Mean Life ± SEM (Day)	75th Percentile ± SEM (Day)	Maximal Lifespan ± SEM (Day)	% Mean Lifespan change	% 75th Percentile change	% Maximal Lifespan change	p Value (Log Rank Test)
Wild Type; L4440 RNAi	14,33 ± 1,66	16 ± 1,41	19,67 ± 0,27	-	-	-	-
Wild Type;daf-16 RNAi	13 ± 0,82	13,67 ± 1,09	16,33 ± 1,36	-9,28	-14,56	-16,98	<0,0001
Wild Type; L4440 RNAi + ThT	11,67 ± 1,44	14,67± 0,72	19,33± 0,98	-18,56	-8,31	-1,73	<0,05
Wild Type; daf-16 RNAi + ThT	9,33 ± 0,27	11,67 ± 0,27	14 ± 0,94	-34,89	-27,06	-28,83	<0,0001

Table 17. The changes in the life span of wild type animals supplemented with 100 μM Thioflavin T (ThT) following RNAi knock-down of *daf-16* at 25°C.

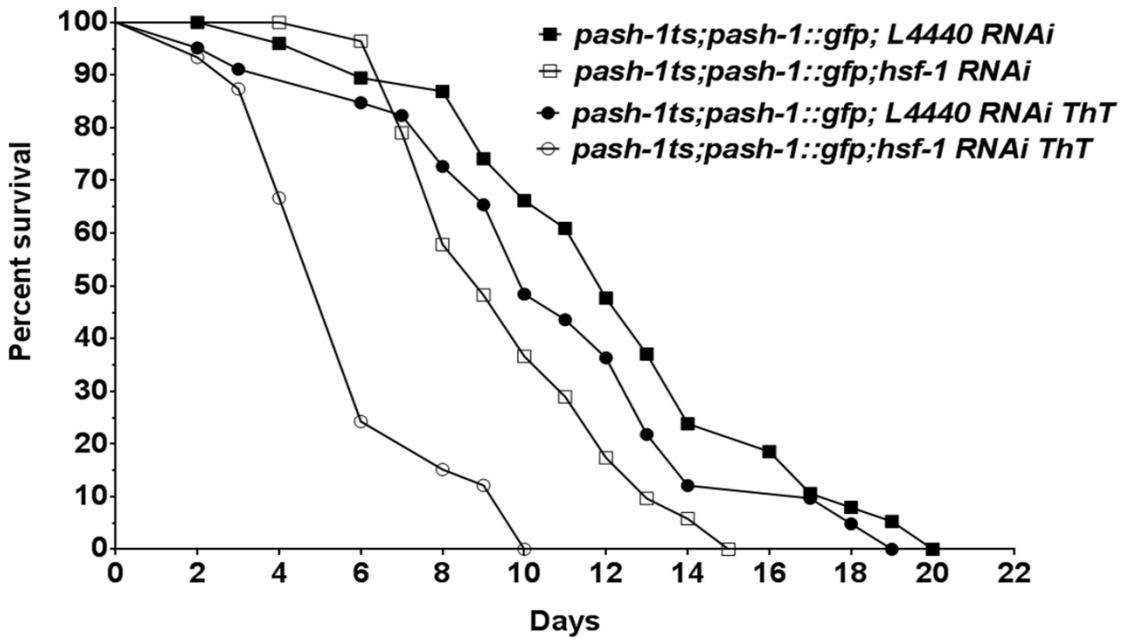

Figure 49. The effect of RNAi knock-down of *hsf-1* on the life span of *pash-1* rescue animals supplemented with 100 μM Thioflavin T (ThT) at 25°C.

Strain	Mean Life ± SEM (Day)	75th Percentile ± SEM (Day)	Maximal Lifespan ± SEM (Day)	% Mean Lifespan change	% 75th Percentile change	% Maximal Lifespan change	p Value (Log Rank Test)
pash-1ts;pash-1::gfp; L4440 RNAi	13,75 ± 0,89	15,33 ± 0,67	20 ± 0	-	-	-	-
pash-1ts;pash-1::gfp;hsf-1 RNAi	10,50 ± 0,56	12 ± 0,41	14,5± 0,25	-23,64	-21,72	-27,50	<0,001
pash-1ts;pash-1::gfp; L4440 RNAi + ThT	9,75 ± 0,41	11,67 ± 0,62	18,25 ± 0,65	-29,09	-23,87	-8,75	N.S.
pash-1ts;pash-1::gfp; hsf-1 RNAi + ThT	7,33 ± 0,54	7,67 ± 0,62	11,33 ± 1,47	-46,69	-49,97	-43,35	<0,0001

Table 18. The changes in the life span of *pash-1* rescue animals supplemented with 100 μM Thioflavin T (ThT) following RNAi knock-down of *hsf-1* at 25°C.

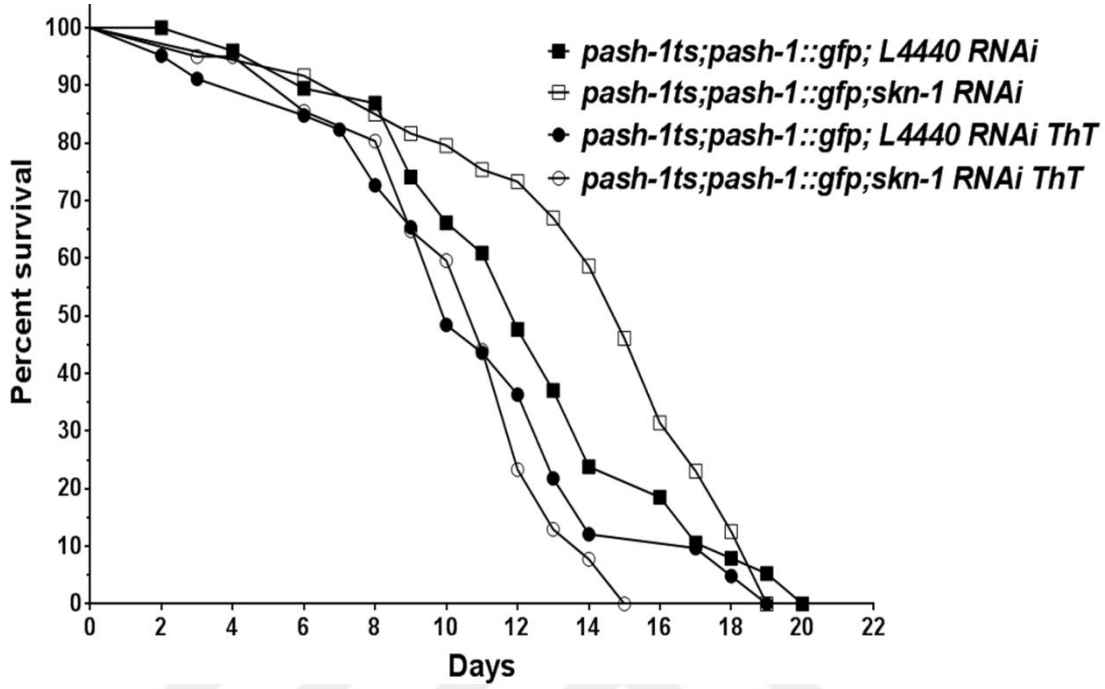

Figure 50. The effect of RNAi knock-down of *skn-1* on the life span of *pash-1* rescue animals supplemented with 100 μM Thioflavin T (ThT) at 25°C.

Strain	Mean Life ± SEM (Day)	75th Percentile ± SEM (Day)	Maximal Lifespan ± SEM (Day)	% Mean Lifespan change	% 75th Percentile change	% Maximal Lifespan change	p Value (Log Rank Test)
pash-1ts;pash-1::gfp; L4440 RNAi	13,33± 1,09	15,33 ± 0,72	20 ± 0	-	-	-	-
pash-1ts;pash-1::gfp;skn-1 RNAi	13,67 ± 0,54	15,33± 0,72	18± 0,47	2,55	0,00	-10,00	n.s.
pash-1ts;pash-1::gfp; L4440 RNAi + ThT	9 ± 0,47	13,33 ± 0,72	18 ± 0,82	-32,48	-13,05	-10,00	n.s.
pash-1ts;pash-1::gfp; skn-1 RNAi + ThT	9,33 ± 0,72	11,67 ± 0,27	15,67 ± 0,27	-30,01	-23,87	-21,65	<0,01

Table 19. The changes in the life span of *pash-1* rescue animals supplemented with 100 μM Thioflavin T (ThT) following RNAi knock-down of *skn-1* at 25°C.

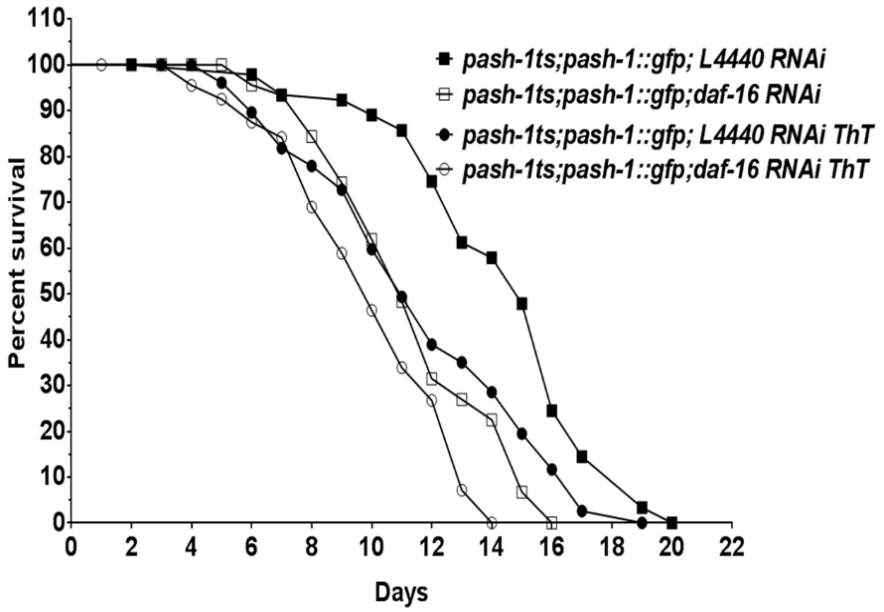

Figure 51. The effect of RNAi knock-down of *hsf-1* on the life span of *pash-1* rescue animals supplemented with 100 μM Thioflavin T (ThT) at 25°C.

Strain	Mean Life ± SEM (Day)	75th Percentile ± SEM (Day)	Maximal Lifespan ± SEM (Day)	% Mean Lifespan change	% 75th Percentile change	% Maximal Lifespan change	p Value (Log Rank Test)
pash-1ts;pash-1::gfp; L4440 RNAi	13,33± 1,09	15,33 ± 0,72	20 ± 0	-	-	-	-
pash-1ts;pash-1::gfp;daf-16 RNAi	13,67 ± 0,54	15,33± 0,72	18± 0,47	2,55	0,00	-10,00	<0,0001
pash-1ts;pash-1::gfp; L4440 RNAi + ThT	9 ± 0,47	13,33 ± 0,72	18 ± 0,82	-32,48	-13,05	-10,00	<0,0001
pash-1ts;pash-1::gfp; daf-16 RNAi + ThT	9,33 ± 0,72	11,67 ± 0,27	15,67 ± 0,27	-30,01	-23,87	-21,65	<0,0001

Table 20. The changes in the life span of *pash-1* rescue animals supplemented with 100 μM Thioflavin T (ThT) following RNAi knock-down of *daf-16* at 25°C.

3.6.4. ThT suppresses *unc-52ts* proteotoxicity in *pash-1ts* animals

We next questioned whether ThT could also suppress the effects of expression of *unc-52ts* in *pash-1ts* animals. Remarkably, on the ThT containing plates *pash-1ts;unc-52ts* double mutants lived 35% longer as compared to control animals (**Figure 52; Table 21**). Moreover, ThT treatment did not extend the lifespan of *unc-52ts,* and in *pash-1ts;unc-52ts* double mutant animals expressing wild type *pash-1* (**Figures 53-54, and Table 21**). The expression

of metastable UNC-52 in *pash-1ts* mutant background caused severe loss of locomotion **(Figure 28)**. However, ThT treatment suppressed the considerable portion of motility defects, ranging from 50%-70% from day 2 to day 5, respectively (**Figure 55**). Moreover, ThT also suppressed the motility defects of *unc-52ts* on day 9 and day 10 **(Figure 56).** On the other hand, ThT treatment became redundant when the wild type *pash-1* gene was expressed in the *unc-52ts;pash-1ts* double mutants (**Figures 55-56)**. These results further prove that expression of mutant UNC-52 protein challenges the proteostasis in *pash-1ts* animals, which can be rescued by ThT treatment.

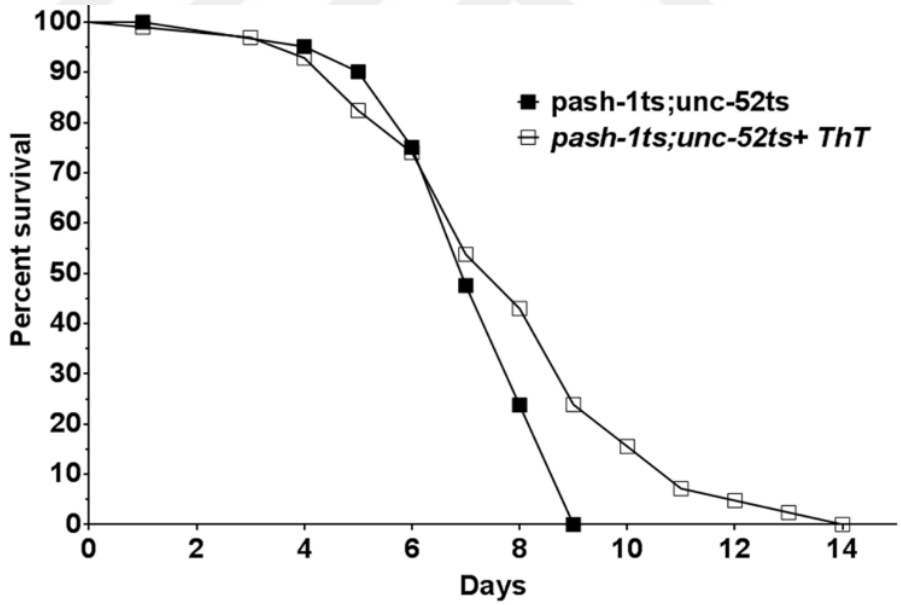

Figure 52. Life span of *pash-1ts;unc-52ts* animals supplemented with 100 μM Thioflavin T (ThT) at 25°C.

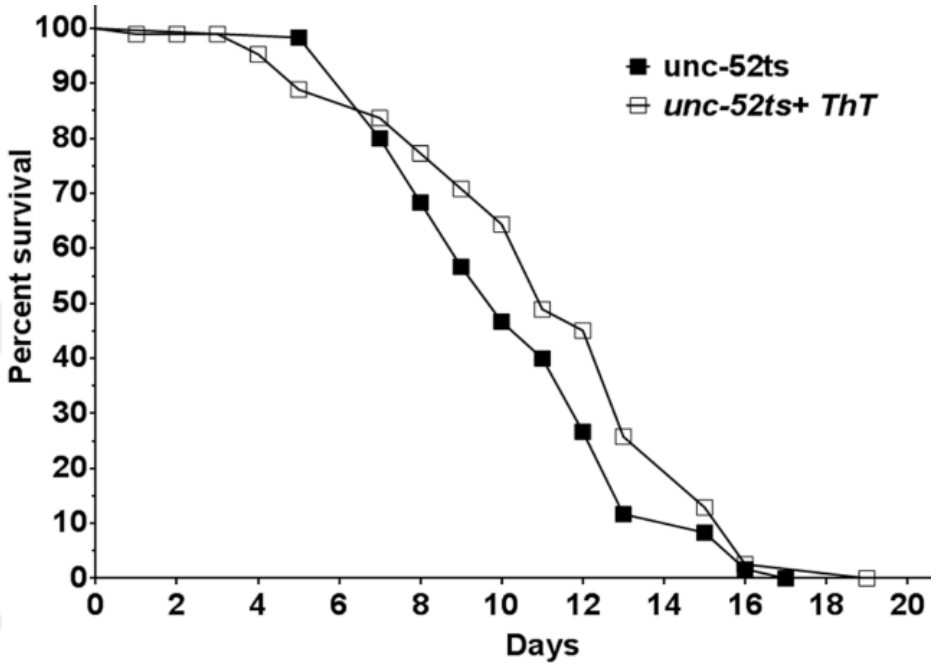

Figure 53. Life span of *unc-52ts* animals supplemented with 100 μM Thioflavin T (ThT) at 25°C.

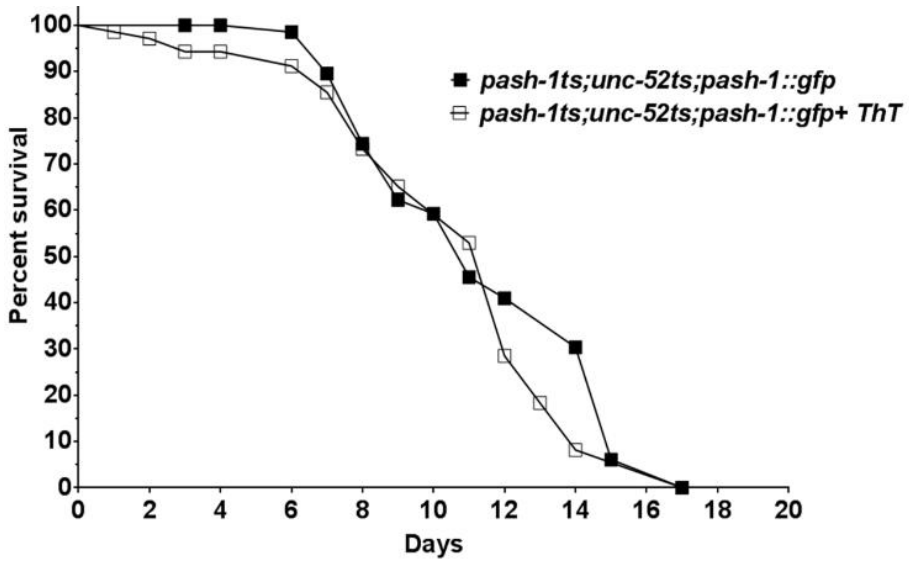

Figure 54. Life span of *pash-1ts;unc-52ts* double mutant expressing wild type *pash-1* animals supplemented with 100 μM Thioflavin T (ThT) at 25°C.

Strain	Mean Life ± SEM (Day)	75th Percentile ± SEM (Day)	Maximal Lifespan ± SEM (Day)	% Mean Lifespan change	% 75th Percentile change	% Maximal Lifespan change	p Value (Log Rank Test)
pash-1ts;unc-52ts	7 ± 0,47	7,67 ± 0,27	9,33 ± 0,27	-	-	-	-
pash-1ts;unc-52ts + ThT	7 ± 0,82	9 ± 0	12,67 ± 0,54	0,00	17,34	35,80	<0,01
unc-52ts	11,33 ± 0,72	13,33 ± 0,72	17,33 ± 0,27	-	-	-	-
unc-52ts+ ThT	10 ± 0,47	12,33 ± 0,54	16,67 ± 1,52	-11,74	-7,50	-3,81	n.s.
pash-1ts;unc-52ts;pash-1::gfp	10 ± 0,71	14,50 ± 0,35	17,50 ± 0,29	-	-	-	-
pash-1ts;unc-52ts;pash-1::gfp + ThT	9 ± 1,73	11 ± 1,15	16 ± 0,58	-10,00	-24,14	-8,57	n.s.

Table 21. The changes in the life span of *pash-1ts;unc-52ts, unc-52ts and pash-1ts;unc-52ts;pash-1::gfp* animals in the presence of 100 μM Thioflavin T (ThT) at 25°C.

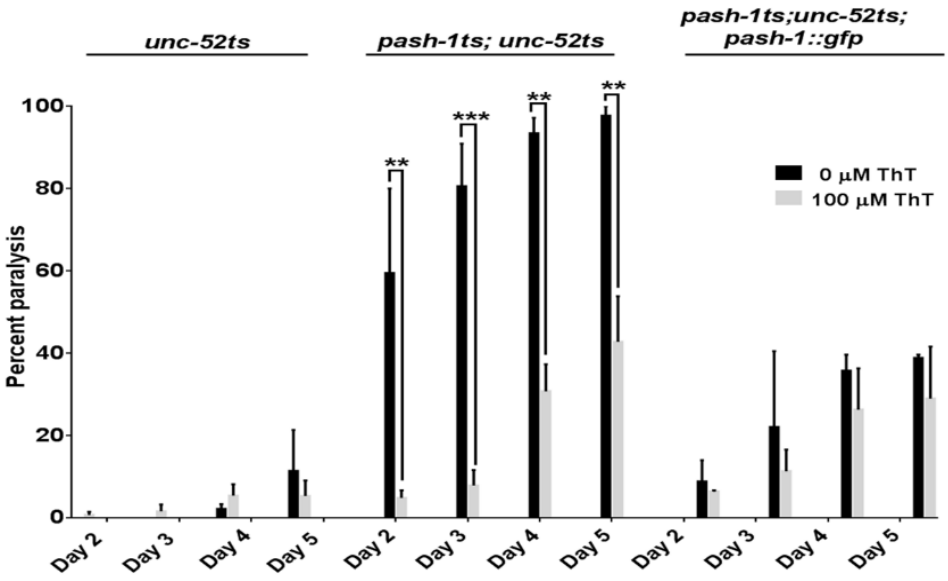

Figure 55. The motility of *unc-52ts*, *pash-1ts;unc-52ts*, and *pash-1ts; unc-52ts* double mutant expressing wild type *pash-1* animals supplemented with 100 μM Thioflavin T (ThT) on days 2 to 5 at 25°C. Results show the mean ± SEM of three independent experiments (**p<0.01, and ***p<0.001).

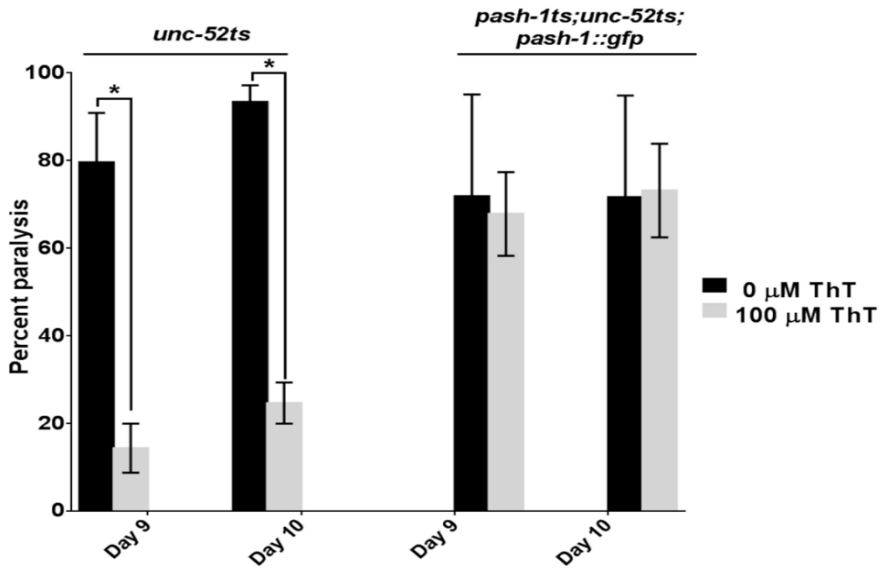

Figure 56. The motility of *unc-52ts* and *pash-1ts; unc-52ts* double mutant expressing wild type *pash-1* animals supplemented with 100 μM Thioflavin T (ThT) on days 9 and 10 at 25°C. Results show the mean ± SEM of three independent experiments (*p<0.05).

3.6.5. ThT also requires HSF-1 at 20˚C

Due to the temperature dependent effect of ThT on wild type nematodes, I have tested its activity in miRNA biogenesis impaired animals at 20°C and 25°C **(please see 3.6.1. and 3.6.2)**. At both temperatures, ThT extended the life span of miRNA biogenesis defective animals **(Figures 32, and 36; and Tables 10-11)**. Therefore, I have investigated whether ThT would also require *hsf-1* at 20°C. Parallel to the findings at 25°C, I have shown that the effect of ThT also required *hsf-1* at 20°C **(Figures 45-46, and 57-58; and Tables 15 and 22)** [182]. RNAi knock-down of *hsf-1* decreased the positive effect of ThT treatment on life span of wild type animals by 60% at 20°C (**Figures 57 and Table 22).** Tht could no longer suppressed the motility defects upon lowering the levels of *hsf-1* (**Figure 58**). Measured by qPCR, the efficiency of RNAi treatment was comparable in ThT containing and control plates (**Figure**

59). These results suggested that ThT acts on proteostasis through the same pathway(s) at both temperatures.

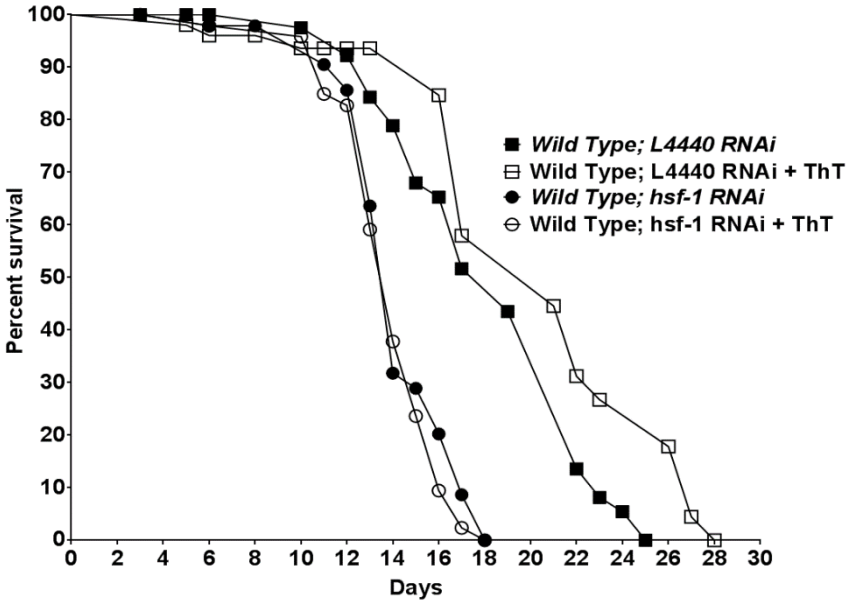

Figure 57. The effect of RNAi knock-down of *hsf-1* on the life span of wild type animals supplemented with 100 μM Thioflavin T (ThT) at 20°C.

Strain	Mean Life ± SEM (Day)	75th Percentile ± SEM (Day)	Maximal Lifespan ± SEM (Day)	% Mean Lifespan change	% 75th Percentile change	% Maximal Lifespan change	p Value (Log Rank Test)
Wild Type; L4440 RNAi	19,33 ± 0,72	23,33 ± 0,98	28,33 ± 1,44	-	-	-	-
Wild Type; L4440 RNAi + ThT	22 ± 0,82	26,33 ± 0,27	32 ± 1,25	13,81	12,86	12,95	<0,0001
Wild Type;hsf-1 RNAi	15 ± 0,47	16,33 ± 0,27	19,33 ± 1,09	-	-	-	-
Wild Type; hsf-1 RNAi + ThT	14 ± 0,94	15,33 ± 0,54	17 ± 0,47	-6,67	-6,12	-12,05	n.s.

Table 22. The changes in the life span of wild type animals supplemented with 100 μM Thioflavin T (ThT) following RNAi knock-down of *hsf-1* at 20°C.

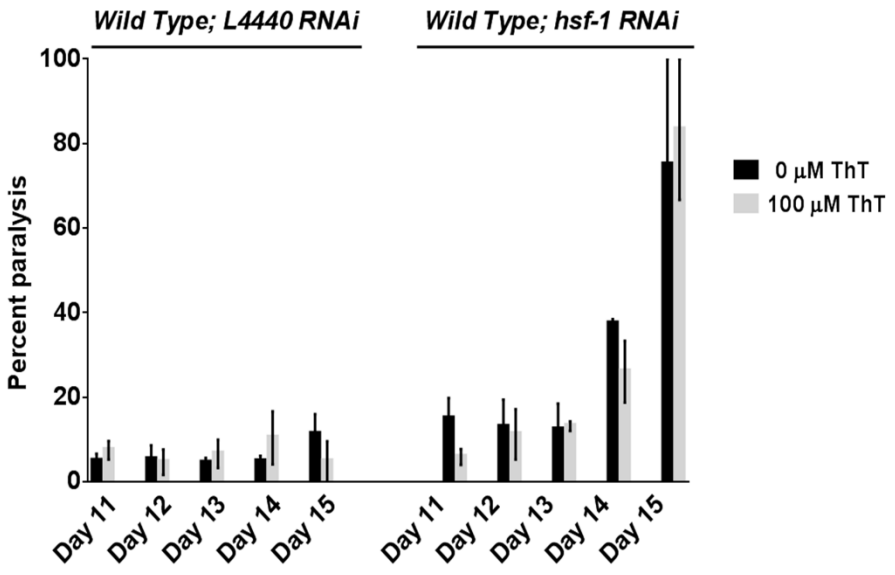

Figure 58. The effect of RNAi knock-down of *hsf-1* on the motility of wild type animals supplemented with 100 μM Thioflavin T (ThT) on days 11 to 15 at 20°C. Results show the mean ± SEM of three independent experiment.

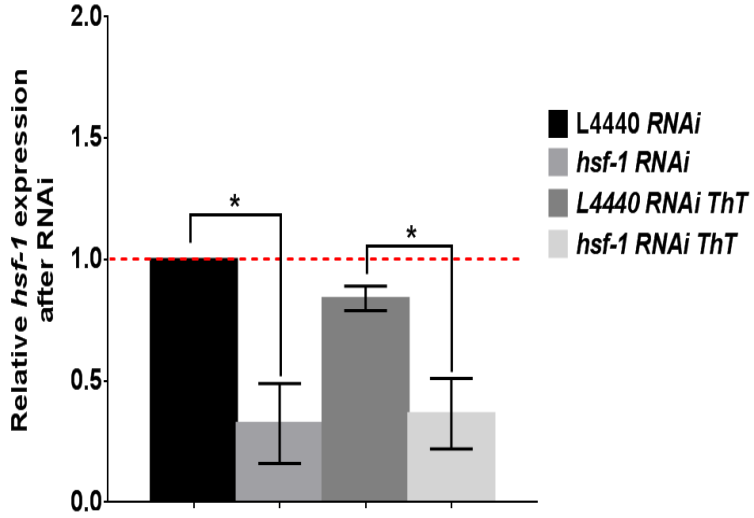

Figure 59. RNAi knock-down efficiency of *hsf-1* in wild type, animals supplemented with 100 μM Thioflavin T (ThT) determined by quantitative RT-PCR on day 3 at 20°C. Results show the mean ± SEM of three independent experiments (*p<0.05).

3.7. Proteotoxicity posed by the loss of miRNA synthesis did not simply result from the general up-regulation of protein levels.

miRNAs mediate post-transcriptional gene regulation by either increasing the mRNA degradation or inhibiting the protein translation. Indeed, transcriptome analysis of *dcr-1*, *alg-1* and *pash-1* mutants indicated an elevated level of mRNAs [8, 201, 202]. Changes in protein abundance during aging has been examined, where it has been shown that 30% of the proteins with 2-fold or higher increase in abundance during aging were also up regulated in *dcr-1* mutant animals [88]. This raises the possibility that the loss of miRNA mediated gene regulation could lead to an increase in protein abundance, leading to higher levels of protein aggregation and posing a challenge to protein folding environment in miRNA biogenesis defective animals.

We asked whether insult to proteostasis in *pash-1ts* animals was because of the change in global protein abundance. To evaluate this, we inhibited protein synthesis by RNAi knockdown of a translation initiation factor, eIF4E/*ife-2*, as the RNAi-knockdown of *ife-2* was previously shown to prolong the life span of wild type animals at 25°C [203]. Despite the 90% reduction in *ife-2* levels in *pash-1ts* animals, neither the life span nor the motility of *pash-1ts* animals changed at the restrictive temperature (**Figures 60-62; and Table 23**). However, RNAi knockdown of *ife-2* extended the life span of wild type and *pash-1ts* rescue animals, by 14% and 10%, respectively (**Figure 61; Table 23**). Thus, the proteostasis defect observed in *pash-1ts* animals does not solely result from the increased level of the proteins, rather reflect a functional defect in proteostasis in miRNA biogenesis deficient animals.

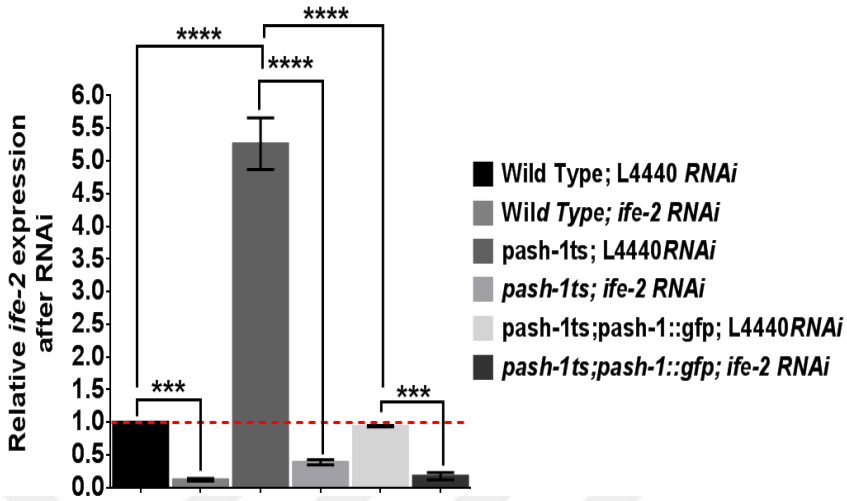

Figure 60. RNAi knock-down efficiency of *ife-2* in wild type, *pash-1ts* and *pash-1* rescue animals determined by quantitative RT-PCR on day 3 at 25°C. Results show the mean ± SEM of three independent experiments (***p<0.001 and ****p<0.0001).

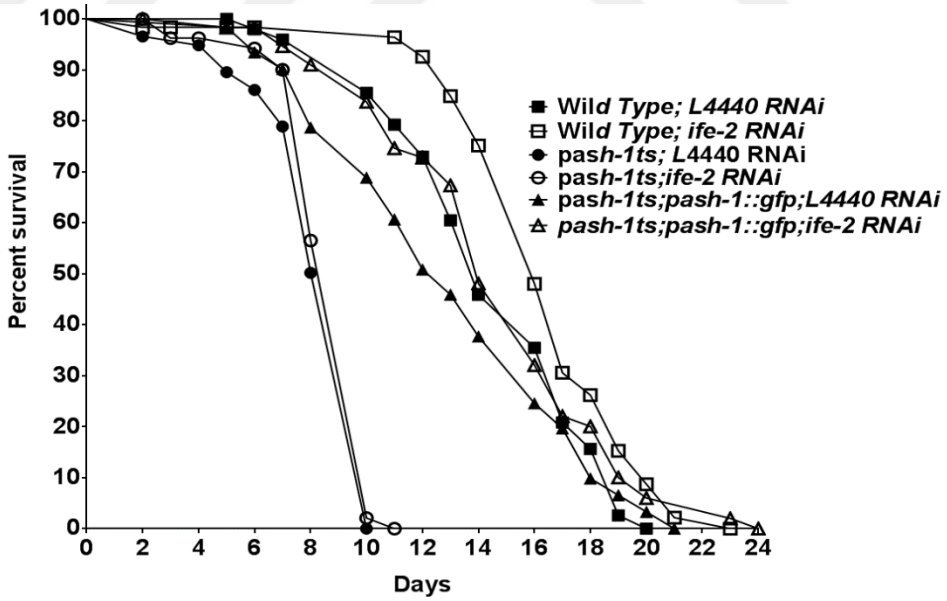

Figure 61. The effect of RNAi knock-down of *ife-2* on the life span of wild type, *pash-1ts* and *pash-1* rescue animals at 25°C.

Strain	Mean Life ± SEM (Day)	75th Percentile ± SEM (Day)	Maximal Lifespan ± SEM (Day)	% Mean Lifespan change	% 75th Percentile change	% Maximal Lifespan change	p Value (Log Rank Test)
Wild Type; L4440 RNAi	15 ±0,57	17,67± 0,27	20,67± 0,54	-	-	-	-
Wild Type; ife-2 RNAi	17 ±0,57	20 ±0,82	23,67± 0,98	13,33	13,21	14,52	<0,01
pash-1ts; L4440 RNAi	7,67 ±0,27	9,33 ±0,54	11 ±0,47	-	-	-	-
pash-1ts; ife-2 RNAi	8 ±0	9,67 ±0,27	11,33± 0,27	4,35	3,57	3,03	n.s.
pash-1ts;pash-1::gfp; L4440 RNAi	14± 0,58	16,33± 0,27	21,67± 0,54	-	-	-	-
pash-1ts;pash-1::gfp; ife-2 RNAi	15± 0,58	17,67± 0,54	24 ±0,47	7,14	8,16	10,77	<0,05

Table 23. The changes in the life span of wild type, *pash-1ts* and *pash-1* rescue animals following RNAi knock-down of *ife-2* at 25°C.

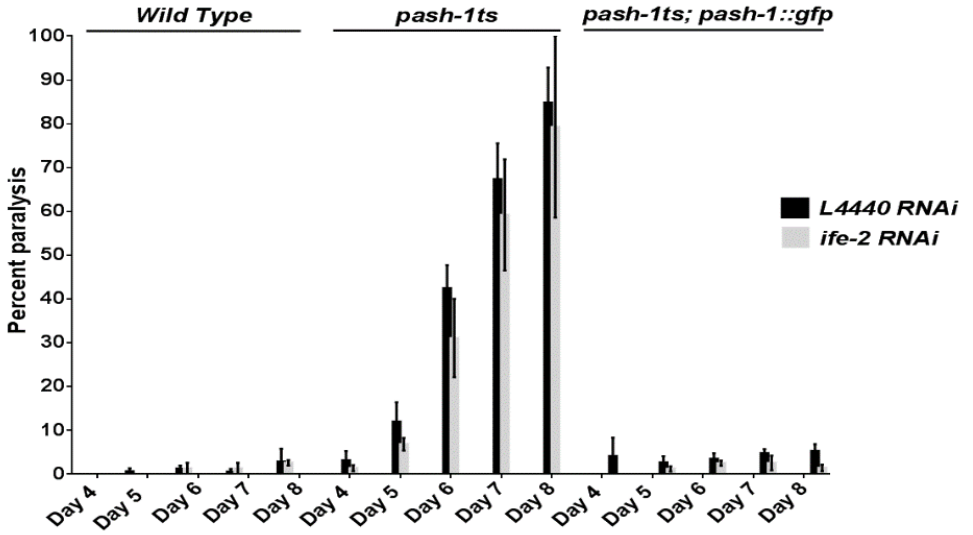

Figure 62. The effect of RNAi knock-down of *ife-2* on the motility of wild type, *pash-1ts*, and *pash-1* rescue animals on days 4 to 8 at 25°C. Results show the mean ± SEM of three independent experiment.

3.8. Absence of miRNAs led to a chaperome imbalance in *C. elegans*.

To investigate where the defect lies in the PN, we analyzed the levels and activities of its essential components in *pash-1ts* animals. As the key players, molecular chaperones assist the folding and refolding of proteins to reach their functional native state; thereby they form the first line of defense against the formation of toxic oligomers and protein aggregations. As we previously showed that lowering *hsf-1* in *pash-1ts* animals did not reduce the lifespan of these mutants, suggesting that the function of *hsf-1* is already impaired (**Figure 38**). *hsf-1* is one of the critical regulators of chaperone levels. Therefore, we determined the mRNA levels of a total of 24 molecular chaperones along with known *hsf-1* targets residing in the cytosol (*hsp-70* family members (*F44E5.4*, *C12C8.1*, and *hsp-1)*; *hsp-90* homolog *daf-21*; small heat shock proteins (*hsp-43a*, *hsp-43b*, *hsp-25*, *hsp-12* family members, *Q9N350*, *ZK1128.7* and *hsp-16* family members)), in the endoplasmic reticulum (*hsp-4*), and in the mitochondria (*hsp-6,* and *hsp-60*) by quantitative RT-PCR. Of all the molecular chaperones we analyzed, relative to *pash-1* rescue strain, 14 of them remained unchanged after normalizing to wild type animals (**Figure 63**). The four of them were up regulated (class I), one of which is known to be induced in the presence of stress by HSF-1 (*F44E5.4*) (**Figure 64**). *F08H9.4b* and *hsp-16.11* (class II), upregulated in *pash-1ts* mutants compared to wild type animals, were also upregulated in *pash-1* rescue transgenic animals (**Figure 64**). Of the known *hsf-1* targets we analyzed, *hsp-16.2*, *daf-21*, and *C12C8.1* did not significantly changed, while *F44E5.4*, was up regulated in *pash-1ts* animals suggesting that either these chaperones were also regulated by other transcription factors, or the ability of *hsf-1* to regulate these chaperones was intact in *pash-1ts* mutants (**Figures 63-64**).

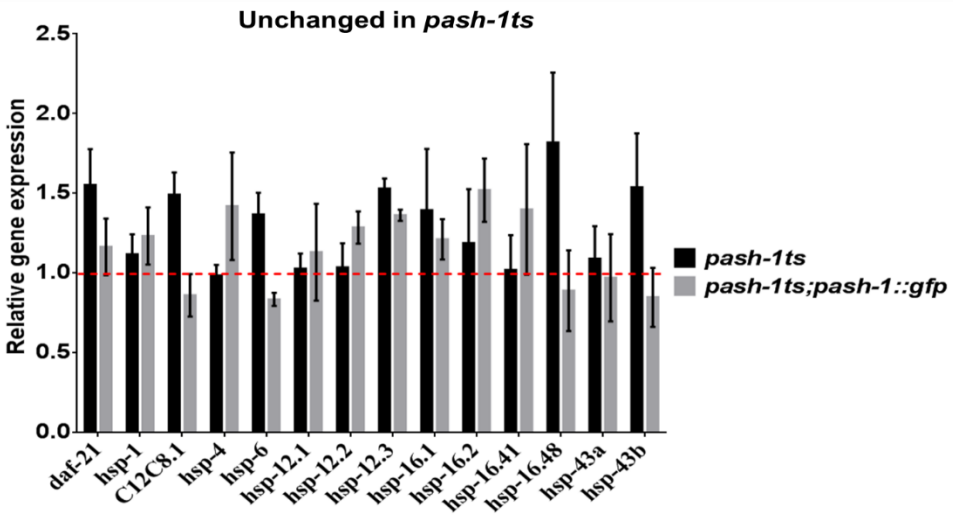

Figure 63. Quantitative RT-PCR results of unchanged chaperones in *pash-1ts* animals relative to wild type animals on day 4 at 25°C. Results show the mean ± SEM of six independent experiments. Red dashed line indicates the corresponding gene levels in the wild type animals.

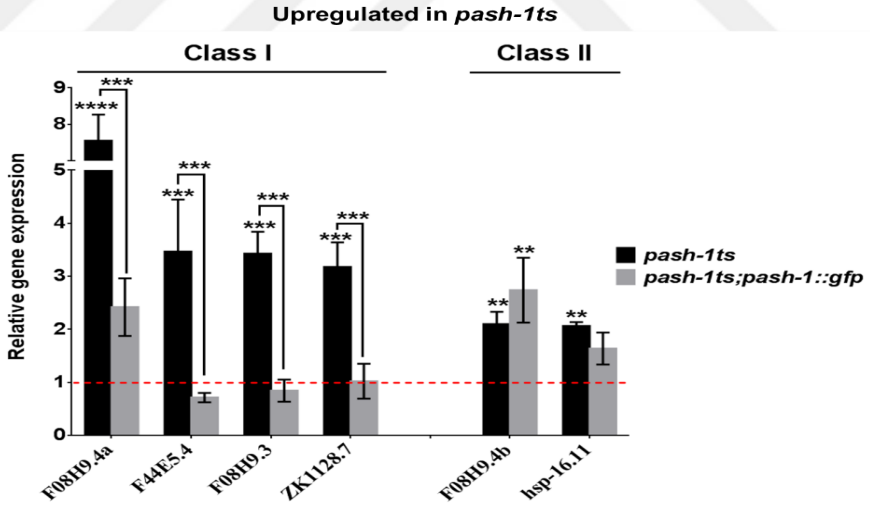

Figure 64. Quantitative RT-PCR results of upregulated chaperones in *pash-1ts* animals relative to wild type animals on day 4 at 25°C. Class I chaperones were upregulated in *pash-1ts* relative to wild type and *pash-1* rescue animals. Class II chaperones were also upregulated in *pash-1* rescue animals relative to wild type. Results show the mean ± SEM of six independent experiments. Red dashed line indicates the corresponding gene levels in the wild type animals (**p<0.01, ***p<0.001, and ****p<0.0001).

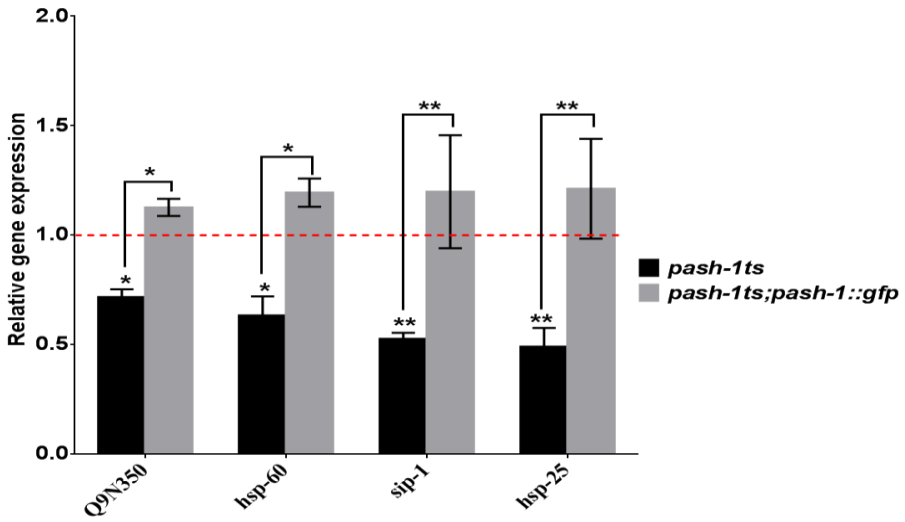

Figure 65. Quantitative RT-PCR results of downregulated chaperones in *pash-1ts* animals relative to wild type animals on day 4 at 25°C. Results show the mean ± SEM of six independent experiments. Red dashed line indicates the corresponding gene levels in the wild type animals (*p<0.05, and **p<0.01).

Noticeably, three small heat shock proteins (*sip-1*, *hsp-25* and *Q9N350*) and *hsp-60* were down regulated,which might be the underlying reason why animals unable to synthesize miRNAs are more susceptible to proteostatic insults (**Figure 65**). Overall, our results implied that the altered chaperome might be the one of reason underlying the increased proteotoxicity in *pash-1ts* animals.

3.9. The transcript levels of longevity determinant proteasome genes, *pbs-5* and *rpn-6.1* increased in *pash-1ts* mutant animals.

We next inquired about the degradative capacity of the *pash-1ts* animals, which might contribute to the accumulation of protein aggregates and appearance of related phenotypes. Misfolded proteins are removed by ubiquitin-proteasome system (UPS) in the cells. The 26S/30S proteasome is composed of a 20S core structure, containing three different

proteolytic activities, and 19S cap structure, playing a regulatory role. Upon binding of the 19S regulatory subunit, the activity of 20S catalytic core is enhanced to degrade proteins. ATPases of 19S regulatory subunit (*rpt* genes) are involved in binding to substrates, ubiquitin removal and translocation into 20S core. Rpt proteins of the 19S subunit contribute to the gate opening in the 20S core structure.

Analysis of the mRNA levels of ATPases of 19S regulatory subunit revealed no significant change in *pash-1ts* mutants in comparison to *pash-1* rescue animals **(Figure 66)**. Except for *rpn-6.1*, other nonATPase subunits were also at comparable levels to *pash-1* rescue animals (**Figure 67**). Even though overexpression of *rpn-6.1* was shown to augment the interaction between 19S and 20S subunits and thereby to enhance the proteasome activity and extend the life span [173], higher levels of *rpn-6.1* failed to affect the proteasome activity in *pash-1ts* animals. Next, we examined the 20S catalytic core subunits and observed no change in the mRNA levels of α-subunits (**Figure 68)**. Interestingly, of the 7 β-subunits we analyzed, *pbs-5* possessing the chymotrypsin-like activity was found to be higher in *pash-1ts* (**Figure 69)**. Unexpectedly, the levels of *pbs-5* and *pbs-2* in *pash-1* rescue animals were lower as compared to wild type worms, yet these animals phenotypically behaved like wild type (**Figure 69)**.

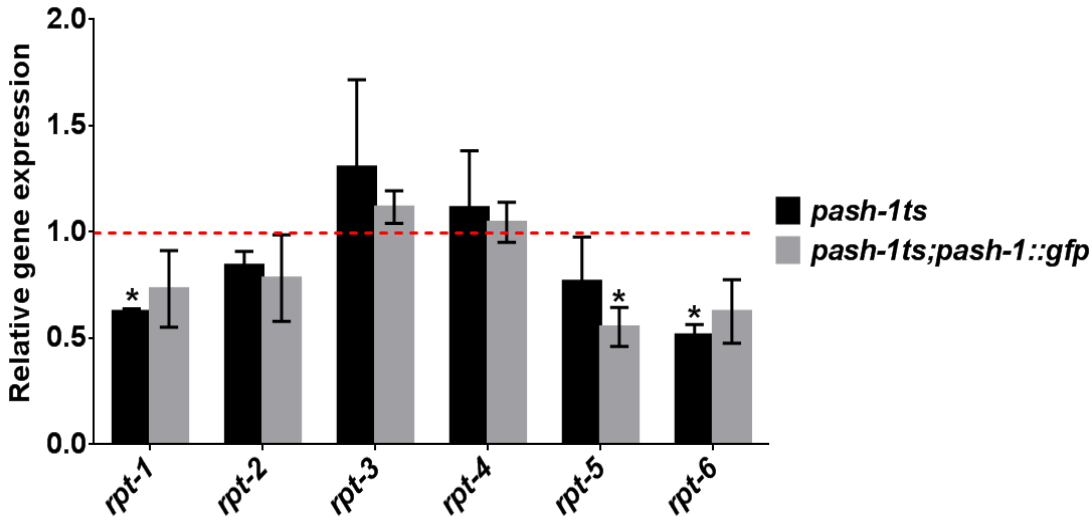

Figure 66. QuantitativeRT-PCR results of 19S ATPases of proteasome in *pash-1ts* and *pash-1* rescue animals on day 4 at 25°C. Results show the mean ± SEM of six independent experiments. Red dashed line indicates the corresponding gene levels in the wild type animals.

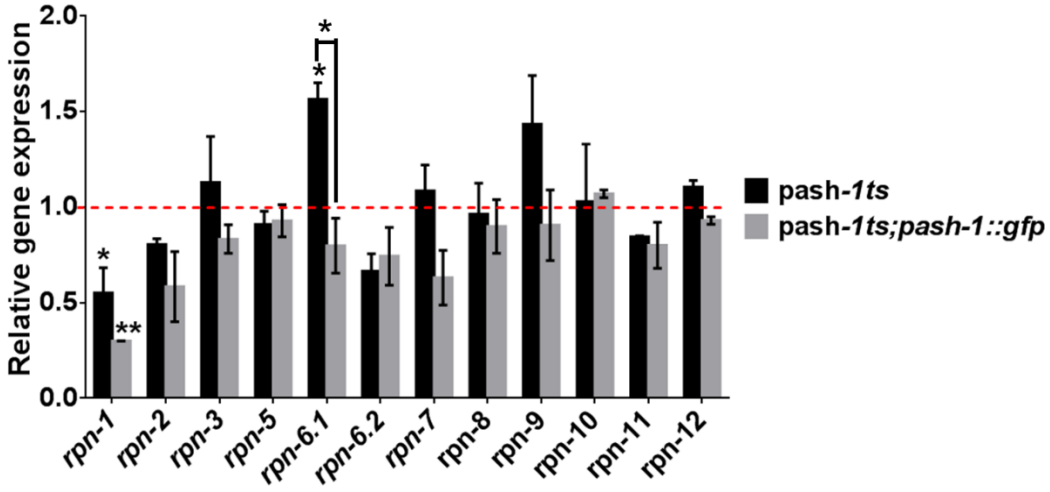

Figure 67. Quantitative RT-PCR results of 19S non-ATPases in *pash-1ts* and *pash-1* rescue animals on day 4 at 25°C. Bar graphs represent the mean ± SEM. Red dashed line indicates the wild type level (*p<0.05, and **p<0.01).

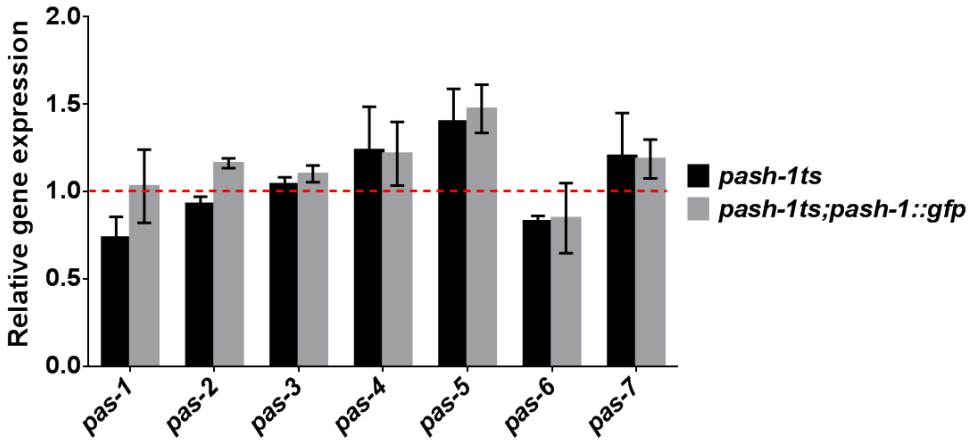

Figure 68. Quantitative RT-PCR results of 20S α subunits of proteasome in *pash-1ts* and *pash-1* rescue animals on day 4 at 25°C. Results show the mean ± SEM of six independent experiments. Red dashed line indicates the corresponding gene levels in the wild type animals.

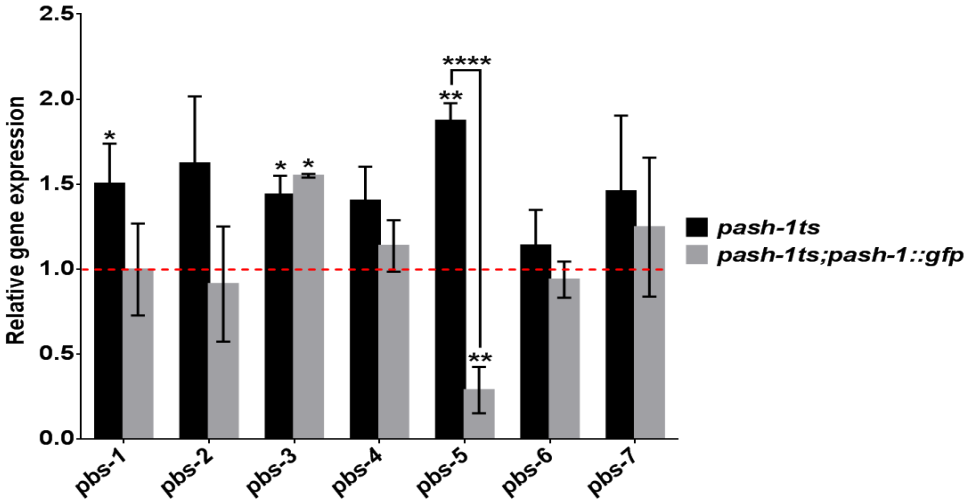

Figure 69. Quantitative RT-PCR results of 20S β subunits of proteasome in *pash-1ts* and *pash-1* rescue animals on day 4 at 25°C. Results show the mean ± SEM of six independent experiments. Red dashed line indicates the corresponding gene levels in the wild type animals (*p<0.05, **p<0.01 and ****p<0.0001).

3.10. Autophagy was not functional in *pash-1ts* animals.

Autophagy functions in complementary to ubiquitin-proteasome system to remove the misfolded proteins and aggregations. Highly conserved Atg proteins act in consequential steps of autophagy, which begins with the formation of isolation membrane near the substrate, then followed by the completion of autophagosome structure and eventually joined by lysosome to degrade the substrate. Regulated by TOR signaling, UNC-51 in a complex with ATG-13 is involved in the initiation of autophagy. ATG-6 homolog, BEC-1 functions in the nucleation and formation of initial membrane around the substrate.

Following the maturation of autophagy vesicles, LGG-1 (Atg-8/LC3 homolog) on the outer membrane is cleaved off by ATG-4 to be recycled, while LGG-1 in the inner membrane is degraded after joining of the lysosome. LGG-1::GFP reporter has been commonly used to visualize autophagy vesicle formation in the pharynx, intestine and seam cells [204]. When LGG-1::GFP transgenic animals crossed to the *pash-1ts* animals, the number of punctae formation was less than that of *pash-1* rescue and wild type animals **(Figure 70)**. Indeed, LGG-1 had a diffuse cytoplasmic localization in *pash-1ts* animals **(Figure 70)**. These suggested that pash-1ts animals fail to form autophagic vesicles.

Inactivation of autophagy genes causes rapid aging [205]. To further test the function of autophagy in *pash-1ts* animals, we lowered the mRNA levels of *unc-51* and *bec-1*, acting prior to vesicle formation, by RNAi. Relative to control RNAi, down regulation of *unc-51* and *bec-1* in wild type and *pash-1* rescue animals shortened the mean lifespan by 13% and 25%, respectively (**Figures 71-72; and Tables 24-25**). In addition, we observed an increase in the motility defects of wild type and *pash-1* rescue animals between day 10 and day 12 (**Figures**

73-76). As *pash-1ts* mutant animals lived at most 10 days, they could not tested on later time points. Reducing *unc-51* and *bec-1* did not significantly affect the mean lifespan or the motility defects of *pash-1ts* animals, indicating autophagy might be already impaired (**Figures 71-73, and 75; Tables 24-25**).

Both *unc-51* and *bec-1* genes are predicted targets of miRNAs. Therefore, absence of miRNA gene regulation might increase the levels of these genes in *pash-1ts* animals. However, when I examined the mRNA level of *unc-51* in *pash-1ts* animals maintained on control RNAi, I determined that the mRNA level of *unc-51* was 0.3 fold higher compared to wild type animals treated with control RNAi, suggesting *unc-51* might be a direct target of miRNAs **(Figure 77)**. On the other hand, mRNA level of *bec-1* in *pash-1ts* animals grown on control RNAi treated plates were similar to that of *bec-1* in wild type animals treated with control RNAi (**Figure 78**). In addition, the efficiency of RNAi knockdown was comparable in all three strains **(Figures 78-79)**. Collectively, these results suggested that in order to initiate the autophagy ongoing miRNA synthesis is required in the adult animals.

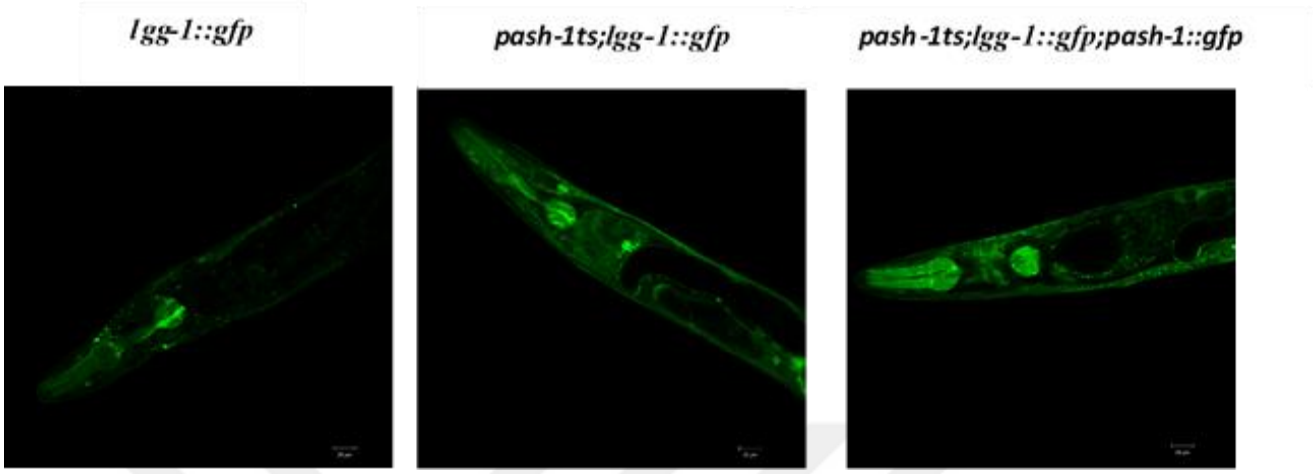

Figure 70. Visualization of autophagic vesicles by LGG-1::GFP in 3-day adult wild type, *pash-1ts* and *pash-1* rescue animals at 25°C. Images were taken by Janine Kirstein.

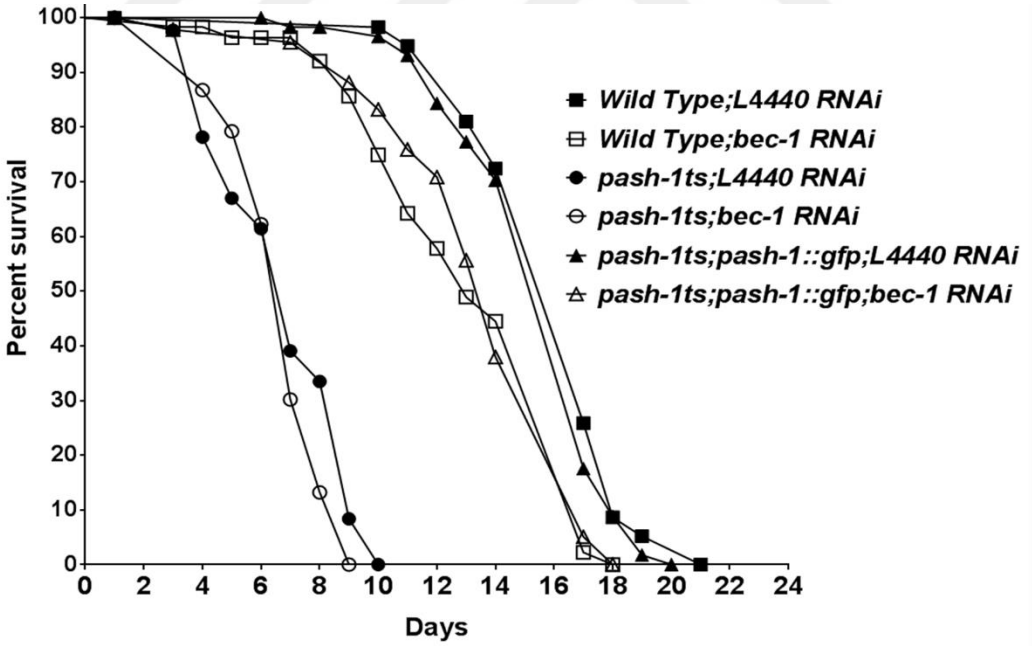

Figure 71. The effect of RNAi knock-down of *bec-1* on the life span of wild type, *pash-1ts* and *pash-1* rescue animals at 25°C.

Strain	Mean Life ± SEM (Day)	75th Percentile ± SEM (Day)	Maximal Lifespan ± SEM (Day)	% Mean Lifespan change	% 75th Percentile change	% Maximal Lifespan change	p Value (Log Rank Test)
Wild Type; L4440 RNAi	15,33 ± 0,98	17 ± 0,82	21 ± 0,47	-	-	-	-
Wild Type;bec-1 RNAi	13,33 ± 0,27	16,33 ± 0,27	18 ± 0,47	-13,05	-3,94	-14,29	<0,0001
pash-1ts; L4440 RNAi	7,33 ± 0,27	9 ± 0,47	11 ± 0,47	-	-	-	-
pash-1ts; bec-1 RNAi	7,33 ± 0,27	8,67 ± 0,54	10,50 ± 0,87	0,00	-3,67	-4,55	n.s.
pash-1ts;pash-1::gfp; L4440 RNAi	16,50 ± 0,29	17 ± 0	21 ± 0,82	-	-	-	-
pash-1ts;pash-1::gfp; bec-1 RNAi	12,33 ± 0,98	14,33 ± 1,44	17,67 ± 0,27	-25,27	-15,71	-15,86	<0,001

Table 24. The changes in the life span of wild type, *pash-1ts* and *pash-1* rescue animals following RNAi knock-down of *bec-1* at 25°C.

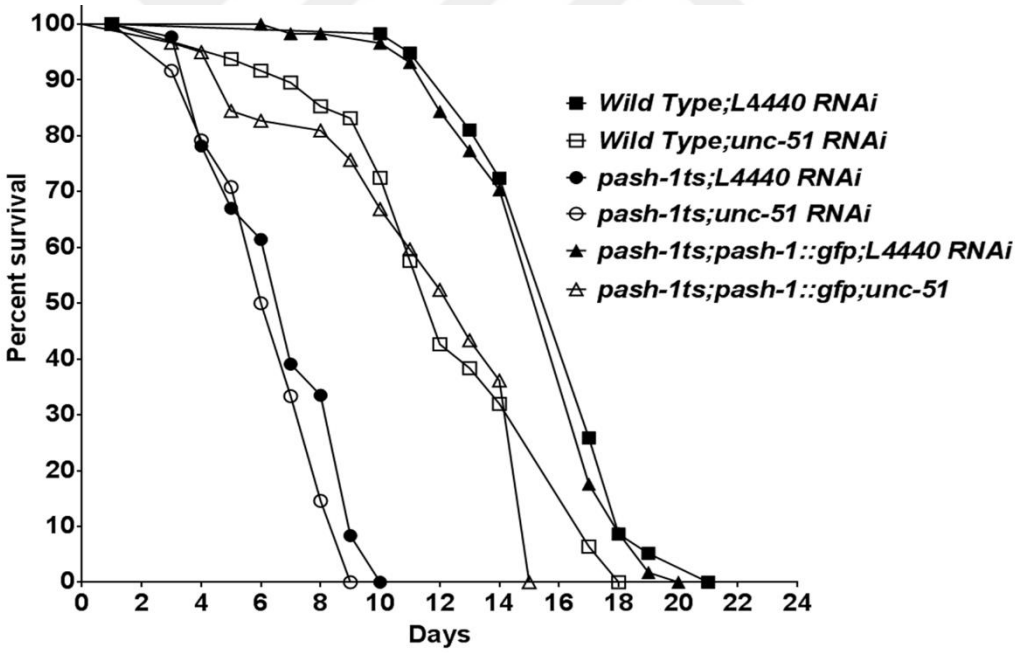

Figure 72. The effect of RNAi knock-down of *unc-51* on the life span of wild type, *pash-1ts* and *pash-1* rescue animals at 25°C.

Strain	Mean Life ± SEM (Day)	75th Percentile ± SEM (Day)	Maximal Lifespan ± SEM (Day)	% Mean Lifespan change	% 75th Percentile change	% Maximal Lifespan change	p Value (Log Rank Test)
Wild Type; L4440 RNAi	15,33 ± 0,98	17 ± 0,82	21 ± 0,47	-	-	-	-
Wild Type;unc-51 RNAi	13,33 ± 0,54	17,33 ± 0,27	18 ± 0	-13,05	1,94	-14,29	<0,0001
pash-1ts; L4440 RNAi	7,33 ± 0,27	9 ± 0,47	11 ± 0,47	-	-	-	-
pash-1ts; unc-51 RNAi	8 ± 0,94	9,33 ± 0,72	10,67 ± 0,72	9,14	3,67	-3,00	n.s.
pash-1ts;pash-1::gfp; L4440 RNAi	16,50 ± 0,29	17 ± 0	21 ± 0,82	-	-	-	-
pash-1ts;pash-1::gfp;unc-51 RNAi	12,33 ± 0,54	14 ± 1,25	16,67 ± 0,72	-25,27	-17,65	-20,62	<0,0001

Table 25. The changes in the life span of wild type, *pash-1ts* and *pash-1* rescue animals following RNAi knock-down of *unc-51* at 25°C.

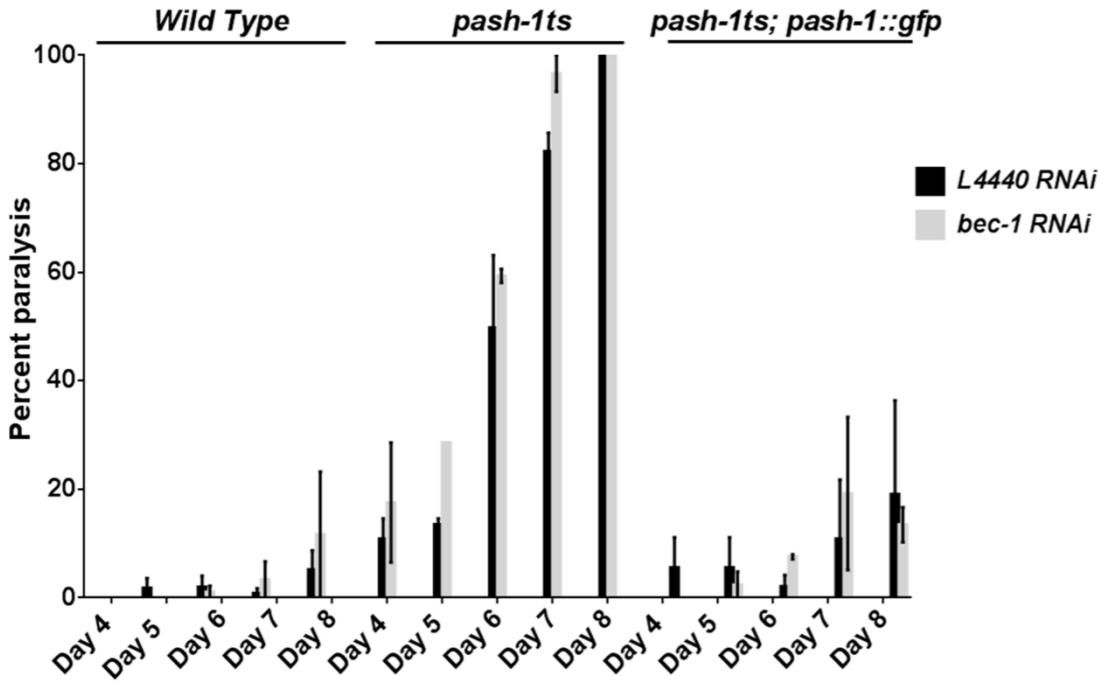

Figure 73. The effect of RNAi knock-down of *bec-1* on the motility of wild type, *pash-1ts*, and *pash-1* rescue animals on days 4 to 8 at 25°C. Results show the mean ± SEM of three independent experiment.

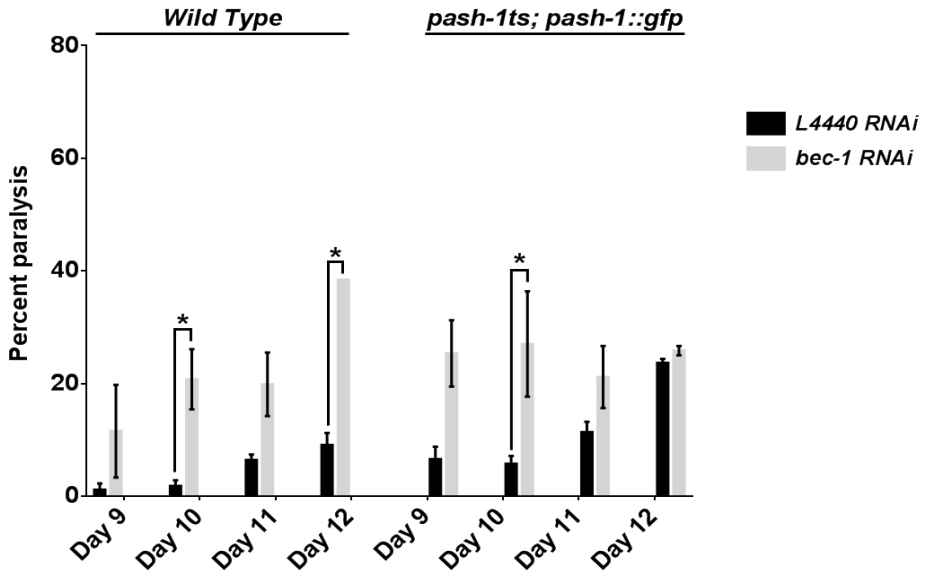

Figure 74. The effect of RNAi knock-down of *bec-1* on the motility of wild type, and *pash-1* rescue animals on days 9 to 12 at 25°C. Results show the mean ± SEM of three independent experiment (*p<0.05).

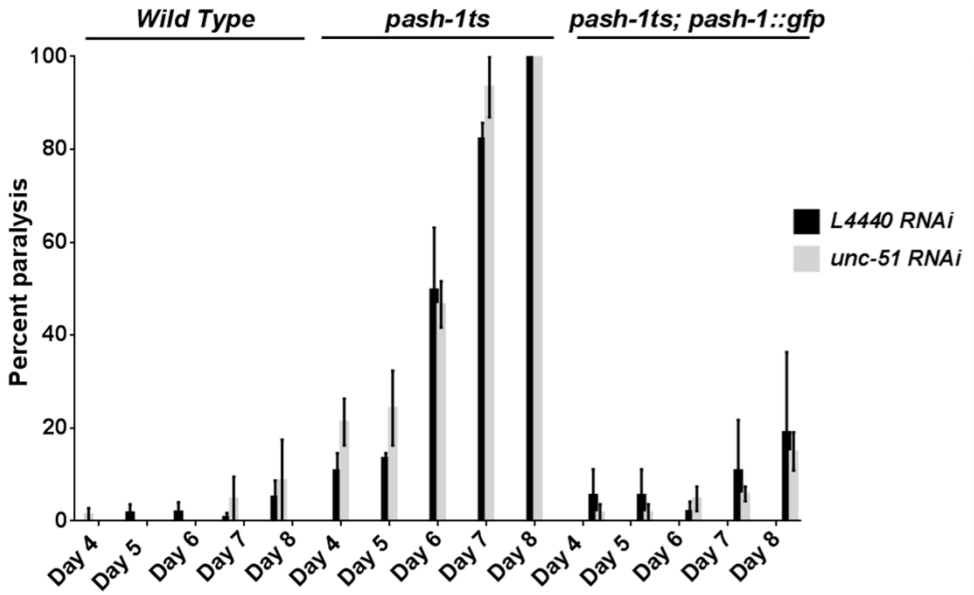

Figure 75. The effect of RNAi knock-down of *unc-51* on the motility of wild type, *pash-1ts*, and *pash-1* rescue animals on days 4 to 8 at 25°C. Results show the mean ± SEM of three independent experiment.

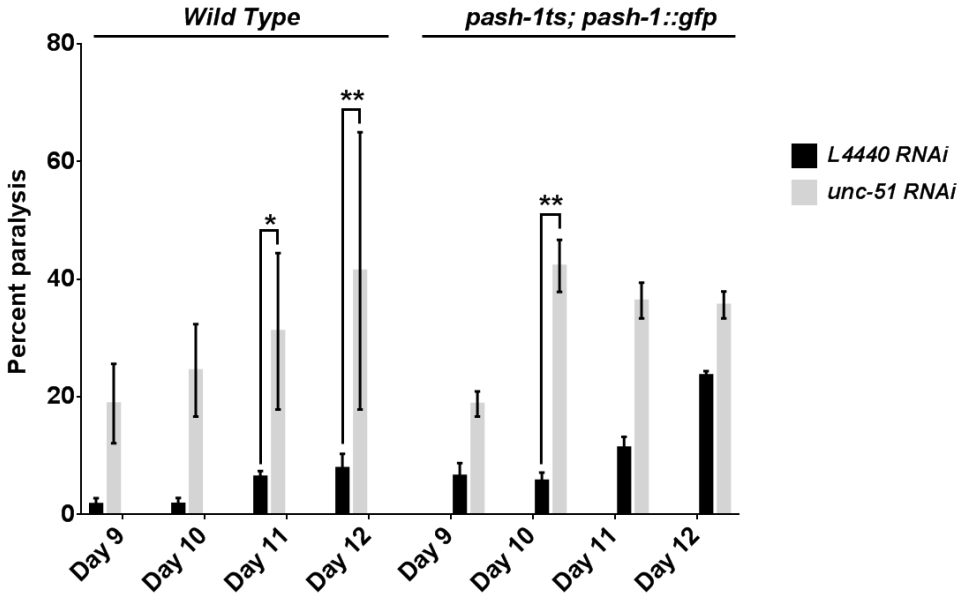

Figure 76. The effect of RNAi knock-down of *unc-51* on the motility of wild type, and *pash-1* rescue animals on days 9 to 12 at 25°C. Results show the mean ± SEM of three independent experiment (*p<0.05 and **p<0.01).

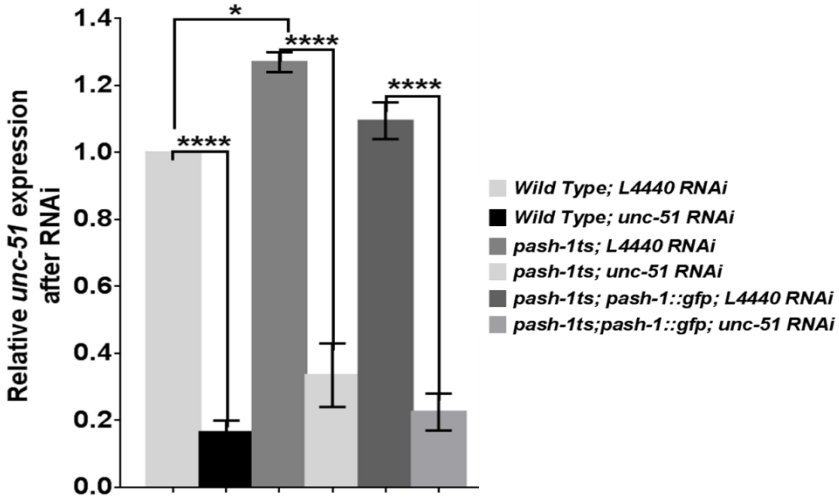

Figure 77. RNAi knock-down efficiency of *unc-51* in wild type, *pash-1ts* and *pash-1* rescue animals determined by quantitative RT-PCR on day 3 at 25°C. Results show the mean ± SEM of three independent experiments (*p<0.05, and ****p<0.0001).

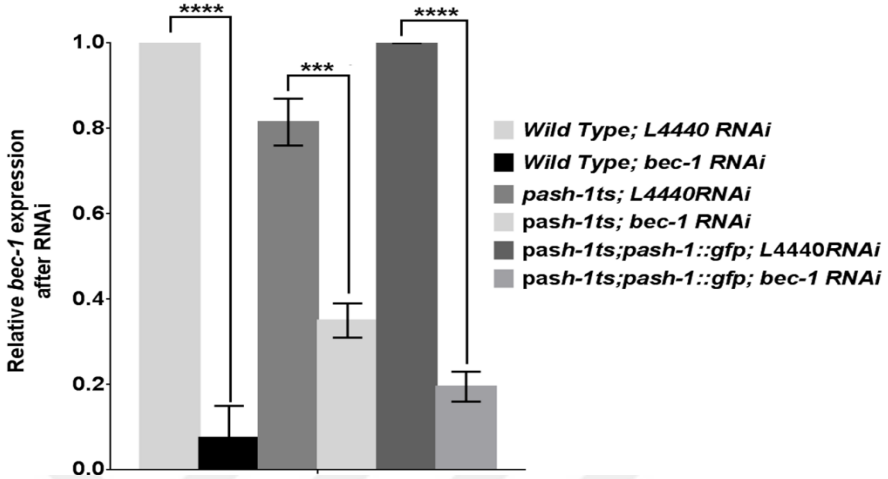

Figure 78. RNAi knock-down efficiency of *bec-1* in wild type, *pash-1ts* and *pash-1* rescue animals determined by quantitative RT-PCR on day 3 at 25°C. Results show the mean ± SEM of three independent experiments (***$p<0.001$ and ****$p<0.0001$).

CHAPTER 4: DISCUSSION

Within the last three decades, an intensive effort has been dedicated to answer one of the most fundamental questions in biology how and why do organisms age? In this regard, many studies have been investigated to examine the genes involved in aging [87]. In parallel to these studies, a growing number of evidence showed that many of the aging regulating miRNAs **(Table 1)** have been linked to stress response regulating transcription factors. For example, *lin-4* requires DAF-16 for the regulation of longevity and *mir-71* regulates the aging through DAF-16, SKN-1 and PHA-4 [64, 68, 69, 71]. However, these studies did not further address whether the defects in the animals upon the knock-out of these miRNAs are related to decline of proteostasis. Therefore, I have studied on the miRNA biogenesis defective nematodes to better understand the involvement of miRNAs in the biology of proteostasis.

To test how PN is affected upon the elimination of miRNA biogenesis, I have challenged the protein folding environment by heat shock which globally denatures the proteins and causes protein aggregations [103]. If the PN is intact, destructive effect of heat shock can be compensated. Otherwise, organisms cannot survive after heat shock. Thus, decline in thermotolerance is an indication of the defects in proteostasis [206, 207]. Our results demonstrated that animals unable to synthesize miRNAs became sensitive to heat stress.

To further investigate whether the defects in *pash-1ts* animals are related to decline of PN, I examined the toxicity of Q40m and mutated UNC-52 in the absence of miRNAs. In here, the idea is that if the PN is impaired in the suppression of miRNA biogenesis, animals should be more susceptible to proteotoxicity. Upon the elimination of miRNA biogenesis, the proteotoxicity of Q40m or mutated UNC-52 became more visible. More importantly, rapid

aging phenotype of *pash-1* could be rescued by the enhancement of proteostasis using ThT, which strongly suggests that PN is regulated by miRNAs in adult nematodes. Additionally, *pash-1ts* adult animals gave rise to more protein aggregation than wild type and *pash-1* rescue animals. It would be of great interest to determine the identity of proteins that aggregate in the absence of miRNAs. Overall, these results showed that miRNA biogenesis is necessary to ensure cellular health and prevent protein aggregation related damages in adult nematodes.

Because many temperature sensitive (ts) mutant proteins are heavily dependent on the cellular folding environment, they represent highly sensitive indicators of a disruption in proteostasis. Therefore, I investigated whether the proteostatic defects in *pash-1ts* animals is due to the aggregation of mutated PASH-1 or loss of miRNA biogenesis. To test this, I have knocked down *pash-1* by RNAi in *pash-1ts* mutant. If the proteostatic challenge is because of the aggregation of mutated PASH-1 in *pash-1ts* animals, lowering PASH-1 level should suppress the aging and aging associated defects. Neither the life span extension nor the suppression of motility have been observed in *pash-1ts* animals upon *pash-1* RNAi. Consistently, the elimination of other miRNA biogenesis genes also shortened the life span of animals. Collectively, these results suggested that miRNA biogenesis is required to prevent rapid aging phenotypes in *C. elegans*. The phenotypes observed in *pash-1ts* animals were not simply due to the aggregation of mutant PASH-1 protein.

Proteostasis compromises of a highly interconnected network (PN) integrating the regulation of stress response, molecular chaperones and protein degradation systems to control the abundance and the proper folding of proteome. As a next step, I aimed to understand which component(s) of PN is affected upon the elimination of miRNA

biogenesis. For this purpose I, first, examined whether the effect of elimination of miRNAs on proteostasis is through the alterations in proteome abundance. In recent reports, it has been shown that the proteome abundance is tightly controlled by PN and alterations in proteome composition can exhaust the proteostasis [88, 208]. Majority of mRNAs is subjected to miRNA regulation in *C. elegans*; therefore, the elimination of miRNA biogenesis can greatly influence the proteome composition and abundance [8, 201, 202]. However, RNAi knock-down of eIF4E/*ife-2* has no effect on *pash-1ts* mutant animals suggesting that proteotoxic defect in the absence of miRNAs, does not result from the altered proteome abundance.

PN is transcriptionally controlled by a set of transcription factors including HSF-1, SKN-1 and DAF-16 in *C. elegans*. Inhibition of these transcription factors can cause shortened life span and aging associated defects such as the loss of motility. Interestingly, RNAi knockdown of *hsf-1* and *skn-1* has no impact on the life span of *pash-1ts* animals while RNAi knockdown of *daf-16* slightly reduced the life span of *pash-1ts* animals compared to wild type and *pash-1* rescue animals. These results suggested that the function of HSF-1 and SKN-1 were impaired and DAF-16 was significantly lost its function in the absence of miRNAs. Based on these results, one could hypothesize that miRNAs can regulate the activity of these transcription factors either by binding to their 3' UTR or through their regulators. Indeed, HSF-1 was shown to be regulated by HSP-90, HSP-70 or DHIC **(please see 1.3.1.1 for more details)** and the mRNA level of *F44E5.4* (one HSP-70 isoform in *C. elegans*) significantly increased in *pash-1ts* mutant animals. Potentially elevated level of *F44E5.4* can prevent the nuclear localization of HSF-1 upon stress. I believe adult specific elimination of *F44E5.4* in *pash-1ts* mutant background would be valuable to further

investigate the regulation of miRNAs on HSF-1 activity. Moreover, even though *daf-21* (only member of the *hsp-90* in *C. elegans*) and other *hsp-70* isoforms were not significantly elevated in *pash-1ts,* they are still good candidates to further test the activity of HSF-1 in *pash-1ts* background. Lastly, how DHIC is regulated by miRNAs remains to be explored.

Insulin/insulin like signaling (IIS) negatively regulates DAF-16 activity **(please see 1.3.1.1 for more details)**. So far, *mir-71* and *mir-239* have been shown to antagonistically act on IIS/DAF-16 pathway in *C. elegans* [68]. Interestingly, these miRNAs have not been associated with any abnormal developmental defects suggesting that they only function in the regulation of aging through IIS/DAF-16.

It should also be taken into account stress response regulating transcription factors can act through miRNAs. Although these transcription factors are one of the highly studied genes in *C. elegans,* mostly their protein coding targets have been characterized. At this stage, assuming that they only act through protein coding genes would be underestimation of the potential targets of these factors. More studies should focus on how stress response regulating transcription factors regulate the expression of non-coding RNAs including miRNAs.

Lastly, it is also possible that miRNAs and these transcription factors can act on common targets to regulate aging and proteostasis. Relatively well known targets of stress response regulating transcription factors are molecular chaperones that take roles in protein folding [91]. Molecular chaperones show the largest transcriptional increase in response to thermal stress. Most of the molecular chaperones are regulated by HSF-1, but few of them require DAF-16 and SKN-1 suggesting that these proteins are part of a fundamental defense against

proteotoxic stress [91, 209, 210]. Hence, I analyzed the gene expression of 24 molecular chaperones by quantitative RT-PCR in *pash-1ts* animals. mRNA level of majority of the chaperones were similar to those of mRNA level in wild type and *pash-1* rescue animals. However, the transcript level of mitochondrial chaperone, *hsp-60*, and cytoplasmic small chaperones, *hsp-25, Q9N350* and *sip-1*, were decreased in *pash-1ts* animals compared to wild type and *pash-1* rescue level. On the other hand, mRNA level of *F08H9.4a*, *F44E5.4*, *F08H9.3* and *ZK1128.7*, categorized as class I chaperones, were increased in *pash-1ts* mutants compared to wild type and *pash-1* rescue animals. In addition, class II chaperones, *F08H9.4b* and *hsp-16.11*, were increased compared to wild type, these chaperones were also up regulated in *pash-1* rescue animals. Therefore, it is very unlikely that these two chaperones contribute to the phenotypes observed in *pash-1ts* animals. To address how the changes in the chaperone levels affect rapid aging of *pash-1ts* animals, one can take several approaches. To narrow down the number of the molecular chaperones to examine, the mRNA levels of these chaperones in *pash-1* overexpressing transgenic animals and ThT treated *pash-1ts* animals could be measured, the chaperones that show opposite expression patterns to *pash-1ts* animals would be most likely candidates to study further. Moreover, it would be very valuable to reduce the level of class I chaperones in *pash-1ts* animals and perform the life span assay to see whether it would cause life span extension in the absence of miRNAs, assuming that some of the overexpressed chaperones could be detrimental to *pash-1ts* animals, as this has been observed upon overexpression of *daf-21* in the wild type animals [130, 211].

To gain better understanding on how protein folding environment is negatively affected by the downregulated small heat shock proteins in *pash-1ts* animals, how the overexpression

of *hsp-60*, *sip-1*, *hsp-25* and *Q9N350* affect the lifespan of *pash-1ts* animals should be examined. To ensure overexpression of these genes, transgenes should contain a promoter and a 3' UTR sequences that devoid of miRNA mediated regulation.

I have also tested protein degradation systems involved in PN. First, I examined the mRNA level of proteasome components. Recently, increasing *pbs-5* and *rpn-6.1* have been shown to sufficient to augment the activity of proteasome in wild type animals [173, 174]. Surprisingly, these two genes were upregulated in *pash-1ts* mutants compared to wild type and *pash-1* rescue animals. However, *pash-1ts* animals did not phenocopy the *pbs-5* or *rpn-6.1* overexpressing transgenic animals. This may imply that despite the increased level of *pbs-5* and *rpn-6.1*, proteasome may not be functional in the absence of miRNAs. To address whether proteasome is functional in *pash-1ts* animals, one need to test the trypsin, chymotrypsin, and caspase-like activity. On top of these experiments, proteasome activity might be tested by the degradation of UbV-GFP, an engineered substrate of proteasome, in *pash-1ts* background [212]. Additionally, ubiquitinated protein level in *pash-1ts* animals compared to wild type and *pash-1* rescue may indicate whether ubiquitination process is under the miRNA regulation in *C. elegans*.

Proteasome machinery is assembled with the following steps: (i) biosynthesis of α and ß subunits, (ii) arrangement of α subunits with the assistance of proteasome assembling chaperones (PAC), (iii) conjugation of α and ß subunits with accessory proteins and lastly (iv) dimerization of half α-ß subunit complex **(please see 1.3.1.4 for more details)** [170]. Even though our quantitative RT-PCR analysis showed that α and ß subunits can be produced at near wild type levels in *pash-1ts* animals. The potential defects in the remaining

steps in the absence of miRNAs remain to be explored. Therefore, examining the level and activity of PAC and accessory proteins in *pash-1ts* animals might shed lights into how proteasome activity is affected in *pash-1ts* animals.

Moreover, why these genes are upregulated in *pash-1ts* mutants remain elusive. It is possible that up regulation of both components constitutes a futile effort against the increased proteotoxicity in *pash-1ts* mutants or they might be the targets of miRNAs.

Another protein degradation system in PN is autophagy. In here, our results indicated that autophagy is not functional in the absence of miRNAs. I showed that lowering the transcript level of *unc-51* and *bec-1* by RNAi does not shorten the life span of *pash-1ts* mutants while wild type and *pash-1* rescue animals are short-lived upon the RNAi knock-down of *unc-51* and *bec-1*. To further investigate the autophagic activity in miRNA biogenesis defective animals, we visualized LGG-1::GFP in *pash-1ts* animals. We observed that unlike wild type and *pash-1* rescue animals, autophagic vesicles could not be formed in *pash-1ts* mutants. Rather, LGG-1 has a diffuse cytoplasmic localization in the absence of miRNAs. Overall, these results suggested that autophagy was impaired in the absence of miRNAs. One reason behind the inactivation of autophagy in *pash-1ts* animals might be the hyper-activation of negative regulators of autophagy. For example, TOR suppresses the induction of autophagy by preventing the phosphorylation of UNC-51 [158]. Therefore, I speculate that TOR might be hyper-active in the absence of miRNAs. To test this, one can potentially knock down the components of TOR complex by RNAi and visualize the formation of autophagic vesicles by LGG-1::GFP in *pash-1ts* animals. Moreover, recently HSF-1 has been proposed to induce the autophagy in *C. elegans*. Another reason of failure of autophagy induction in *pash-1ts* animals might be due to impaired HSF-1 activity [213].

Using tissue specific *pash-1* rescue lines Lehrbach and his colleagues have shown that neuronal rescue of miRNA biosynthesis almost completely restores the life span similar to wild type levels [8]. Another report showed that *mir-71* expression in neurons alone regulates the longevity through the modulation of transcriptional activity of DAF-16 in the intestine [64]. These suggested that some of the cellular functions controlled by miRNAs influence the life span in a cell non-autonomous manner. Proteostasis might be the one of these mechanisms because growing number of reports indicated that proteostasis is also regulated by cell non-autonomous manner. Tissue specific gene expression studies showed that neuronal overexpression of HSF-1 can extend the life span of nematodes in intestinal *daf-16* expression dependent manner [214]. Moreover, challenging the proteostasis in a particular tissue can lead to upregulation of chaperones in other tissues [130].

CHAPTER 5: CONCLUSION

Overall, this thesis has focused on the identification the roles of miRNAs in proteostasis network in adult *C. elegans*. Since intact proteostasis is necessary for the healthy aging, I asked whether the rapid aging phenotype of animals, unable to synthesize miRNA, is due to decline in proteostatic capacity. In regard to this, I have first studied on the effect of disrupting miRNA biogenesis on proteotoxicity. Then I systemically analyzed the components of proteostasis network in the animals unable to synthesize miRNAs. This study proposes that miRNAs are involved in many aspects of proteostasis in *C. elegans*. In future, which miRNA(s) is required for functional proteostasis not only in *C. elegans*, but also in other animals will be of great interest to understand not only the biology of proteostasis, but also for the diagnostic and therapeutic purposes against aging associated diseases.

Moreover, even though I have examined the involvement of miRNAs in aging through the regulation of proteostasis, it does not exclude the possibility of the effects of miRNAs on aging through other cellular processes. For example, it has been suggested that miRNAs can also regulate the aging by affecting the metabolism and genomic stability [8, 68, 215].

APPENDIX

Strain Name	Genotype
N2	*Wild Type*
SAR55	*pash-1(mj100)*
SX1359	*pash-1(mj100); mjEx331 [eft-3p::pash-1::GFP::unc-54 3'UTR + myo-2p::mCherry::unc-54 3'UTR]*
SAR93	*funIs001[eft-3::pash-1::GFP::unc-54 3' UTR + myo-2p::mCherry:: unc-54 3' UTR]*
SAR94	*mjEx331 [eft-3p::pash-1::GFP::unc-54 3'UTR + myo-2p::mCherry::unc-54 3'UTR]*
AM141	*rmIs133 [unc-54p::Q40::YFP]*
SAR54	*pash-1(mj100); rmIs133 [unc-54p::Q40::YFP]*
SAR60	*pash-1(mj100); rmIs133 [unc-54p::Q40::YFP]; mjEx331 [eft-3p::pash-1::GFP::unc-54 3'UTR + myo-2p::mCherry::unc-54 3'UTR]*
SAR16	*unc-52(e669su250)II*
SAR15	*pash-1(mj100) I, unc-52(e669su250)II*
SAR35	*pash-1(mj100) I; unc-52(e669su250)II; mjEx331 [eft-3p::pash-1::GFP::unc-54 3' UTR + myo-2p::mCherry::unc-54 3' UTR]*
DA2123	*adIs2122 [lgg-1p::GFP::lgg-1 + rol-6(su1006)]*
SAR30	*pash-1(mj100); adIs2122 [lgg-1p::GFP::lgg-1 + rol-6(su1006)]*
SAR92	*pash-1 (mj100) I; adIs2122[lgg-1::GFP::lgg-1 + rol-6(su1006)]; mjEx331[eft-3p::pash-1::gfp+myo-2p::mCherry]*

Appendix 1. Strains used in the study.

	Forward (5' to 3')	Reverse (5' to 3')
cdc-42	CTGCTGGACAGGAAGATTACG	CTCGGACATTCTCGAATGAAG
unc-51	GAATCAGACAACATGCTCCACATCC	GGTAGGGCTCCGTGATCCATT
bec-1	GCCAGATTCAGCGGATTCCGA	CGAAGAGCGTCAGAGCAATCATTACA
daf-21	CTTGACAAGATTCGCTACCAG	GCTTGAAGAGCCTCCATGAAGG
C12C8.1	ACTCATGTGTCGGTATTTATC	ACGGGCTTTCCTTGTTTT
F44E5.4	AATGAACCAACTGCTGCTGCTCTT	TGTCCTTTCCGGTCTTCCTTTTG
hsp-1	CTCGAGTCATACGCCTTCAACCTTA	GGCCAATCCTTCCAAATCCTTCTG
hsp-4	GGGGACAATCATTGGTATCG	ACGCAACGTATGATGGAGTG
hsp-6	GTTATCGAGAACGCAGAAGGAG	CATCCTTAGTAGCTTGACGCTG
hsp-60	CATGCTCGTCGGAGTCAAC	TTTGTGATCTTTGGGCTTCC
hsp-43a	CTTCTCATTCTTACAGCTACCA	CCAGCAGTATTATATGACCCACTTG
hsp-43b	CTTCTCATTCTTACAGCTACCA	CTGTCCGCTCACTTGTTGTG
hsp-25	CTTCGTCTCAGATTTGACGTAGCT	GAAGGAATTCCTGGTTGTACTCTCT
hsp-16.49	CAATTTTTCCGACAATATTGGAGAGATTGT	GATCGTTTCGAGTATCCATGCTCT
hsp-16.48	TTTCCGACAATATTGGAGAGATTGTAA	CGTTTCGAGTATCCATGCTCTGAT
hsp-16.41	CCGATAATATTGGGGAGATTGTAAATGA	CAAGTATCCATGTTCCGATTTTGTTTC
hsp-16.11	GGCTCAGATGGAACGTCAA	GCTTGAACTGCGAGACATTG
hsp-16.2	ACTTTACCACTATTTCCGTCCAGC	CCTTGAACCGCTTCTTTCTTTG
hsp-16.1	CTCCATCTGAATCTTCTGAGATTGTT	CCATGTTCAGTCTTTAATTCTTGTTCTCC
sip-1	ACAACATCGTGCCACAACAG	TGGTCATCTGTCCTTCCTTG
F08H9.3	CAGATTGTCGGAATGAGATTGTCG	GACGTCAACATCTTCTGGCAAG
F08H9.4a	CCAATGACCGATGATTCTGAGATAATG	CACCATGTTCATTCTCCACGTC
F08H9.4b	GCTGTAAATCTCAATGTCTCCAACT	CTTGAGAACGACTTTCTCGATGC
Q9N350	ATTCCAGGAATGCCGGACCT	CGACGACGGTTACCTTTAACGA
ZK128.7	GTTTTTCGAGAAAGTACTCAATCCCG	GAGTTGTTGGGTGATAGCTTGAG
hsp-12.6	ATGATGAGCGTTCCAGTGATGGCTGACG	TTAATGCATTTTTCTTGCTTCAATGTGAAGAATTCC
hsp-12.3	AAAGGAGATGGAGTTGTTAAGGTTCTG	GTGTGAGCCATGTGGATCTCA
hsp-12.2	GACGGAGTTGTCAAGGTCCA	TCACTGCGGGTCTCGTGA
hsp-12.1	CCTTCAGCATAACGATGGTGTC	ACGATTATCATGTCGCAAATG
pas-1	GGCTGATCTCAACCAGTATTACACA	GAACAAAAGAGCACATCCCAAAC
pas-2	CGGCCGTAATGCAGGAATAT	AAGAAGCGATGCTCCAAACG
pas-3	CGGAGAGGAAATGCCAGTTG	ACGGTCTCTTTCCTCCAATCTG
pas-4	GTCGTACCACCAGGATCACAAA	TGCTGCAGCTCATCATTAACTTTT
pas-5	CAACATATTGGCGTCACATTCG	TGCCCGTTCGACCAGAGT
pas-6	CGAGAAATCAACTCCGGAACA	AAGTGTGTCGCGAAGAGCAA
pas-7	TTTCCAAGTCGAGTACGCTCAA	TTGCCACGAATTGCAATCAT
pbs-1	TCAGCACTGGAACCACTCTCA	TCGGTTCCGACGACAACTC
pbs-2	ATTTTGGAGCGTGATTTTAAGGTT	GGCGCGTTGGACAAGCT
pbs-3	GCTCCACGCGATTTCGTT	GCGCCAGAAGTTTTCACAAAC
pbs-4	GGGCAACAGCCGTACTTGTT	CGATCCATAATGGCATAGCAGAA
pbs-5	CTGCAATTTGTGCCACATCAC	TCACGTCCATTGGTGGAAGA
pbs-6	GATATGAGCGTCCGGAACTCA	ACGGAACGAATCCTTCATCAA
pbs-7	CTCTACGCCAAACGTTGCAA	ACTCCGGCGACAACAAGTG
rpt-1	TGGAAACATCAAGGTGCTTATGG	CTCATGAGAGCGGGATCGA
rpt-2	CCTGACGCCGCTAGCAAA	GCAACTTCAGACGGCATCTG
rpt-3	TGGAGAAGGACCACGAATGG	GATGGGCTGTTTTCCTTTGC
rpt-4	GTCAAGTTGTCCGACGGATTC	TGGCAAACATTCCAGCTTCTG
rpt-5	GAAGATGAATGTCAACAAGGATGTAAA	TGCATTGTGCTCCGTTGAAG
rpt-6	CCGAAGAATCCGATGAGAAAAC	CACTTTTTGCTGCGCATCA
rpn-1	CGGAAAGCCAAAGACAATCAC	GAGATATTCATCGTTCGCCAACT
rpn-2	TGACATTGTTGAACAGATGGAGATC	TGCGGCTGCGTTTGAA
rpn-3	ATACATTGTGGCGAAGGCTATTG	TGTACCGAGGTCCATCACGAA
rpn-5	GGAGAGCACAACATGCGTATGA	CAGCGAGACGTTCGAAAGTG
rpn-6.1	AATATTGGAAAAGCACCTGAAATGT	TTTGATGTGGAAGTGAAGTCATTGT
rpn-6.2	AACTTGGCGAAGGCAAAGAC	AAGCAAACGCCGAATTGGT
rpn-7	TCATTCAGTTGGCCGCTCTT	TGTGGCGATAGATAGCGATCAA
rpn-8	TCAGGAAGTTCACGATGATGGA	TCTGAAGGCACATGCTCGAA
rpn-9	GGGTGCAGCCAAGAGTTTTAGA	GGAGTTGACATCGTTCCTCCAT
rpn-10	AGTACTATGATTTGTGTCGACAATTCG	GGAGCCGAGTTGGTTGGAA
rpn-11	ACGTTTTCGCTATGCCACAGT	TGGATCGACCGCTTCGA
rpn-12	CAAAGGAGCCAAAAGATCTTGTC	CACTGAGAACCTTCGTCAACTCA
drsh-1	CATATGGCAATAAATGGAGAGGA	TGGGTCGAAACACTCATCAGGC
dcr-1	CAAAGCAAGCCCGTGTTGGT	CAATTCATCACCTTCAGCGTTGG
alg-1/2	CAATTACCTGGCGGCAACCA	CAAGCAGCTGATAATCTCGCGAT
pash-1	GAAGGCGTCAAAAATCCTGCACAG	TTTAAAACTGGAACTGGAGCCCG
daf-16	CGAAGCCGATTAAGACGGAACCA	CGGTAGTGGCATTGGCTTGAAGT
hsf-1	GAAATGTTTTGCCGCATTTT	CCTTGGGACAGTGGAGTCAT
skn-1	ACCAAACGATGTGTTCCC	TGTGAGTGATATGGATCGAAC
ife-2	GCAACTGGACCTGGTGGTATCTGA	CTGATGGTGGATTGAGCCCACT

Appendix 2. List of primers used in the study.

BIBLIOGRAPHY

1. Wightman, B., I. Ha, and G. Ruvkun, *Posttranscriptional regulation of the heterochronic gene lin-14 by lin-4 mediates temporal pattern formation in C. elegans.* Cell, 1993. **75**(5): p. 855-862.
2. Pasquinelli, A.E., et al., *Conservation of the sequence and temporal expression of let-7 heterochronic regulatory RNA.* Nature, 2000. **408**(6808): p. 86-89.
3. Lee, R.C., R.L. Feinbaum, and V. Ambros, *The C. elegans heterochronic gene lin-4 encodes small RNAs with antisense complementarity to lin-14.* Cell, 1993. **75**: p. 843-854.
4. Reinhart, B.J., et al., *The 21-nucleotide let-7 RNA regulates developmental timing in Caenorhabditis elegans.* Nature, 2000. **403**(6772): p. 901-906.
5. Bartel, D.P., *MicroRNAs.* Cell, 2004. **116**(2): p. 281-297.
6. Brennecke, J., et al., *bantam Encodes a Developmentally Regulated microRNA that Controls Cell Proliferation and Regulates the Proapoptotic Gene hid in Drosophila.* Cell, 2003. **113**(1): p. 25-36.
7. Lewis, B.P., C.B. Burge, and D.P. Bartel, *Conserved Seed Pairing, Often Flanked by Adenosines, Indicates that Thousands of Human Genes are MicroRNA Targets.* Cell, 2005. **120**(1): p. 15-20.
8. Lehrbach, N.J., et al., *Post-develpmental microRNA expression is required for normal physiology, and regulates aging in parallel to insulin/IGF-1 signaling in C. elegans.* RNA, 2012. **18**: p. 2220-2235.
9. Brenner, S., *The genetics of Caenorhabditis elegans.* Genetics, 1974. **77**(1): p. 71-94.

10. Raizen, D.M., et al., *Lethargus is a Caenorhabditis elegans sleep-like state.* Nature, 2008. **451**(7178): p. 569-572.

11. Ward, S. and J. Carrel, *Fertilization and sperm competition in the nematode Caenorhabditis elegans.* Dev Biol, 1979. **73**(2): p. 304-321.

12. Golden, J.W. and D.L. Riddle, *The Caenorhabditis elegans dauer larva: Developmental effects of pheromone, food, and temperature.* Developmental Biology, 1984. **102**(2): p. 368-378.

13. Chalfie, M., et al., *Green fluorescent protein as a marker for gene expression.* Science, 1994. **263**: p. 802-805.

14. Sulston, J.E. and H.R. Horvitz, *Post-embryonic cell lineages of the nematode Caenorhabditis elegans.* Dev. Biol, 1977. **56**: p. 110-156.

15. Kimble, J. and D. Hirsh, *The postembryonic cell lineages of the hermaphrodite and male gonads in Caenorhabditis elegans.* Developmental Biology, 1979. **70**(2): p. 396-417.

16. Sulston, J.E., et al., *The embryonic cell lineage of the nematode Caenorhabditis elegans.* Developmental Biology, 1983. **100**(1): p. 64-119.

17. Chamberlain, J.S. and G.M. Benian, *Muscular dystrophy: The worm turns to genetic disease.* Current Biology. **10**(21): p. R795-R797.

18. Benian, G.M. and H.F. Epstein, *Caenorhabditis elegans Muscle A Genetic and Molecular Model for Protein Interactions in the Heart.* 2011. **30322**.

19. Zarkower, D., *Somatic sex determination* WormBook

2006: p. 1-12.

20. C. elegans Sequencing Consortium, *Genome Sequence of the Nematode C. elegans: A Platform for Investigating Biology.* Science, 1998. **282**(5396): p. 2012.

21. Schwarz, E.M., *Genomic classification of protein-coding gene families* 2005: p. 1-23.

22. Kaletta, T. and M.O. Hengartner, *Finding function in novel targets: C. elegans as a model organism.* Nat Rev Drug Discov, 2006. **5**(5): p. 387-399.

23. Shaye, D.D. and I. Greenwald, *OrthoList: A Compendium of C. elegans Genes with Human Orthologs.* PLOS ONE, 2011. **6**(5): p. e20085.

24. Kamath, R.S., et al., *Systematic functional analysis of the Caenorhabditis elegans genome using RNAi.* Nature, 2003. **421**(6920): p. 231-237.

25. Fire, A., et al., *Potent and specific genetic interference by double-stranded RNA in Caenorhabditis elegans.* Nature, 1998. **391**(6669): p. 806-811.

26. Markaki, M. and N. Tavernarakis, *Modeling human diseases in Caenorhabditis elegans.* Biotechnology Journal, 2010. **5**(12): p. 1261-1276.

27. Golden, J.W. and D.L. Riddle, *A pheromone-induced developmental switch in Caenorhabditis elegans: Temperature-sensitive mutants reveal a wild-type temperature-dependent process.* Proceedings of the National Academy of Sciences, 1984. **81**(3): p. 819-823.

28. Thomas, J.H., D.A. Birnby, and J.J. Vowels, *Evidence for Parallel Processing of Sensory Information Controlling Dauer Formation in Caenorhabditis Elegans.* Genetics, 1993. **134**(4): p. 1105-1117.

29. Xu, P., et al., *The Drosophila MicroRNA Mir-14 Suppresses Cell Death and Is Required for Normal Fat Metabolism.* Current Biology, 2003. **13**(9): p. 790-795.

30. Kaufman, E.J. and E.A. Miska, *Seminars in Cell & Developmental Biology The microRNAs of Caenorhabditis elegans.* Seminars in Cell and Developmental Biology, 2010. **21**(7): p. 728-737.

31. Kim, V.N., J. Han, and M.C. Siomi, *Biogenesis of small RNAs in animals.* Nat Rev Mol Cell Biol, 2009. **10**(2): p. 126-139.

32. Ha, M. and V.N. Kim, *Regulation of microRNA biogenesis.* Nat Rev Mol Cell Biol, 2014. **15**(8): p. 509-524.

33. Okamura, K., *Diversity of animal small RNA pathways and their biological utility.* Wiley Interdisciplinary Reviews: RNA, 2012. **3**(3): p. 351-368.

34. Lee, Y., et al., *MicroRNA genes are transcribed by RNA polymerase II.* The EMBO Journal, 2004. **23**(20): p. 4051-4060.

35. Cai, X., C.H. Hagedorn, and B.R. Cullen, *Human microRNAs are processed from capped, polyadenylated transcripts that can also function as mRNAs.* RNA, 2004. **10**(12): p. 1957-1966.

36. Denli, A.M., et al., *Processing of primary microRNAs by the Microprocessor complex.* Nature, 2004. **432**(7014): p. 231-235.

37. Basyuk, E., et al., *Retroviral Genomic RNAs Are Transported to the Plasma Membrane by Endosomal Vesicles.* Developmental Cell, 2003. **5**(1): p. 161-174.

38. Lund, E., et al., *Nuclear Export of MicroRNA Precursors.* Science, 2004. **303**(5654): p. 95.

39. Büssing, I., et al., *The nuclear export receptor XPO-1 supports primary miRNA processing in C. elegans and Drosophila.* The EMBO Journal, 2010. **29**(11): p. 1830-1839.

40. Grishok, A., et al., *Genes and Mechanisms Related to RNA Interference Regulate Expression of the Small Temporal RNAs that Control C. elegans Developmental Timing.* Cell, 2001. **106**(1): p. 23-34.

41. Hutvágner, G., et al., *A Cellular Function for the RNA-Interference Enzyme Dicer in the Maturation of the let-7 Small Temporal RNA.* Science, 2001. **293**(5531): p. 834.

42. Ketting, R.F., et al., *Dicer functions in RNA interference and in synthesis of small RNA involved in developmental timing in C. elegans.* Genes & Development, 2001. **15**(20): p. 2654-2659.

43. Lagos-Quintana, M., et al., *Identification of Novel Genes Coding for Small Expressed RNAs.* Science, 2001. **294**(5543): p. 853.

44. Westholm, J.O. and E.C. Lai, *Mirtrons: microRNA biogenesis via splicing.* Biochimie, 2011. **93**(11): p. 1897-1904.

45. Aravin, A.A., et al., *The Small RNA Profile during Drosophila melanogaster Development.* Developmental Cell, 2003. **5**(2): p. 337-350.

46. Lagos-Quintana, M., et al., *New microRNAs from mouse and human.* RNA, 2003. **9**(2): p. 175-179.

47. Alvarez-Saavedra, E. and H.R. Horvitz, *Many families of Caenorhabditis elegans microRNAs are not essential for development or viability.* Current biology : CB, 2010. **20**(4): p. 367-373.

48. Miska, E.A., et al., *Most Caenorhabditis elegans microRNAs Are Individually Not Essential for Development or Viability.* PLOS Genetics, 2007. **3**(12): p. e215.

49. Ambros, V., *MicroRNAs: Genetically Sensitized Worms Reveal New Secrets.* Current Biology, 2010. **20**(14): p. R598-R600.

50. Brenner, J.L., et al., *Identification of mutant phenotypes associated with loss of individual microRNAs in sensitized genetic backgrounds in Caenorhabditis elegans.* Current biology : CB, 2010. **20**(14): p. 1321-1325.

51. Eacker, S.M., T.M. Dawson, and V.L. Dawson, *Understanding microRNAs in Neurodegeneration.* Nature reviews. Neuroscience, 2009. **10**(12): p. 837-841.

52. Johnson, C.D., et al., *The let-7 MicroRNA Represses Cell Proliferation Pathways in Human Cells.* Cancer Research, 2007. **67**(16): p. 7713.

53. Sherrard, R., et al., *miRNAs cooperate in apoptosis regulation during C . elegans development.* 2017: p. 209-222.

54. Wightman, B., et al., *Negative regulatory sequences in the necessary to generate a temporal switch during Caenorhabditis elegans development.* 1991: p. 1813-1824.

55. Slack, F.J., et al., *The lin-41 RBCC Gene Acts in the C. elegans Heterochronic Pathway between the let-7 Regulatory RNA and the LIN-29 Transcription Factor.* Molecular Cell, 2000. **5**(4): p. 659-669.

56. Boyerinas, B., et al., *The role of let-7 in cell differentiation and cancer.* 2010.

57. Shaw, W.R., et al., *The Conserved miR-51 microRNA Family Is Redundantly Required for Embryonic Development and Pharynx Attachment in Caenorhabditis elegans.* Genetics, 2010. **185**(3): p. 897-905.

58. Pierce-Shimomura, J.T., et al., *The homeobox gene lim-6 is required for distinct chemosensory representations in C. elegans.* Nature, 2001. **410**(6829): p. 694-698.

59. Chang, S., et al., *MicroRNAs act sequentially and asymmetrically to control chemosensory laterality in the nematode.* Nature, 2004. **430**(7001): p. 785-789.

60. Johnston, R.J., et al., *MicroRNAs acting in a double-negative feedback loop to control a neuronal cell fate decision.* Proceedings of the National Academy of Sciences of the United States of America, 2005. **102**(35): p. 12449-12454.

61. Simon, D.J., et al., *The MicroRNA miR-1 Regulates a MEF-2-Dependent Retrograde Signal at Neuromuscular Junctions.* Cell, 2008. **133**(5): p. 903-915.

62. Vidigal, J.A. and A. Ventura, *The biological functions of miRNAs: lessons from in vivo studies.* Trends in Cell Biology, 2015. **25**(3): p. 137-147.

63. Kato, M., et al., *Age-associated changes in expression of small, noncoding RNAs, including microRNAs, in C. elegans.* RNA, 2011. **17**(10): p. 1804-1820.

64. Boulias, K. and H.R. Horvitz, *Article The C . elegans MicroRNA mir-71 Acts in Neurons to Promote Germline-Mediated Longevity through Regulation of DAF-16 / FOXO.* Cell Metabolism, 2012. **15**(4): p. 439-450.

65. Smith-Vikos, T. and F.J. Slack, *MicroRNAs and their roles in aging.* Journal of Cell Science, 2012. **125**(1): p. 7-17.

66. Ibáñez-Ventoso, C. and M. Driscoll, *MicroRNAs in C. elegans Aging: Molecular Insurance for Robustness?* Current Genomics, 2009. **10**(3): p. 144-153.

67. Griffiths-Jones, S., et al., *MicroRNA evolution by arm switching.* EMBO reports, 2011. **12**(2): p. 172.

68. Lencastre, A.D., et al., *MicroRNAs both promote and antagonize longevity in C. elegans.* 2011. **20**(24): p. 2159-2168.

69. Boehm, M. and F. Slack, *A developmental timing microRNA and its target regulate life span in C. elegans.* Science (New York, N.Y.), 2005. **310**(5756): p. 1954-1957.

70. Baugh, L.R. and P.W. Sternberg, *DAF-16/FOXO Regulates Transcription of cki-1/Cip/Kip and Repression of lin-4 during C. elegans L1 Arrest.* Current Biology, 2006. **16**(8): p. 780-785.

71. Smith-Vikos, T., et al., *MicroRNAs mediate dietary-restriction-induced longevity through PHA-4/FOXA and SKN-1/Nrf transcription factors.* Current biology : CB, 2014. **24**(19): p. 2238-2246.

72. Dallaire, A., et al., *Down regulation of miR-124 in both Werner syndrome DNA helicase mutant mice and mutant Caenorhabditis elegans wrn-1 reveals the importance of this microRNA in accelerated aging.* Aging (Albany NY), 2012. **4**(9): p. 636-647.

73. Niccoli, T. and L. Partridge, *Ageing as a Risk Factor for Disease.* Current Biology, 2012. **22**(17): p. R741-R752.

74. Uno, M. and E. Nishida, *Lifespan-regulating genes in C. elegans.* 2016(August 2015).

75. López-Otín, C., et al., *The Hallmarks of Aging.* Cell, 2013. **153**(6): p. 1194-1217.

76. Moskalev, A.A., et al., *The role of DNA damage and repair in aging through the prism of Koch-like criteria.* Ageing Research Reviews, 2013. **12**(2): p. 661-684.

77. Blackburn, E.H., C.W. Greider, and J.W. Szostak, *Telomeres and telomerase: the path from maize, Tetrahymena and yeast to human cancer and aging.* Nat Med, 2006. **12**(10): p. 1133-1138.

78. Harries, L.W., et al., *Human aging is characterized by focused changes in gene expression and deregulation of alternative splicing.* Aging cell, 2011. **10**(5): p. 868-878.

79. Shaw, A.C., et al., *Aging of the Innate Immune System.* Current opinion in immunology, 2010. **22**(4): p. 507-513.

80. Green, D.R., L. Galluzzi, and G. Kroemer, *Mitochondria and the autophagy-inflammation-cell death axis in organismal aging.* Science (New York, N.y.), 2011. **333**(6046): p. 1109-1112.

81. Douglas, P.M. and A. Dillin, *Protein homeostasis and aging in neurodegeneration.* The Journal of Cell Biology, 2010. **190**(5): p. 719-729.

82. Taylor, R.C. and A. Dillin, *Aging as an Event of Proteostasis Collapse.* Cold Spring Harbor Perspectives in Biology, 2011. **3**(5): p. a004440.

83. Klass, M.R., *Aging in the nematode Caenorhabditis elegans: Major biological and environmental factors influencing life span.* Mechanisms of Ageing and Development, 1977. **6**: p. 413-429.

84. Johnson, T.E. and W.B. Wood, *Genetic analysis of life-span in Caenorhabditis elegans.* Proceedings of the National Academy of Sciences, 1982. **79**(21): p. 6603-6607.

85. Klass, M., P.N. Nguyen, and A. Dechavigny, *Age-correlated changes in the DNA template in the nematode Caenorhabditis elegans.* Mechanisms of Ageing and Development, 1983. **22**(3): p. 253-263.

86. Kenyon, C., et al., *A C. elegans mutant that lives twice as long as wild type.* Nature 1993.

87. Johnson, T.E., *25 Years after age-1: Genes, Interventions and the Revolution in Aging Research.* Experimental gerontology, 2013. **48**(7): p. 640-643.

88. Walther, Dirk M., et al., *Widespread Proteome Remodeling and Aggregation in Aging C. elegans.* Cell, 2015. **161**(4): p. 919-932.

89. Labbadia, J. and R.I. Morimoto, *The Biology of Proteostasis in Aging and Disease.* Annual review of biochemistry, 2015. **84**: p. 435-464.

90. David, D.C., et al., *Widespread Protein Aggregation as an Inherent Part of Aging in C. elegans.* PLoS Biology, 2010. **8**(8): p. e1000450.

91. Hsu, A.-L., C.T. Murphy, and C. Kenyon, *Regulation of Aging and Age-Related Disease by DAF-16 and Heat-Shock Factor.* Science, 2003. **300**(5622): p. 1142.

92. Morley, J.F., et al., *The threshold for polyglutamine-expansion protein aggregation and cellular toxicity is dynamic and influenced by aging in Caenorhabditis elegans.* Proceedings of the National Academy of Sciences of the United States of America, 2002. **99**(16): p. 10417-10422.

93. Morley, J.F. and R.I. Morimoto, *Regulation of Longevity in Caenorhabditis elegans by Heat Shock Factor and Molecular Chaperones.* Molecular Biology of the Cell, 2004. **15**(2): p. 657-664.

94. Knowles, T.P.J., M. Vendruscolo, and C.M. Dobson, *The amyloid state and its association with protein misfolding diseases.* Nat Rev Mol Cell Biol, 2014. **15**(6): p. 384-396.

95. Labbadia, J. and R.I. Morimoto, *Repression of the heat shock response is a programmed event at the onset of reproduction.* Molecular cell, 2015. **59**(4): p. 639-650.

96. Haigis, M.C. and B.A. Yankner, *The Aging Stress Response.* Molecular cell, 2010. **40**(2): p. 333-344.

97. Kourtis, N. and N. Tavernarakis, *Cellular stress response pathways and ageing: intricate molecular relationships.* The EMBO Journal, 2011. **30**(13): p. 2520-2531.

98. Ben-Zvi, A., E.A. Miller, and R.I. Morimoto, *Collapse of proteostasis represents an early molecular event in Caenorhabditis elegans aging.* Proceedings of the National Academy of Sciences of the United States of America, 2009. **106**(35): p. 14914-14919.

99. Shemesh, N., N. Shai, and A. Ben-Zvi, *Germline stem cell arrest inhibits the collapse of somatic proteostasis early in Caenorhabditis elegans adulthood.* Aging Cell, 2013. **12**(5): p. 814-822.

100. Henis-Korenblit, S., et al., *Insulin/IGF-1 signaling mutants reprogram ER stress response regulators to promote longevity.* Proceedings of the National Academy of Sciences of the United States of America, 2010. **107**(21): p. 9730-9735.

101. Tullet, J.M.A., et al., *Direct inhibition of the longevity promoting factor SKN-1 by Insulin-like signaling in C. elegans.* Cell, 2008. **132**(6): p. 1025-1038.

102. Ogg, S., et al., *The Fork head transcription factor DAF-16 transduces insulin-like metabolic and longevity signals in C. elegans.* Nature, 1997. **389**(6654): p. 994-999.

103. Lithgow, G.J., et al., *Thermotolerance and extended life-span conferred by single-gene mutations and induced by thermal stress.* Proceedings of the National Academy of Sciences of the United States of America, 1995. **92**(16): p. 7540-7544.

104. Volovik, Y., et al., *Temporal Requirements of Heat Shock Factor-1 for Longevity Assurance.* Aging cell, 2012. **11**(3): p. 491-499.

105. Hajdu-Cronin, Y.M., W.J. Chen, and P.W. Sternberg, *The L-Type Cyclin CYL-1 and the Heat-Shock-Factor HSF-1 Are Required for Heat-Shock-Induced Protein Expression in Caenorhabditis elegans.* Genetics, 2004. **168**(4): p. 1937-1949.

106. Xiao, X., et al., *HSF1 is required for extra-embryonic development, postnatal growth and protection during inflammatory responses in mice.* The EMBO Journal, 1999. **18**(21): p. 5943.

107. Morton, E.A. and T. Lamitina, *C. elegans HSF-1 is an essential nuclear protein that forms stress granule-like structures following heat shock.* Aging cell, 2013. **12**(1): p. 112-120.

108. Holmberg, C.I., et al., *Multisite phosphorylation provides sophisticated regulation of transcription factors.* Trends in Biochemical Sciences, 2002. **27**(12): p. 619-627.

109. Westerheide, S.D. and R.I. Morimoto, *Heat Shock Response Modulators as Therapeutic.* 2005. **280**(39): p. 33097-33100.

110. Morimoto, R.I., *Regulation of the heat shock transcriptional response : cross talk between a family of heat shock factors , molecular chaperones , and negative regulators.* 1998: p. 3788-3796.

111. Chiang, W.-C., et al., *A complex containing DDL-1 and HSF-1 links insulin-like signaling to heat-shock response in C. elegans.* Cell, 2012. **148**(1-2): p. 322-334.

112. Westerheide, S.D., et al., *Stress-Inducible Regulation of Heat Shock Factor 1 by the Deacetylase SIRT1.* Science (New York, N.Y.), 2009. **323**(5917): p. 1063-1066.

113. Raychaudhuri, S., et al., *Interplay of Acetyltransferase EP300 and the Proteasome System in Regulating Heat Shock Transcription Factor 1.* Cell, 2014. **156**(5): p. 975-985.

114. Jia, K., D. Chen, and D.L. Riddle, *The TOR pathway interacts with the insulin signaling pathway to regulate C. elegans larval development, metabolism and life span.* Development, 2004. **131**(16): p. 3897-906.

115. Murphy, C.T., *The search for DAF-16/FOXO transcriptional targets: Approaches and discoveries.* Experimental Gerontology, 2006. **41**(10): p. 910-921.

116. Ogg, S. and G. Ruvkun, *The C. elegans PTEN Homolog, DAF-18, Acts in the Insulin Receptor-like Metabolic Signaling Pathway.* Molecular Cell, 1998. **2**(6): p. 887-893.

117. Wook Oh, S., et al., *Identification of direct DAF-16 targets controlling longevity, metabolism and diapause by chromatin immunoprecipitation.* Nat Genet, 2006. **38**(2): p. 251-257.

118. Barbieri, M., et al., *Insulin/IGF-I-signaling pathway: an evolutionarily conserved mechanism of longevity from yeast to humans.* American Journal of Physiology - Endocrinology And Metabolism, 2003. **285**(5): p. E1064.

119. Riddle, D.L. and P.S. Albert, *Genetic and Environmental Regulation of Dauer Larva Development*, in *C. elegans II*, D.L. Riddle, et al., Editors. 1997, Cold Spring Harbor Laboratory Press: Cold Spring Harbor (NY).

120. Wang, J., et al., *RNAi Screening Implicates a SKN-1–Dependent Transcriptional Response in Stress Resistance and Longevity Deriving from Translation Inhibition.* PLOS Genetics, 2010. **6**(8): p. e1001048.

121. Inoue, H., et al., *The C. elegans p38 MAPK pathway regulates nuclear localization of the transcription factor SKN-1 in oxidative stress response.* Genes & Development, 2005. **19**(19): p. 2278-2283.

122. Glover-Cutter, K.M., S. Lin, and T.K. Blackwell, *Integration of the Unfolded Protein and Oxidative Stress Responses through SKN-1/Nrf.* PLoS Genetics, 2013. **9**(9): p. e1003701.

123. Soukas, A.A., et al., *Rictor/TORC2 regulates fat metabolism, feeding, growth, and life span in Caenorhabditis elegans.* Genes & Development, 2009. **23**(4): p. 496-511.

124. An, J.H., et al., *Regulation of the Caenorhabditis elegans oxidative stress defense protein SKN-1 by glycogen synthase kinase-3.* Proceedings of the National Academy of Sciences of the United States of America, 2005. **102**(45): p. 16275-16280.

125. Bishop, N.A. and L. Guarente, *Two neurons mediate diet-restriction-induced longevity in C. elegans.* Nature, 2007. **447**(7144): p. 545-549.

126. Robida-Stubbs, S., et al., *TOR signaling and rapamycin influence longevity by regulating SKN-1/Nrf and DAF-16/FoxO.* Cell Metab, 2012. **15**(5): p. 713-24.

127. Bowerman, B., B.A. Eaton, and J.R. Priess, *skn-1, a maternally expressed gene required to specify the fate of ventral blastomeres in the early C. elegans embryo.* Cell, 1992. **68**(6): p. 1061-1075.

128. Paek, J., et al., *Mitochondrial SKN-1/Nrf mediates a conserved starvation response.* Cell Metab, 2012. **16**(4): p. 526-37.

129. Haslbeck, M. and E. Vierling, *A first line of stress defense: Small heat shock proteins and their function in protein homeostasis.* Journal of Molecular Biology, 2015. **427**(7): p. 1537-1548.

130. van Oosten-Hawle, P., R.S. Porter, and R.I. Morimoto, *Regulation of organismal proteostasis by trans-cellular chaperone signaling.* Cell, 2013. **153**(6): p. 1366-1378.

131. Clark, J.I. and P.J. Muchowski, *Small heat-shock proteins and their potential role in human disease.* Current Opinion in Structural Biology, 2000. **10**(1): p. 52-59.

132. Ritossa, F.M., *Experimental activation of specific loci in polytene chromosomes of Drosophila.* Experimental Cell Research, 1964. **35**(3): p. 601-607.

133. Brehme, M., et al., *A Chaperome Sub-Network Safeguards Proteostasis in Aging and Neurodegenerative Disease.* Cell reports, 2014. **9**(3): p. 1135-1150.

134. Eichner, T., et al., *Conformational Conversion during Amyloid Formation at Atomic Resolution.* Molecular Cell, 2011. **41**(2): p. 161-172.

135. Kayed, R., et al., *Common Structure of Soluble Amyloid Oligomers Implies Common Mechanism of Pathogenesis.* Science, 2003. **300**(5618): p. 486.

136. Mayer, M.P., *Gymnastics of Molecular Chaperones.* Molecular Cell, 2010. **39**(3): p. 321-331.

137. Buchner, J., *Supervising the fold: functional principles of molecular chaperones.* The FASEB Journal, 1996. **10**(1): p. 10-19.

138. Bukau, B., J. Weissman, and A. Horwich, *Molecular Chaperones and Protein Quality Control.* Cell, 2006. **125**(3): p. 443-451.

139. Preissler, S. and E. Deuerling, *Ribosome-associated chaperones as key players in proteostasis.* Trends in Biochemical Sciences, 2012. **37**(7): p. 274-283.

140. Hartl, F.U., A. Bracher, and M. Hayer-Hartl, *Molecular chaperones in protein folding and proteostasis.* Nature, 2011. **475**(7356): p. 324-332.

141. Brychzy, A., et al., *Cofactor Tpr2 combines two TPR domains and a J domain to regulate the Hsp70/Hsp90 chaperone system.* The EMBO Journal, 2003. **22**(14): p. 3613-3623.

142. Shorter, J. and S. Lindquist, *Hsp104 Catalyzes Formation and Elimination of Self-Replicating Sup35 Prion Conformers.* Science, 2004. **304**(5678): p. 1793.

143. Behrends, C., et al., *Chaperonin TRiC Promotes the Assembly of polyQ Expansion Proteins into Nontoxic Oligomers.* Molecular Cell, 2006. **23**(6): p. 887-897.

144. Massey, A.C., C. Zhang, and A.M. Cuervo, *Chaperone-mediated autophagy in aging and disease.* Curr Top Dev Biol, 2006. **73**: p. 205-35.

145. Roelofs, J., et al., *Chaperone-mediated pathway of proteasome regulatory particle assembly*. Nature, 2009. **459**(7248): p. 861-865.

146. Glickman, M.H. and A. Ciechanover, *The ubiquitin-proteasome proteolytic pathway: destruction for the sake of construction.* Physiol Rev, 2002. **82**(2): p. 373-428.

147. Majeski, A.E. and J.F. Dice, *Mechanisms of chaperone-mediated autophagy.* Int J Biochem Cell Biol, 2004. **36**(12): p. 2435-44.

148. Fabrizio, P., et al., *Genome-wide screen in Saccharomyces cerevisiae identifies vacuolar protein sorting, autophagy, biosynthetic, and tRNA methylation genes involved in life span regulation.* PLoS Genet, 2010. **6**(7): p. e1001024.

149. Hansen, M., et al., *A role for autophagy in the extension of lifespan by dietary restriction in C. elegans.* PLoS Genet, 2008. **4**(2): p. e24.

150. Hars, E.S., et al., *Autophagy regulates ageing in C. elegans.* Autophagy, 2007. **3**(2): p. 93-5.

151. Melendez, A., et al., *Autophagy genes are essential for dauer development and life-span extension in C. elegans.* Science, 2003. **301**(5638): p. 1387-91.

152. Salminen, A. and K. Kaarniranta, *Regulation of the aging process by autophagy.* Trends Mol Med, 2009. **15**(5): p. 217-24.

153. Komatsu, M., et al., *Loss of autophagy in the central nervous system causes neurodegeneration in mice.* Nature, 2006. **441**(7095): p. 880-4.

154. Hara, T., et al., *Suppression of basal autophagy in neural cells causes neurodegenerative disease in mice.* Nature, 2006. **441**(7095): p. 885-9.

155. Bishop, N.A., T. Lu, and B.A. Yankner, *Neural mechanisms of ageing and cognitive decline.* Nature, 2010. **464**(7288): p. 529-535.

156. Terman, A., *The effect of age on formation and elimination of autophagic vacuoles in mouse hepatocytes.* Gerontology, 1995. **41 Suppl 2**: p. 319-26.

157. Vittorini, S., et al., *The age-related accumulation of protein carbonyl in rat liver correlates with the age-related decline in liver proteolytic activities.* J Gerontol A Biol Sci Med Sci, 1999. **54**(8): p. B318-23.

158. Johnson, S.C., P.S. Rabinovitch, and M. Kaeberlein, *mTOR is a key modulator of ageing and age-related disease.* 2013.

159. Kihara, A., et al., *Two distinct Vps34 phosphatidylinositol 3-kinase complexes function in autophagy and carboxypeptidase Y sorting in Saccharomyces cerevisiae.* J Cell Biol, 2001. **152**(3): p. 519-30.

160. Reggiori, F., et al., *The Atg1-Atg13 complex regulates Atg9 and Atg23 retrieval transport from the pre-autophagosomal structure.* Dev Cell, 2004. **6**(1): p. 79-90.

161. Reggiori, F. and D.J. Klionsky, *Atg9 sorting from mitochondria is impaired in early secretion and VFT-complex mutants in Saccharomyces cerevisiae.* J Cell Sci, 2006. **119**(Pt 14): p. 2903-11.

162. Finley, D., *Recognition and processing of ubiquitin-protein conjugates by the proteasome.* Annu Rev Biochem, 2009. **78**: p. 477-513.

163. Hanna, J. and D. Finley, *A proteasome for all occasions.* FEBS Letters, 2007. **581**(15): p. 2854-2861.

164. Wong, E. and A.M. Cuervo, *Integration of Clearance Mechanisms: The Proteasome and Autophagy.* Cold Spring Harbor Perspectives in Biology, 2010. **2**(12): p. a006734.

165. Labbadia, J. and R.I. Morimoto, *Proteostasis and longevity: when does aging really begin?* F1000Prime Reports, 2014. **6**: p. 7.

166. Kisselev, A.F., et al., *The sizes of peptides generated from protein by mammalian 26 and 20 S proteasomes. Implications for understanding the degradative mechanism and antigen presentation.* J Biol Chem, 1999. **274**(6): p. 3363-71.

167. Chen, S., et al., *Structural basis for dynamic regulation of the human 26S proteasome.* Proc Natl Acad Sci U S A, 2016. **113**(46): p. 12991-12996.

168. Husnjak, K., et al., *Proteasome subunit Rpn13 is a novel ubiquitin receptor.* Nature, 2008. **453**(7194): p. 481-8.

169. Goldberg, A.L., *Functions of the proteasome: from protein degradation and immune surveillance to cancer therapy.* Biochem Soc Trans, 2007. **35**(Pt 1): p. 12-7.

170. Chondrogianni, N. and E.S. Gonos, *Proteasome activation as a novel antiaging strategy.* IUBMB Life, 2008. **60**(10): p. 651-655.

171. Huber, N., et al., *Age-related decrease in proteasome expression contributes to defective nuclear factor-kappaB activation during hepatic ischemia/reperfusion.* Hepatology, 2009. **49**(5): p. 1718-28.

172. Tsakiri, E.N., et al., *Proteasome dysfunction in Drosophila signals to an Nrf2-dependent regulatory circuit aiming to restore proteostasis and prevent premature aging.* Aging cell, 2013. **12**(5): p. 802-813.

173. Vilchez, D., et al., *RPN-6 determines C. elegans longevity under proteotoxic stress conditions.* Nature, 2012. **489**(7415): p. 263-268.

174. Chondrogianni, N., et al., *20S proteasome activation promotes life span extension and resistance to proteotoxicity in Caenorhabditis elegans.*

175. Pathare, G.R., et al., *The proteasomal subunit Rpn6 is a molecular clamp holding the core and regulatory subcomplexes together.* Proceedings of the National Academy of Sciences of the United States of America, 2012. **109**(1): p. 149-154.

176. Muntau, A.C., et al., *Innovative strategies to treat protein misfolding in inborn errors of metabolism: pharmacological chaperones and proteostasis regulators.* J Inherit Metab Dis, 2014. **37**(4): p. 505-23.

177. Mu, T.W., et al., *Chemical and biological approaches synergize to ameliorate protein-folding diseases.* Cell, 2008. **134**(5): p. 769-81.

178. Arakawa, T., et al., *Small molecule pharmacological chaperones: From thermodynamic stabilization to pharmaceutical drugs.* Biochim Biophys Acta, 2006. **1764**(11): p. 1677-87.

179. Underhaug, J., O. Aubi, and A. Martinez, *Phenylalanine Hydroxylase Misfolding and Pharmacological Chaperones.* Current Topics in Medicinal Chemistry, 2012. **12**(22): p. 2534-2545.

180. Bernier, V., et al., *Pharmacological chaperones: potential treatment for conformational diseases.* Trends Endocrinol Metab, 2004. **15**(5): p. 222-8.

181. Kim, K.H., et al., *Acute Exercise Induces FGF21 Expression in Mice and in Healthy Humans.* PLOS ONE, 2013. **8**(5): p. e63517.

182. Alavez, S., et al., *Amyloid-binding compounds maintain protein homeostasis during ageing and extend lifespan.* Nature, 2011. **472**(7342): p. 226-9.

183. Khurana, R., et al., *Mechanism of thioflavin T binding to amyloid fibrils.* Journal of Structural Biology, 2005. **151**(3): p. 229-238.

184. Rual, J.-F., et al., *Toward Improving Caenorhabditis elegans Phenome Mapping With an ORFeome-Based RNAi Library.* Genome Research, 2004. **14**(10b): p. 2162-2168.

185. Hoogewijs, D., et al., *quantitative sod gene expression analysis in C . elegans.* 2008. **8**: p. 1-8.

186. Schmittgen, T.D. and K.J. Livak, *Analyzing real-time PCR data by the comparative C T method.* 2008. **3**(6): p. 1101-1108.

187. Mitchell, D.H., et al., *Synchronous growth and aging of Caenorhabditis elegans in the presence of fluorodeoxyuridine.* J Gerontol, 1979. **34**(1): p. 28-36.

188. Gandhi, S., et al., *A simple method for maintaining large, aging populations of Caenorhabditis elegans.* Mechanisms of Ageing and Development, 1980. **12**(2): p. 137-150.

189. Lehrbach, N.J., *2220.full.* RNA, 2012. **18**: p. 2220-2235.

190. Davies, S.K., A.M. Leroi, and J.G. Bundy, *Fluorodeoxyuridine affects the identification of metabolic responses to daf-2 status in Caenorhabditis elegans.* Mechanisms of Ageing and Development, 2012. **133**(1): p. 46-49.

191. Van Raamsdonk, J.M. and S. Hekimi, *FUdR causes a twofold increase in the lifespan of the mitochondrial mutant gas-1.* Mechanisms of Ageing and Development, 2011. **132**(10): p. 519-521.

192. Rooney, J.P., et al., *Effects of 5'-Fluoro-2-deoxyuridine on Mitochondrial Biology in Caenorhabditis elegans.* Experimental gerontology, 2014. **0**: p. 69-76.

193. Tang, M., et al., *Correlation Assessment among Clinical Phenotypes, Expression Analysis and Molecular Modeling of 14 Novel Variations in the Human Galactose-1-phosphate Uridylyltransferase Gene.* Human mutation, 2012. **33**(7): p. 1107-1115.

194. Acsadi, G., et al., *Novel Mutation in Spectrin-like Repeat 1 of Dystrophin Central Domain Causes Protein Misfolding and Mild Becker Muscular Dystrophy.* The Journal of Biological Chemistry, 2012. **287**(22): p. 18153-18162.

195. Steffan, J.S. and L.M. Thompson, *Targeting aggregation in the development of therapeutics for the treatment of Huntington's disease and other polyglutamine repeat diseases.* Expert Opinion on Therapeutic Targets, 2003. **7**(2): p. 201-213.

196. Wang, H., et al., *Suppression of polyglutamine-induced toxicity in cell and animal models of Huntington's disease by ubiquilin.* Human Molecular Genetics, 2006. **15**(6): p. 1025-1041.

197. *Gidalevitz T, Prahlad V, Morimoto RI: The stress of protein misfolding: from single cells to multicellular organisms. Cold Spring Harb Perspect Biol 2011, 3(6). doi: 10.1101/cshperspect.a009704.*

198. Biancalana, M. and S. Koide, *Molecular Mechanism of Thioflavin-T Binding to Amyloid Fibrils.* Biochimica et biophysica acta, 2010. **1804**(7): p. 1405-1412.

199. Picken, M.M. and G.A. Herrera, *Thioflavin T Stain: An Easier and More Sensitive Method for Amyloid Detection*, in *Amyloid and Related Disorders: Surgical Pathology and Clinical Correlations*, P.F.M.M. Picken Md, M.D.P.D.A. Dogan, and M.D.G.A. Herrera, Editors. 2012, Humana Press: Totowa, NJ. p. 187-189.

200. Fay, D.S., et al., *In Vivo Aggregation of / 3-Amyloid Peptide Variants.* 1998.

201. Zisoulis, D.G., et al., *Comprehensive discovery of endogenous Argonaute binding sites in Caenorhabditis elegans.* Nature structural & molecular biology, 2010. **17**(2): p. 173-179.

202. Welker, N.C., et al., *Dicer's helicase domain discriminates dsRNA termini to promote an altered reaction mode.* Molecular cell, 2011. **41**(5): p. 589-599.

203. Hansen, M., et al., *Lifespan extension by conditions that inhibit translation in Caenorhabditis elegans.* Aging Cell, 2007. **6**(1): p. 95-110.

204. Zhang, H., et al., *Guidelines for monitoring autophagy in Caenorhabditis elegans.* Autophagy, 2015. **11**(1): p. 9-27.

205. Toth, M.L., et al., *Longevity pathways converge on autophagy genes to regulate life span in Caenorhabditis elegans.* Autophagy, 2008. **4**(3): p. 330-8.

206. Prahlad, V., T. Cornelius, and R.I. Morimoto, *Regulation of the cellular heat shock response in Caenorhabditis elegans by thermosensory neurons.* Science, 2008. **sas320**.

207. Balch, W.E., et al., *Adapting Proteostasis for Disease Intervention.* Science, 2008. **319**(5865): p. 916.

208. Ciryam, P., et al., *Widespread Aggregation and Neurodegenerative Diseases Are Associated with Supersaturated Proteins.* CellReports, 2013. **5**(3): p. 781-790.

209. Blackwell, T.K., et al., *SKN-1/Nrf, stress responses, and aging in Caenorhabditis elegans.* Free radical biology & medicine, 2015. **88**(Pt B): p. 290-301.

210. Mertensk̈otter, A., et al., *The p38 MAPK PMK-1 shows heat-induced nuclear translocation, supports chaperone expression, and affects the heat tolerance of Caenorhabditis elegans.* Cell Stress & Chaperones, 2013. **18**(3): p. 293-306.

211. Zou, J., et al., *Repression of heat shock transcription factor HSF1 activation by HSP90 (HSP90 complex) that forms a stress-sensitive complex with HSF1.* Cell, 1998. **94**(4): p. 471-80.

212. Segref, A., S. Torres, and T. Hoppe, *A Screenable in vivo Assay to Study Proteostasis Networks in Caenorhabditis elegans.* Genetics, 2011. **187**(4): p. 1235-1240.

213. Kumsta, C., et al., *Hormetic heat stress and HSF-1 induce autophagy to improve survival and proteostasis in C. elegans.* Nature Communications, 2017. **8**: p. 14337-14337.

214. Douglas, P.M., et al., *Heterotypic Signals from Neural HSF-1 Separate Thermotolerance from Longevity.* Cell Reports, 2015. **12**(7): p. 1196-1204.

215. Dowen, R.H., et al., *A microRNA program in the C. elegans hypodermis couples to intestinal mTORC2/PQM-1 signaling to modulate fat transport.* Genes Dev, 2016. **30**(13): p. 1515-28.